

ABSTRACT

Title of Document: **MULTILAYERED SPHERES, TUBES AND SURFACES
SYNTHESIZED BY “INSIDE-OUT” POLYMERIZATION**

Brady C. Zarket , Doctor of Philosophy, 2017

Directed By: Professor Srinivasa R. Raghavan
Department of Chemical and Biomolecular Engineering

Numerous materials in nature, including eggs, onions, spinal discs, and blood vessels, have multiple layers. Each layer in these materials has a distinct composition and thereby a unique function in the overall material. Our work is motivated by the need to find a simple, versatile route for the synthesis of such multilayered materials. Toward this goal, we have devised a technique termed “inside-out polymerization” to synthesize multilayered materials with precise control over the composition and thickness of each layer. Each layer is a crosslinked polymer gel and it grows from the surface of the previous layer, with this growth being controlled by precursor molecules present in the core of the structure. Using this technique, we synthesize multilayer structures in three different geometries, as described below.

First, we outline our technique and use it to create multilayered polymer capsules. In particular, we create interesting capsules with concentric layers of non-responsive and stimuli-responsive polymers. The thickness of the stimuli-responsive layer varies sharply due to the stimulus while the non-responsive layer remains at the same thickness. In addition, the permeability of small molecules through the stimuli-responsive layers is also altered. This means that these multilayered capsules could be used to conduct pulsatile

release of solutes such as drugs or other chemicals. In addition, we also show that multilayered capsules exhibit improved mechanical properties compared to those of the fragile core.

Next, we extend our technique to the synthesis of multilayered polymer tubes. Our technique provides precise control over the inner diameter of the tube, the number of layers in the tube wall, and the thickness and chemistry of each layer. Tubes can be patterned with different polymers either in the lateral or longitudinal directions. Patterned tubes based on stimuli-responsive polymers exhibit the ability to spontaneously change their lumen diameter in response to stimuli, or to convert from a straight to a curled shape. On the whole, these tubes mimic several features exhibited by blood vessels like veins and arteries.

In our last study, we use our technique to create hair-like structures that grow outward from a base polymer gel. The diameter, length, and spacing of hairs can all be tuned. The addition of hairs serves to increase the net surface area of the base gel by nearly 10-fold. This increase is comparable to the surface area increase provided by hairs called “villi” on the inner walls of small intestines. In accordance with the increased surface area, hairy surfaces extract solutes from a solution much faster than a bare surface. We also impart stimuli-responsive properties to the hairs (e.g., magnetic properties), and we show that hairy gels can be induced to fold into tubes with hairs on the outside or inside. The latter mimics the structure of the small intestine.

**MULTILAYERED SPHERES, TUBES AND SURFACES SYNTHESIZED BY
“INSIDE-OUT” POLYMERIZATION**

By

Brady C. Zarket

Dissertation submitted to the Faculty of the Graduate School of the
University of Maryland, College Park, in partial fulfillment
of the requirements for the degree of
Doctor of Philosophy
2017

Advisory Committee:
Professor Srinivasa R. Raghavan, Chair
Professor Robert M. Briber
Professor Richard V. Calabrese
Professor Ian M. White
Professor Taylor J. Woehl

© Copyright by

Brady C. Zarket

2017

Acknowledgements

First, I would like to thank my advisor, Dr. Srinivasa Raghavan. I have known Dr. Raghavan for over 7 years, and he has been incredibly influential in my professional development. In a way, he is the reason I am where I am today. Dr. Raghavan provided me with my first opportunity to pursue scientific research during my undergraduate studies. This first experience truly transformed me in a profound way. I realized I love science, research and gaining knowledge, and because of this I decided I wished to pursue a career in scientific research. He is one of the best writers and orators I have ever known, and took the time (repeatedly in some cases) to pass on his wealth of knowledge in these areas to me. The value of the discussions about research topics, and guidance through the last 5 years, he has provided cannot be overstated. Dr. Raghavan always encourages his students to pursue interesting topics, rather than confining us to one specific research subject. This made my time in graduate school unique, and incredibly rewarding. I am truly grateful for everything Dr. Raghavan has done for me.

I would like to thank my committee: Dr. Robert Briber, Dr. Ian White, Dr. Richard Calabrese and Dr. Taylor Woehl for taking the time to advise me on the subjects within this dissertation. Additionally, I would like to thank all the undergraduate students who have worked with me during my graduate studies on various projects: Steven Antoszewski, Justin Heckelman, Timothy Coyne, Felix Yuwono, Matthew Bohensky and Hanchu Wang. I would especially like to thank Hanchu Wang. Hanchu has an inquisitive nature, always

asks me intriguing, important questions, and possesses a work ethic which many would envy. I wish you all the best in your future endeavors.

Next, I want to thank my friends and colleagues. Specifically, I would like to thank Dr. Ankit Gargava, Dr. Jasmin Athas, Dr. Annie Lu, Dr. Bani Cipriano, Dr. Tao Gao, Dr. Svetlana Ikonomova, Derrick Ko, Nick Guros and Kerry DeMella for their friendship throughout the years. I would like to thank Dr. Joseph White for his help with everything rheology, Dr. Hyuntaek Oh, Dr. Matthew Dowling, Dr. Chanda Arya and Dr. Xuefeng Li for their helpful discussions about my research activities. I would also like to thank James Liu, Niti Agrawal, Toniya Acharya, Chunxue Zhang and all the Complex Fluids and Nanomaterials lab group members.

Finally, and with my utmost sincerity, I would like to thank my family. My father and mother Frank and Joyce Zarket, and my brother Max Zarket. My family has always been my rock, providing me a strong foundation and support through my studies. I always know that no matter what happens I can trust my family to help me. I could not have made it this far without your support. I don't say it very frequently, but I cannot thank you all enough.

Table of Contents

ABSTRACT	i
Acknowledgements	ii
Table of Contents	iv
List of Figures	vi
Chapter 1	1
Introduction and Overview.....	1
1.1 Problem Description and Motivation	1
1.2 Proposed Approach	3
1.2.1 Multilayered Spherical Capsules	3
1.2.2 Multilayered Tubes.....	4
1.2.3 Hairy Surfaces	5
1.3 Significance of This Work.....	6
Chapter 2	7
Background	7
2.1 Multilayered Materials in Nature	7
2.2 Hydrogel Formation by Free-Radical Polymerization	9
2.3 Stimuli-Responsive Hydrogels.....	11
2.4 Shape-Changing Materials in Nature	13
2.5 Shape-Changing Hydrogels.....	14
Chapter 3	16
Multilayered Spherical Capsules.....	16
3.1 Introduction	16
3.2 Experimental.....	18
3.3 Results and Discussion.....	22
3.3.1 Synthesis of Multilayer Capsules	22
3.3.2 Kinetics of Layer Growth.....	27
3.3.3 Mechanical Properties	29
3.3.4 Stimuli-Responsive Layers.....	32
3.3.5 Solute Release from Temperature-Responsive Capsules	35
3.4 Conclusions	40
Chapter 4	42
Multilayer Tubes	42
4.1 Introduction	42
4.2 Experimental.....	44

4.3 Results and Discussion	47
4.3.1 Synthesis of Single-Layer Tubes.....	47
4.3.2 Kinetics of Layer Growth.....	49
4.3.3 LAP-Crosslinked Tubes and their Staining.....	52
4.3.4 Mechanical Robustness of the Tubes	54
4.3.5 Tubes Patterned with Stimuli-Responsive Polymers.....	55
4.3.6 Multilayered Polymer Tubes	59
4.3.7 Chemical Post-Modification of Tube Layers	62
4.4 Conclusions	63
Chapter 5	64
Hairy Gel Surfaces	64
5.1 Introduction	64
5.2 Experimental.....	65
5.3 Results and Discussion.....	70
5.3.1 Synthesis of Hairy Gel Surfaces.....	70
5.3.2 LAP-Bearing Hairs and their Staining.....	72
5.3.3 Hairy Gels with Tailored Dimensions	74
5.3.4 Dye Adsorption by Hairy vs. Base Gels.....	76
5.3.5 Gels with Stimuli-Responsive Hairs.....	78
5.3.6 Multilayer Hairs.....	80
5.3.7 Hairy Gels with Stimuli-Responsive Bases.....	81
5.4 Conclusions	84
Chapter 6	85
Conclusions and Recommendations.....	85
6.1 Project Summary and Principal Contributions	85
6.2 Recommendations for Future Work	86
6.2.1 Mechanical Properties of Multilayered Capsules.....	86
6.2.2 Multilayered Hydrogel Materials as Tissue Engineering Scaffolds.....	87
6.2.3 Organic-Inorganic Hybrid Materials	88
References	90
List of Publications	100

List of Figures

- Figure 1.1. Micrographs of a stimuli-responsive multilayered capsule.** There are two layers, each of which is a polymer gel. The outer layer is responsive to pH, and thereby its thickness increases dramatically as pH is changed from 3 to 7. The scale bars represent 500 μm3
- Figure 1.2. Schematic and photo of a multilayered polymer tube.** The tube has three distinct layers, each of which is a polymer gel. The middle layer is stained with the dye methylene blue (MB). The scale bar is 2.0 mm.4
- Figure 1.3. Schematic and photos of a hair-covered surface.** The base and hairs are both made of polymer gels. Photos of the system are shown from the side and the top. The scale bars represent 5.0 mm.5
- Figure 2.1. Examples of natural materials that have multiple layers.** (a) Plant seeds. The cross-section of a castor bean seed is shown. (b) Eggs and embryos. The structure of a chicken egg is illustrated. (c) Vegetables and fruits. The structure of an onion is shown in two views. (d) Tissues and body parts. The top-view of a spinal disc located between the vertebrae in the spine is shown.¹ (e) Blood vessels.² The structure of a vein is shown. (f) The wall of a small intestine is shown, highlighting the hair-like structures called villi. ...7
- Figure 2.2. Reactions involved in the crosslinking of N-Isopropylacrylamide (NIPA).** In initiation, the free-radical initiator is cleaved to create radicals. Next, the radicals attack vinyl groups on the monomer (NIPA) and the crosslinker (BIS). The result is a NIPA-BIS network.9
- Figure 2.3. Examples of monomers used for synthesizing stimuli-responsive hydrogels.** Gels of AAm shrink when the solvent composition is changed (e.g., in mixtures of water and acetone). Gels of NIPA shrink upon heating above a critical temperature. Gels of SA shrink when the pH of the solution is lowered below a critical value.....11
- Figure 2.4. Volume change of NIPA gels upon heating.** When a NIPA gel is heated above its LCST of 32°C, it shrinks abruptly, as shown by the above data. Adapted from Hirokawa et. Al.12
- Figure 2.5. Opening of pine cone scales.** Pine cone scales contain layers of tissue which swell to different extents. In a humid environment the outer layer of the scale is more swollen and the scales are closed. When the humidity is low, the outer layer shrinks and the scales open, releasing the seeds that are contained in the pine cone. Adapted from Dunlop et. Al.....13

Figure 2.6. Folding of a bilayer hydrogel. The gel is a sandwich of two layers, one made from acrylamide (AAM) and the other from N,N-dimethylacrylamide (DMAA). The AAM layer shrinks in the presence of acetone, and the resulting swelling mismatch between the layers causes the whole gel to curl.....14

Figure 3.1. Synthesis of multilayer capsules. An alginate gel core is first made (a) and this is loaded with free-radical initiator (b). The gel is then introduced into a solution of monomer 1 (along with cross-linker and accelerant) (c). Upon polymerization, a layer of polymer 1 is formed around the gel core (d). The inset in c shows that this layer is formed by diffusion of initiator outward from the core into the monomer solution. This process is then repeated with the onelayer capsule (e), which is loaded with initiator (f) and then contacted with monomer 2 (g). Upon polymerization, a second layer of polymer 2 is formed (h). The process can be further repeated to introduce additional layers. Scale bars are 500 μm23

Figure 3.2. Images of multilayer capsules at different length scales. (a) Photos of the alginate gel core and the corresponding one-layer and two-layer capsules. (b) Optical micrograph of a capsule with an alginate (Alg) core, an inner layer of N-isopropylacrylamide (NIPA) and an outer layer of N,N'-dimethylacrylamide (DMAA). The overall structure is denoted as Alg-NIPA-DMAA. The scale bar is 500 μm . (c) Scanning electron micrographs of two Alg-NIPA-DMAA capsules (after freeze-drying). The boundaries between the layers can be distinctly seen in both cases. Scale bars in the images are 500 μm25

Figure 3.3. Single-layer capsules over a range of length scales. Optical micrographs are shown of capsules with a crosslinked polymeric shell surrounding a biopolymer gel core. In (a), the core (chitosan/GA) has a diameter of 185 μm , and the shell (SA) has a similar thickness (scale bar is 100 μm). In (b), the core (chitosan/GA) has a diameter of 400 μm and the shell (DMAA) has a thickness of ~ 150 μm (scale bar is 200 μm). In (c), the core (alginate) has a diameter of 2.8 mm and the shell (DMAA) is 250 μm thick (scale bar is 700 μm). In (d), the core (alginate) has a diameter of 6.0 mm and the shell (DMAA) is 230 μm thick (scale bar is 800 μm).26

Figure 3.4. Kinetics of layer growth, visualized directly by optical microscopy. At time $t = 0$, an alginate gel core of 2 mm diameter, loaded with 15 mg/ml ammonium persulfate (APS) initiator, is placed in a solution of 1 M DMAA monomer (together with cross-linker and accelerant). Still images at various time points are shown in a, b, and c, and these reveal the growth of the polymer layer around the core. Scale bars in the images are 200 μm . In d, a plot of the layer thickness h vs. t is shown, and the solid curve through the data is a fit to eq 3.1.....27

Figure 3.5. Contrasting mechanical properties of a core gel particle versus a single-layer capsule. Photos are shown of an Alg gel particle (a) and an Alg-DMAA capsule (b) being compressed between parallel plates. Both have the same core diameter of 4.6 mm, with the DMAA shell being 200 μm thick. Photos a1 to a3: when the Alg gel is compressed

by 50%, it remains squished and does not recover when the compression is removed (plastic response). Photos b1 to b3: when the Alg–DMAA capsule is compressed by 60%, it recovers as soon as the compression is removed (elastic response). Thus, the addition of the thin DMAA shell (1/20th the thickness of the core) dramatically alters the mechanical properties.....30

Figure 3.6. Compression tests on an Alg gel core and an Alg-DMAA capsule. The sample is placed between parallel plates at time zero. During the compression cycle the top plate is brought down, while during the recovery cycle the top plate is lifted up (both at 10% strain per minute). The measured compressive stress is plotted against time in the two plots, with the compressive strain indicated for selected points. (a) When the Alg gel core is compressed up to ~ 50% strain, it is irreversibly squished into a disc shape (plastic behavior). Thus, the sample does not recover when the plate is lifted up. (b) When the Alg-DMAA capsule is compressed up to ~ 50% strain, it responds elastically, and recovers to its initial size when the plate is lifted up during the recovery cycle. A second compression-recovery cycle is then applied on the capsule, and the data for this cycle closely track those from the first cycle.31

Figure 3.7. Multilayer capsules with specific layers responsive to external stimuli. In (a), a two-layer capsule is shown with an inner layer of nonionic polymer (DMAA) and an outer layer of anionic polymer, obtained by copolymerization of DMAA with sodium acrylate (SA) (designated as DMAA–SA). At pH 3, the two layers have the same thickness. At pH 7, the carboxylate groups in the DMAA–SA layer become deprotonated, causing the anionic gel to swell, and thus the thickness of the DMAA–SA layer increases substantially. In (b), a three-layer capsule is shown, where layers 1 and 3 are DMAA (non-responsive), while layer 2 is NIPA (thermoresponsive). At ambient temperature (25°C), all layers are transparent gels. Upon heating to 40°C, which is above the lower critical solution temperature (LCST) of NIPA, the NIPA layer becomes turbid. Scale bars are 500 μm in (a) and 1 mm in (b).34

Figure 3.8. Temperature-responsive release of dye from a two-layer DMAA–NIPA capsule. Here, DMAA is the inner layer and NIPA is the outer layer. At 40 °C (above the LCST of NIPA), the pores in the outer NIPA layer are closed; thus, the dye remains in the capsule. This is indicated by the schematic, and the corresponding micrograph shows a dark capsule due to the turbidity of the outer layer. After a certain time (110 min for the blue curve; 780 min for the red curve), the temperature is lowered to ambient (25 °C). The pores in the NIPA layer open up, causing the dye to release. This is shown by the schematic, and in this case the micrograph shows a transparent capsule. The y-axis is normalized to the dye released into solution after a long time (2 days).36

Figure 3.9. Temperature-responsive release of dye from a two-layer NIPA–DMAA capsule. Here, NIPA is the inner layer and DMAA is the outer layer. At 40°C (above the LCST of NIPA), the pores in the inner NIPA layer are closed. In this case, the dye in the outer DMAA layer alone is released, as shown by the schematic. The corresponding micrograph shows a dark inner portion due to the turbidity of the NIPA layer, while the

outer layer is transparent. At the 45 min mark, the temperature is lowered to ambient (25°C). The pores in the NIPA layer open up, causing the inner dye to also release. This is shown by the schematic and in this case the entire capsule is transparent.39

Figure 4.1. Synthesis of a single-layer polymer tube. First, a cylindrical template of agar of desired diameter is created, as shown in (a) to (d). Then, an agar cylinder of specific size (e) is loaded with free-radical initiator (f), and transferred to a solution of monomer (along with crosslinker and accelerant) (g). The initiator diffuses outward, polymerizing a layer of polymer around the template (h). To yield a hollow tube, the ends are cut off (i) and the structure is heated to ~ 90°C (j), whereupon the agar melts away, leaving behind a hollow tube (k). All scalebars in insets are 4.5mm in length.....47

Figure 4.2. Single-layer tubes of different lumen diameter. All tubes have a wall composed of a DMAA-BIS network and their lumen (inner) diameter ranges from ~ 0.6 mm on the far right to ~ 4.5 mm on the far left. The scale bar is 5mm in length.....49

Figure 4.3. Kinetics of polymer layer growth. An agar cylinder loaded with 15 mg/mL APS was placed in a 10 wt% DMAA solution at time $t = 0$. Time-lapse microscope images collected during the polymerization are presented in (a), (b) and (c), showing the growth of the polymer layer over time. Scale bars in the images are 500 μm . In (d), the thickness h of the polymer layer is plotted as a function of time t , and fit to eq 4.150

Figure 4.4. Kinetics of layer growth around a spherical vs. cylindrical template. The data from Figures 3.4 and 4.3 are replotted above. Each set of data is normalized by the final layer thickness ($h^* = h/h_\infty$). The semilog plots above both follow straight lines, confirming the exponential form for the fit (eq 4.1). From the slope, the rate constants k are calculated, and we find that $k_{\text{sph}} = 0.54$ is much higher than $k_{\text{cyl}} = 0.21$ 51

Figure 4.5. Tube with a polymer layer crosslinked by LAP and staining of this layer. LAP particles serve as crosslinkers for growing polymer chains, leading to a network, as shown by the schematics. A tube with a layer of DMAA-LAP is transparent (a). When placed in a 10 μM solution of methylene blue (MB) for 30 min, the tube wall takes on a light-blue color (b), while incubation in the same solution for 9 h gives it a dark blue color (c). The color is due to adsorption of the cationic MB on the anionic faces of the LAP particles, as shown by the schematics. Scale bars are 5 mm53

Figure 4.6. Photos showing the mechanical properties of tubes. This 1-layer tube of DMAA-LAP is flexible and robust enough to be bent and tied into a knot (a). The images in (b) and (c) show a knotted tube being further stretched up to ~150% of its initial length without breaking. All scale bars are 5mm54

Figure 4.7. Synthesis of laterally patterned tubes, and two examples of the same. (a) The synthesis is achieved by placing an initiator-loaded cylindrical agar template in a rectangular trough containing two or more highly viscous monomer solutions. The solutions do not mix due to their viscosity. (b) A tube with three lateral segments corresponding to DMAA-NIPA-DMAA. When heated above 32°C, the middle NIPA

segment shrinks, and the tube narrows. The lumen diameter (inset micrographs of a separate, microscale tube which shows inner diameter change; scale bar 500 μm) decreases by $\sim 50\%$. (c) A tube with three lateral segments corresponding to DMAA-SA-DMAA. At $\text{pH} > 7$, the SA segment swells and the tube dilates. The lumen diameter increases from 4.5 mm to 5.7 mm. Photograph scale bars are 4.5mm.....56

Figure 4.8. Synthesis of longitudinally patterned (“Janus”) tubes, and an example of the same. (a) The synthesis is achieved by placing an initiator-loaded cylindrical agar template in a rectangular trough containing two viscous monomer solutions, poured one after the other. The solutions do not mix due to their viscosity. (b) The Janus tube has a top half of DMAA and a bottom half of NIPA. When heated above 32°C , the NIPA half shrinks. This in turn causes the tube to curl and coil. Scale bars are 5mm.....58

Figure 4.9. Synthesis of multilayer polymer tubes. A one-layer cylinder (with agar intact) is used as a new template for the synthesis of the next outside layer (a). The template is soaked in initiator (b) and then placed in monomer 2 solution (c), yielding a second polymer layer outside the first. This process is repeated to form additional layers. A three-layer tube is shown schematically in (e) and by a photo in (f). The layers differ in the crosslinker used: layers 1 and 3 have BIS as crosslinker while layer 2 has LAP as crosslinker. The differences between the layers are highlighted by the fact that only the LAP layer strongly binds MB dye, giving it a dark blue color. The scale bar is 2 mm.....60

Figure 4.10. Synthesis of tubes with single-layer and multilayer regions. A one-layer cylinder (with agar intact) is loaded with initiator and placed vertically in a second monomer solution such that only a portion of the cylinder is submerged (a). As a result, the second polymer layer only forms over the submerged portion. Photos of such a tube are shown in different views from the top and sides (b-d). The one-layer portion is DMAA-LAP and the second layer is DMAA-BIS. Only the former strongly binds MB dye, giving it a dark blue color. The scale bars are 5 mm61

Figure 4.11. Post-modification of a specific layer in a multilayer tube. The tube has an outer layer of DMAA and an inner layer of SA, with the latter having carboxylate groups. The tube is reacted with EDC and NHS, and then with a primary amine via the reaction scheme shown in (a). The result is that the carboxylates become attached to the functional group F on the amine. The amine chosen here is fluoresceinamine (F-NH_2) and it imparts fluorescence to the inner layer. A yellow-green color is selectively seen visually for this layer after modification (b). The scale bar in the photo is 2 mm. The cross-section of the tube is viewed under fluorescence microscopy and the inner layer reveals bright green fluorescence (c-e). Scale bars in the images are 500 μm62

Figure 5.1. Synthesis of Hairy Gels. First a base gel, typically of DMAA, is made and cut to the desired size. Second, agar is poured around a syringe needle array (c) and cooled to produce a gel. When the needles are removed, we have a holey agar template with channels (d), which are filled with a monomer solution (e). The base gel is loaded with initiator (f) and placed atop the monomer-filled agar template (g). The initiator diffuses into the

channels and forms polymer (h). Finally, the agar is dissolved by heat (i) to yield a hairy gel (j). Images of hairy gels in (k). All scale bars are 5 mm.....71

Figure 5.2. Staining of LAP-bearing hairs with a cationic dye. The LAP particles serve as crosslinkers for polymer chains in the hairs, as shown by the schematics. The hairs are initially transparent (a). When placed in a 10 μ M solution of methylene blue (MB) for 30 min, the hairs take on a light-blue color (b), while incubation in the same solution for 9 h gives the hairs a dark blue color (c). The color is due to adsorption of the cationic MB on the anionic faces of the LAP particles, as shown by the schematics in (b) and (c). Scale bars in the images are 5 mm73

Figure 5.3. Hairs of varying dimensions and spacing. The height, diameter, and spacing between hairs are varied, as shown in the photos. All hairs were fabricated on a base of the same dimensions, i.e. a 14.5 \times 14.5 mm square.....74

Figure 5.4. Surface area increase for hairy gels vs base gels. The ratio of the surface area of the hairs + base gel, $SA_{(h+b)}$ to the surface area of just a base gel SA_b is plotted in (a) as a function of the hair diameter and in (b) as a function of the total number of hairs. The yellow box demarcates the typical increase in surface area seen for an intestine covered with villi over a flat intestine. Inset (c) shows images of hairy gels with different hair densities, from 5 \times 5 to 8 \times 8 for a constant hair diameter of 0.9 mm. Scale bars are 5mm .75

Figure 5.5. Dye adsorption of hairy vs base gels. A base gel and a hairy gel of identical composition (both contain LAP) are compared for their ability to absorb MB dye from water. Photos of the base gel (a) and hairy gel (b) in MB solution at different time points. The hairy gel samples show a lighter color, indicating more dye removal. (c) Dye% in solution as a function of time plotted for the base and hairy gels, confirming more rapid dye removal by the latter. The inset is a semilog plot of the initial \sim 1 h of the data. The slopes of the lines yield the decay constants k for each gel. The value of k_{hair} is about thrice the value of k_{base} . Scale bars are 5 mm.....77

Figure 5.6. Stimuli-responsive rows of hairs. Rows of magnetically responsive hairs (brown color, due to MNPs in the hairs) (brown) alternate with non-responsive hairs (black due to CB in the hairs) on the base gel. Both photos (top) and schematics (bottom) are shown. In (a), with no magnetic field, both hairs stand vertically. In (b), when a magnet is placed on the left, the magnetic hairs bend toward the gel, while the non-responsive hairs remain vertical. In (c). the magnetic field is removed and all hairs return to the vertical position. Scale bars are 5 mm79

Figure 5.7. Multilayered hairs. Each hair has an inner layer of DMAA-LAP (blue due to adsorbed MB dye) and an outer layer of AAm-BIS. In water (top), both layers are swollen. In 60% acetone the outer AAm layer shrinks and becomes turbid. Scale bars are 5 mm .80

Figure 5.8. Hairy gel with a stimuli-responsive base. The hairs are DMAA-LAP on top of a base of AAm-BIS. The whole gel is placed in a 60% acetone solution. The top-view of the response is shown in (a) and the side view in (b). The base gel shrinks, but the hairs

remain the same height. The dashed lines show the initial dimensions of the base gel. Due to the shrinking, the distance between adjacent hairs shrinks from 2.7 to 1.3 mm. Scale bars are 5 mm81

Figure 5.9. Hairy gel with a bilayer base showing a shape change to an insect-like structure in response to solvent composition. The base has two layers, AAm and DMAA, both crosslinked with BIS, and hairs of DMAA-LAP are grown on the DMAA side of the bilayer. In acetone, the AAm layer shrinks, causing the base to curl into a tube. The DMAA layer, and the hairs, are on the outside of this tube, which thereby resembles an insect...82

Figure 5.10. Hairy gel with a bilayer base showing a shape change to an intestine-like tube in response to solvent composition. The base has two layers, AAm and DMAA, both crosslinked with BIS, and hairs of DMAA-LAP are grown on the AAm side of the bilayer. In acetone, the AAm layer shrinks, causing the base to curl into a tube. The hairs are attached to the AAm layer, which means the hairs are now positioned on the inside of the tube. This structure is similar to that of the small intestine83

Chapter 1

Introduction and Overview

1.1 Problem Description and Motivation

Numerous materials commonly observed in nature are composed of multiple layers. For example, eggs, onions, seeds, spinal discs, blood vessels, and the human gastrointestinal (GI) tract all exhibit a complex multilayer structure (see Chapter 2).¹⁻⁶ The reason for the existence of multiple layers is that each layer has a distinct function. For example, in the egg, the core is the yolk, which contains the genetic material. This is surrounded by the albumin layer, which provides nutrients to the growing embryo in the yolk.¹ The albumin and yolk are then further surrounded by an inorganic shell, which provides protection and mechanical strength to the overall structure.⁷ Each of these layers serves a specific purpose within the whole, and without each one the structure would not properly function.

The prevalence of multilayered materials in nature has stimulated scientists to try and develop synthetic analogues. Man-made multilayered materials have primarily been synthesized through sequential deposition of individual layers, typically onto flat surfaces, but in some cases also around spherical core particles.⁸⁻¹⁴ (Prior work in this area is discussed in further detail in subsequent chapters.) For example, one could start with an anionic sphere (“template”) and deposit a layer of an oppositely charged (cationic) polymer around the sphere.^{15,16} Next, a layer of an anionic polymer could be deposited around the cationic layer. This process can be sequentially repeated to give a sphere with multiple thin

layers of polymers around it. Later, the template may be selectively removed, thereby forming a multilayered capsule.^{15,16} While such layer-by-layer techniques have proven popular in the literature, they have many limitations. Firstly, each layer is necessarily very thin because it has to bind strongly to the layer below. Secondly, due to the necessity for interaction between adjacent layers, the selection of materials is limited (i.e. one cannot deposit adjacent layers of like-charged materials). Furthermore, each layer is interpenetrated with the layers above and below it, i.e., there no distinct separation between adjacent layers.

Other techniques to create true multilayer structures have recently emerged, and these include the use of microfluidics to create multiple emulsions (i.e., oil-in-water-in-oil).¹⁷⁻²² Subsequently, polymerizations can be conducted in each individual phase to generate multiple layers.¹⁹ Alternately, a technique has recently been reported to create multiple concentric layers of a single material around a core, leading to an onion-like structure.^{21,23,24} However, this technique is limited because all the layers are made from the same material. We conclude that current techniques are inadequate for use in fabricating synthetic mimics of natural multilayered structures. Thus, there is a need for a simple, versatile technique to synthesize multilayered structures. Ideally, this technique should offer independent control of the chemistry and contents of each layer as well as the number of layers and the layer dimensions (thickness etc.). For example, we would like to juxtapose different polymeric layers next to each other in a multilayered sphere.

1.2 Proposed Approach

In this dissertation, we describe the synthesis of multilayered materials, where each layer is a cross-linked polymer gel. For this synthesis, we have developed a technique that we call “inside-out” polymerization, i.e., each layer of polymer grows from the core and proceeds outward. We have synthesized multilayered structures in three kinds of geometries, and these are described in brief here.

1.2.1 Multilayered Spherical Capsules

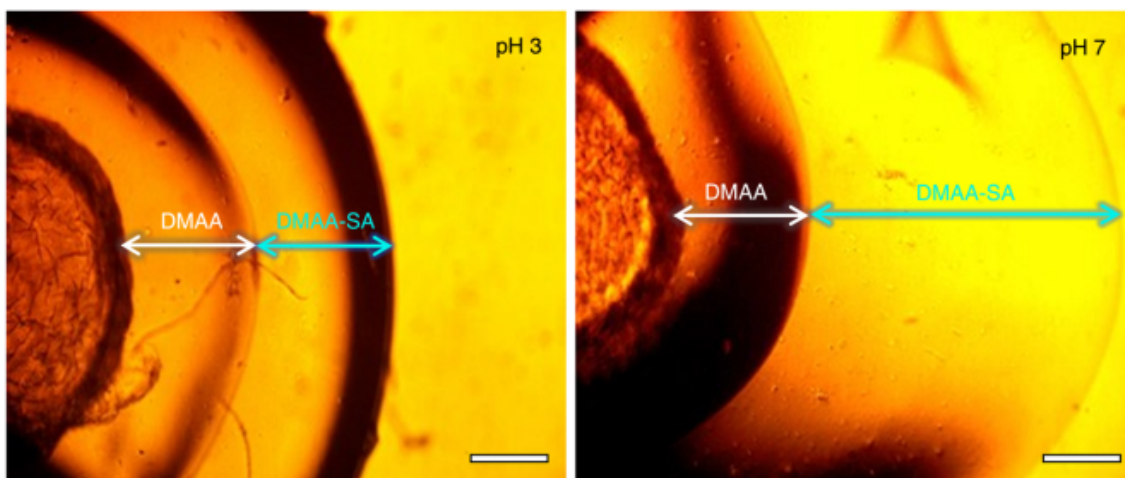


Figure 1.1. Micrographs of a stimuli-responsive multilayered capsule. There are two layers, each of which is a polymer gel. The outer layer is responsive to pH, and thereby its thickness increases dramatically as pH is changed from 3 to 7. The scale bars represent 500 μm .

In Chapter 3, we introduce our technique and show its applicability for the synthesis of multilayered spherical capsules. The key to our technique is that we begin with a core gel particle (“template”) and load it with an initiator used for free-radical polymerization. This particle is placed in a solution containing a monomer and crosslinker. The initiator diffuses outward and initiates the growth of a polymer layer around the template particle.

Next, this one-layer particle is reloaded with initiator and placed into a second (different) monomer solution, whereupon a second layer of polymer forms around the first. The process is then repeated further to create multilayered spheres with a desired composition for each layer. The number of layers and the thickness of each layer can be controlled. The core template may also be dissolved at the end to yield a hollow capsule. Figure 1.1 shows that we can incorporate stimuli-responsive materials into distinct layers. In this case, one of the two layers of the capsule swells significantly when the pH of the solution is changed.

1.2.2 Multilayered Tubes

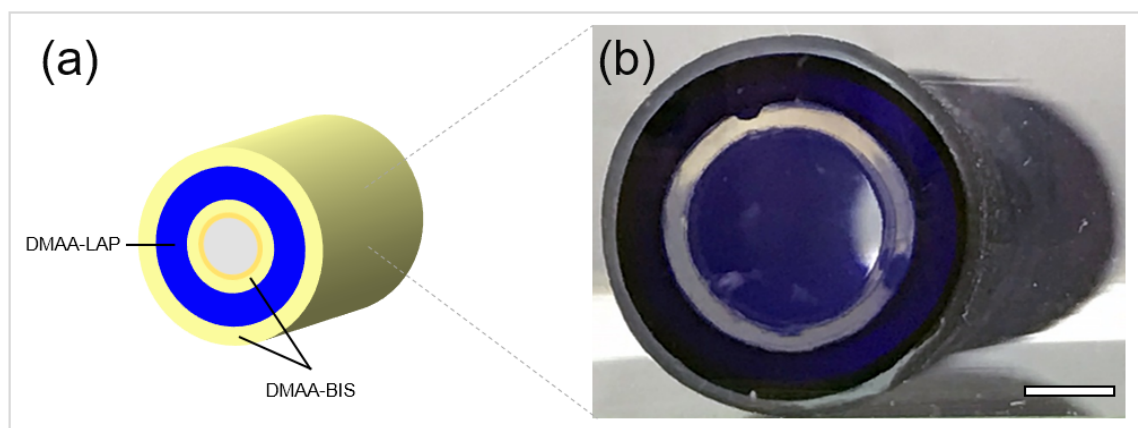


Figure 1.2. Schematic and photo of a multilayered polymer tube. The tube has three distinct layers, each of which is a polymer gel. The middle layer is stained with the dye methylene blue (MB). The scale bar is 2.0 mm.

In Chapter 4, we extend the technique described in Chapter 3 towards the synthesis of multilayer tubes. Here, a sacrificial template cylinder composed of agar is utilized. The agar cylinder is then loaded with initiator, and placed into a monomer solution. The initiator diffuses out of the template cylinder and creates a layer of polymer around the agar cylinder. The process is repeated with a different monomer solution to create the next layer.

Once the multiple layers are formed, the agar template is removed by heating to about 90°C, and the result is a hollow multilayered polymer tube, as shown in Figure 1.2. Stimuli-responsive polymers can be incorporated into the tube walls, and the resulting tubes show constriction and dilatation.

1.2.3 Hairy Surfaces

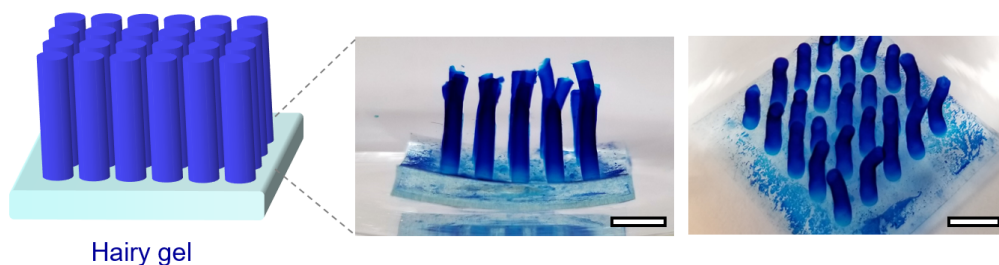


Figure 1.3. Schematic and photos of a hair-covered surface. The base and hairs are both made of polymer gels. Photos of the system are shown from the side and the top. The scale bars represent 5.0 mm.

Finally, in Chapter 5, we demonstrate the use of our “inside-out” polymerization technique to create gels with hair-like protrusions coming off the surface, as shown in Figure 1.3. For this synthesis, we again use an agar template with channels, each of which is filled with monomer solution. Subsequently, an initiator-loaded base gel is introduced over the template. The initiator diffuses from the base gel into the channels, growing hairs from the surface of the base gel. The final hair-covered surface resembles the walls of the GI tract, which contain hair-like protrusions called villi. We demonstrate that the hair-like protrusions increase the rate of adsorption of solutes from water, which is also the function of the villi in the GI tract. The hairs can be made from stimuli-responsive materials and thus be induced to respond to external stimuli.

1.3 Significance of This Work

We believe the significance of this work is two-fold. First, our work represents a significant advancement in the field of soft materials. We have advanced a technique that permits researchers to synthesize multilayered materials with unprecedented control over layer composition and thickness. We have further used this technique to synthesize a variety of new materials, including onion-like spherical particles, multilayered tubes, and hair-covered surfaces. Many of these materials could not have been synthesized with earlier techniques; they are demonstrated for the first time here. Importantly, we have been able to achieve the synthesis of several materials that have structural resemblance to those found in nature.

The additional significance and implications of our study lies in the unique properties of the above materials. For example, multilayered spheres could be useful for the controlled delivery of drugs, cosmetics, or agrochemicals. Multilayered tubes could prove to be valuable constructs for use in tissue engineering and biomaterials, e.g., for the engineering of artificial blood vessels. Hairy surfaces mimic the structure of intestinal walls and could also have biomedical utility due to the increased surface area provided by the hairs. We believe that additional applications in both biological and other contexts will arise as researchers further explore the properties of these materials.

Chapter 2

Background

2.1 Multilayered Materials in Nature

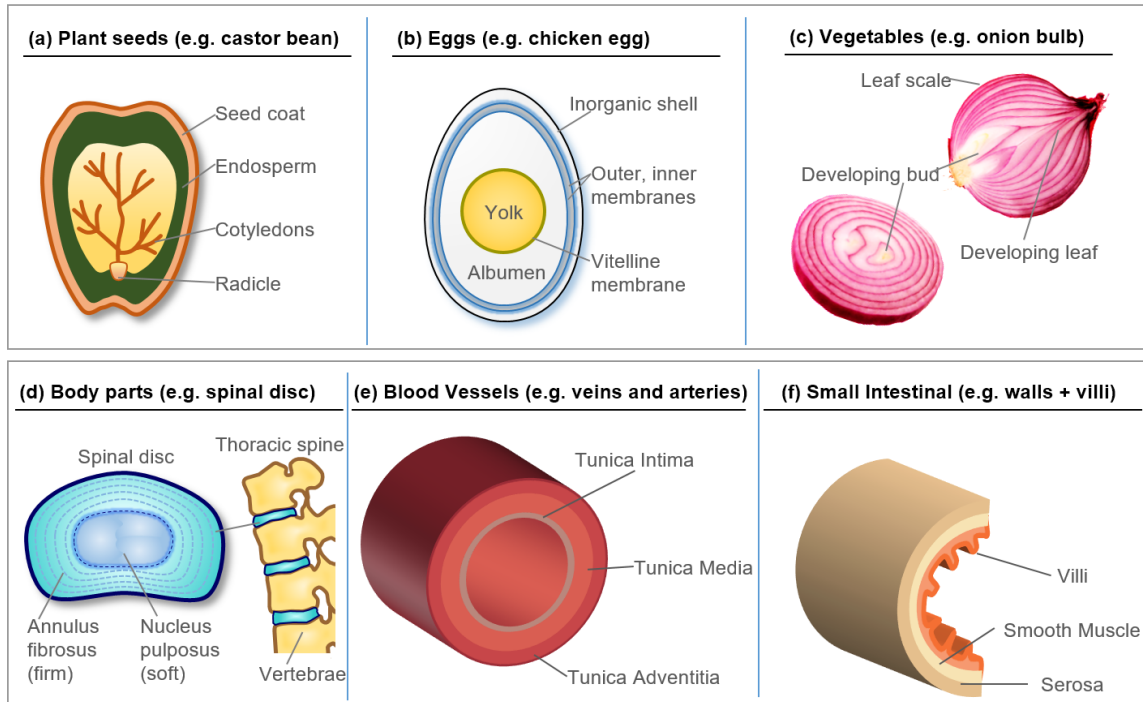


Figure 2.1. Examples of natural materials that have multiple layers. (a) Plant seeds.⁴ The cross-section of a castor bean seed is shown. (b) Eggs and embryos.¹ The structure of a chicken egg is illustrated. (c) Vegetables and fruits. The structure of an onion is shown in two views. (d) Tissues and body parts. The top-view of a spinal disc located between the vertebrae in the spine is shown.¹ (e) Blood vessels.² The structure of a vein is shown. (f) The wall of a small intestine is shown, highlighting the hair-like structures called villi.²⁵

A variety of materials found throughout the natural world are composed of multiple layers, as shown in Figure 2.1. These include near-spherical materials like plant seeds, eggs, and vegetables like the onion.^{1,4} In addition, body parts like the spinal discs between the vertebrae in the spine are also roughly spherical and multilayered.¹ In many such

structures, the layers are arranged in a concentric fashion. Each layer of these materials serves a distinct purpose, and all layers are critical to the functioning of the whole. For example, in the case of an egg, at its center is a fatty core called the yolk, which contains genetic information. Albumin, a nutrient-rich protein gel, surrounds this yolk and provides vital nutrients during maturation of the embryo. The outermost layer of the egg is a hard layer of calcium carbonate, which protects the inner portions of the egg from damage.⁷

Our body also has different kinds of hollow tubes used to ferry contents from one location to another.^{1,3} These tubes usually have multilayered walls^{2,26,27}, as shown in Figure 2.1e and 2.1f. Blood vessels, i.e., veins and arteries are composed of three layers, each with a distinct function. The inner-most layer, the *tunica intima*, is composed of endothelial cells, and it controls the transport of nutrients from blood to the surrounding tissues.² Next, the middle layer, the *tunica media*, is composed of smooth muscle tissue. This layer is elastic and flexible, and it contracts or expands to control the blood pressure. The outermost layer, the *tunica adventitia*, is composed of connective tissue and it provides structural support and protection against damage to the entire vessel. Thus, the individual layers work together to create a functional whole.

2.2 Hydrogel Formation by Free-Radical Polymerization

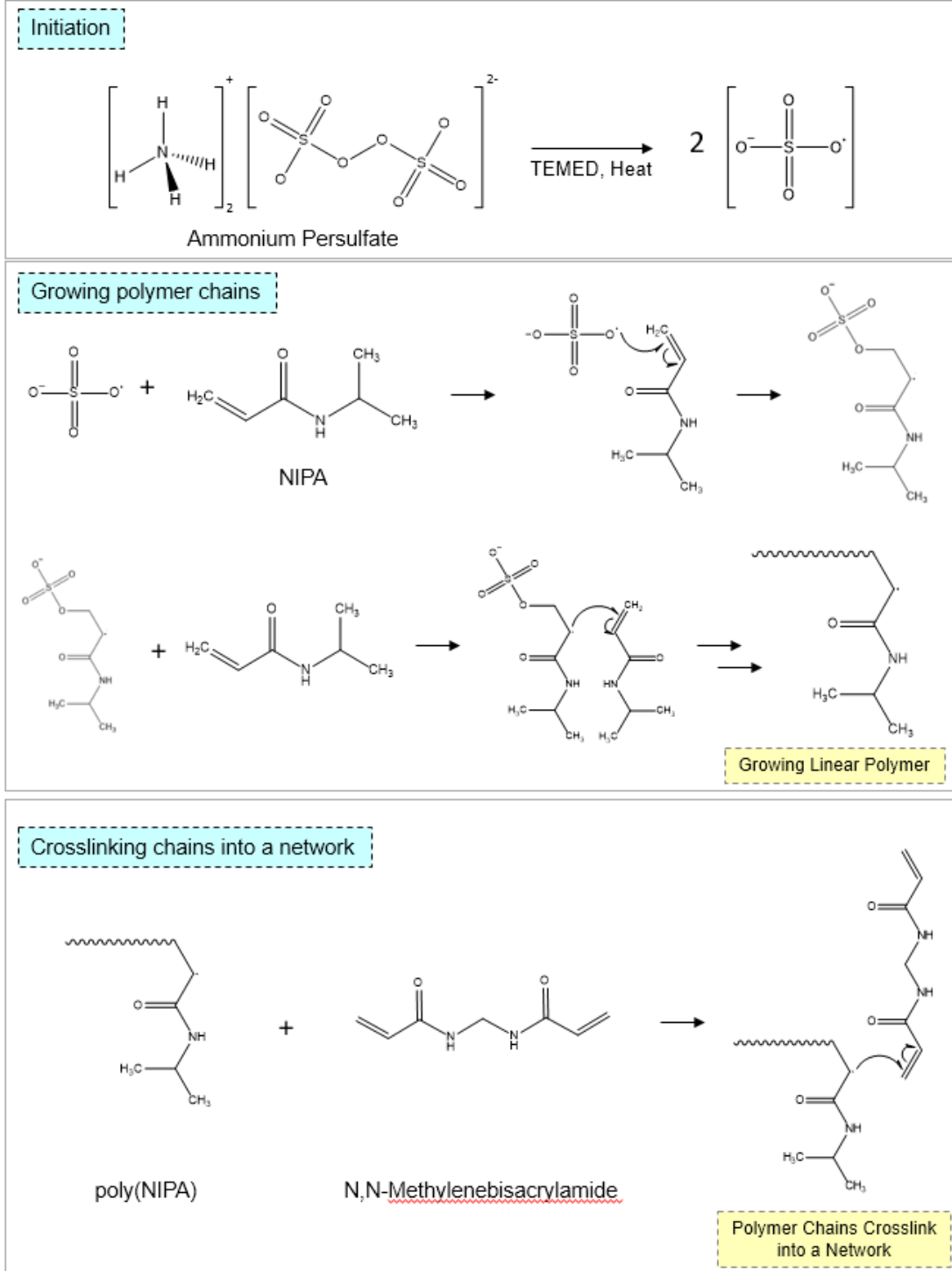


Figure 2.2. Reactions involved in the crosslinking of N-Isopropylacrylamide (NIPA). In initiation, the free-radical initiator is cleaved to create radicals. Next, the radicals attack vinyl groups on the monomer (NIPA) and the crosslinker (BIS). The result is a NIPA-BIS network.

Hydrogels are water-swollen networks of crosslinked polymer chains.^{28,29} The most common method to synthesize hydrogels with covalent crosslinks is through free-radical polymerization.^{28,29} This process involves the interaction between water-soluble monomers and crosslinkers in the presence of free-radical initiators and an additional chemical accelerant. An example of the reactions involved is shown in Figure 2.2. Here, the monomer, N-isopropylacrylamide (NIPA) is combined with the initiator, ammonium persulfate (APS) and the chemical accelerant N,N,N',N'-tetramethylethylenediamine (TEMED). First, the initiator molecule first gets cleaved by heat to generate free-radicals. Next, in the propagation step, the free-radicals interact with the vinyl groups (i.e. carbon-carbon double bonds) on the monomers and crosslinkers, and thus begin the process of growing chains. A monomer like NIPA, with just one vinyl group, can only form linear chains. However, monomers with two or more vinyl groups act as crosslinkers, meaning that one growing chain may now connect to more than one other growing chain, creating a network of polymers. The crosslinker in Figure 2.2 is N,N'-methylenebisacrylamide (BIS), which has two vinyl groups. Typically, the crosslinker is used at a low concentration of about 1% of the monomer on a molar basis. This low concentration allows the polymer chains to reach a considerable length before being crosslinked into a network.

2.3 Stimuli-Responsive Hydrogels

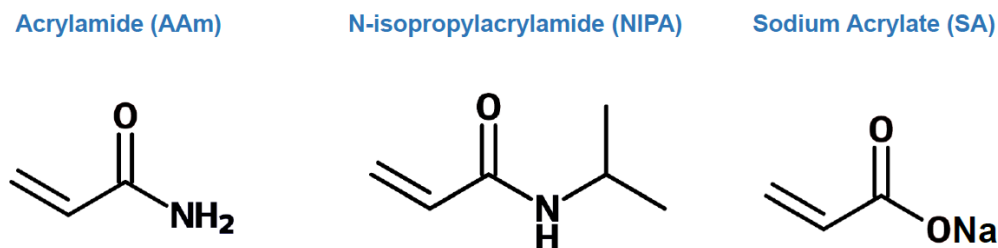


Figure 2.3. Examples of monomers used for synthesizing stimuli-responsive hydrogels. Gels of AAm shrink when the solvent composition is changed (e.g., in mixtures of water and acetone). Gels of NIPA shrink upon heating above a critical temperature. Gels of SA shrink when the pH of the solution is lowered below a critical value.

Hydrogels that respond to external stimuli such as temperature, pH, solvent and light have been reported in literature.²⁸⁻³¹ Gels synthesized from the monomers NIPA, sodium acrylate (SA) and acrylamide (AAM) (shown in Figure 2.3) respond to changes in temperature, pH and solvent composition, respectively.³²⁻³⁴ NIPA is a derivative of AAM with the addition of a hydrophobic isopropyl group, as shown in Figure 2.3. Below 32°C, the isopropyl groups in a NIPA gel are hydrated, and the gel is swollen. Above 32°C, which is the lower critical solution temperature (LCST) of NIPA, the isopropyl groups aggregate due to their hydrophobic nature.^{34,35} This causes water to be expelled from the hydrogel, which results in a sharp reduction in the gel volume, and the gel turning an opaque white color.^{35,36} The volume change with respect to temperature of a NIPA hydrogel in water is shown in Figure 2.4.³⁵ NIPA is one of the most studied thermoresponsive gels due to its LCST being close to human body temperature, i.e., 37°C.

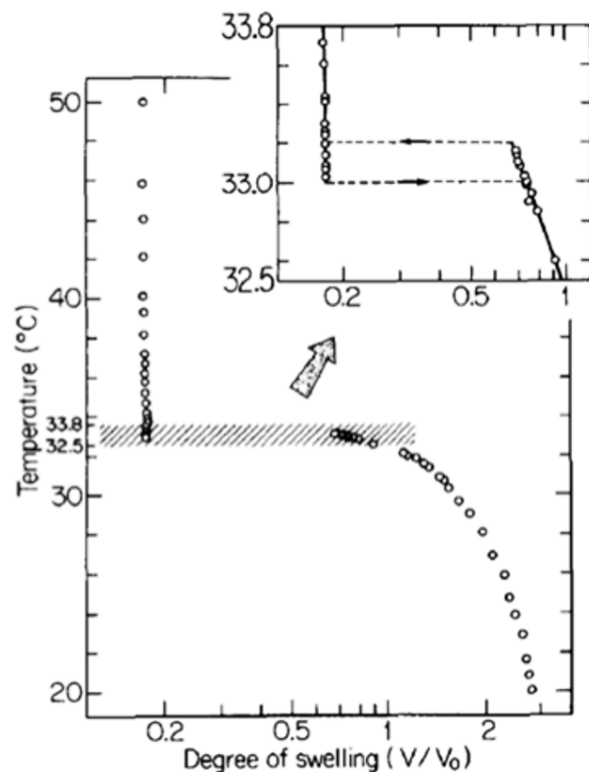


Figure 2.4. Volume change of NIPA gels upon heating. When a NIPA gel is heated above its LCST of 32°C, it shrinks abruptly, as shown by the above data. Adapted from Hirokawa et. Al.³⁵

Hydrogels that respond to pH are engineered through the selection of ionizable monomers, i.e. monomers that have positive or negative charges on the polymer chains.^{32,34} For example, a gel synthesized from SA will be neutral in charge at low pH (~ 3) because the carboxylic acid groups along the chains will be unionized, i.e., $-\text{COONa}$. However, when the pH is raised to about 7, these groups will get ionized and will become negatively charged.³² The charged polymer chains within the network will repel each other, causing the network to expand and swell. Thus, SA gels will exhibit a sharp increase in volume as a function of pH. Gels that respond to changes in solvent are based on polymer backbones that are soluble in one solvent, but not in others. For example, linear chains of poly(AAm) are soluble in water, but insoluble in acetone (a solvent that is miscible with water).²⁸

Correspondingly, gels of AAm that are swollen in water will shrink when the water is replaced with a water-acetone mixture where the acetone content is $> 50\%$.²⁸

2.4 Shape-Changing Materials in Nature

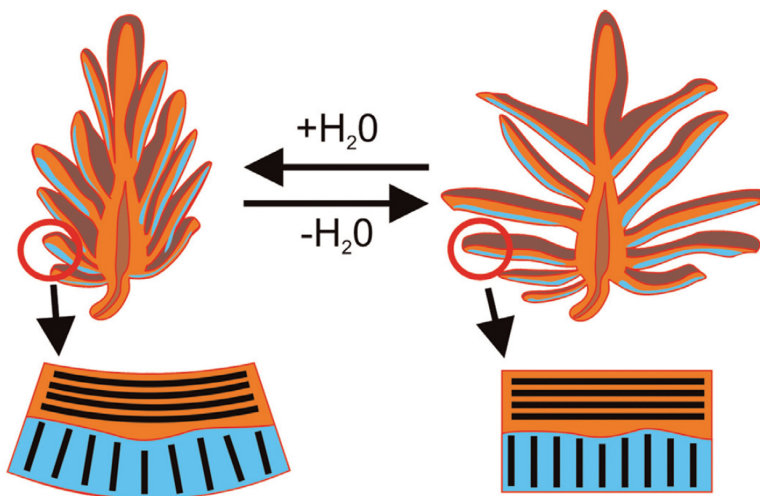


Figure 2.5. Opening of pine cone scales. Pine cone scales contain layers of tissue which swell to different extents. In a humid environment the outer layer of the scale is more swollen and the scales are closed. When the humidity is low, the outer layer shrinks and the scales open, releasing the seeds that are contained in the pine cone. Adapted from Dunlop et. Al.³⁷

In the previous section, we considered isotropic changes in the volume of gels in response to stimuli. That is, the gel swelled or shrunk, but its shape was unchanged (for example, a flat gel sheet remained flat even if it shrunk). Some types of gels can also change their shape in response to stimuli. The most common shape-changes are the folding or bending of flat sheets.^{38,39} Shape-changing materials are frequently observed in nature. This behavior commonly arises in materials that have multiple portions (layers) with different properties. The layers will respond differently to a given stimulus, e.g., swell to different extents, which drives the shape-change.^{38,39} For example, the scales of a pine cone open

and close depending on the ambient humidity (Figure 2.5).^{37,40} This protects the seeds, which are only dispersed in dry conditions. Each scale has two layers.^{37,40} The outer-most layer of the scale shrinks more than the inner layer when the air is dry, which leads to the opening of the scales to disperse seeds. Another example of a natural material that displays a shape change is the Venus flytrap, a carnivorous plant.⁴¹ The leaves of this plant create a pocket in which insects are trapped and digested. When the insect sits in the pocket, different regions of the leaf swell, which causes the leaves to change their curvature and inducing the trap to snap shut.

2.5 Shape-Changing Hydrogels

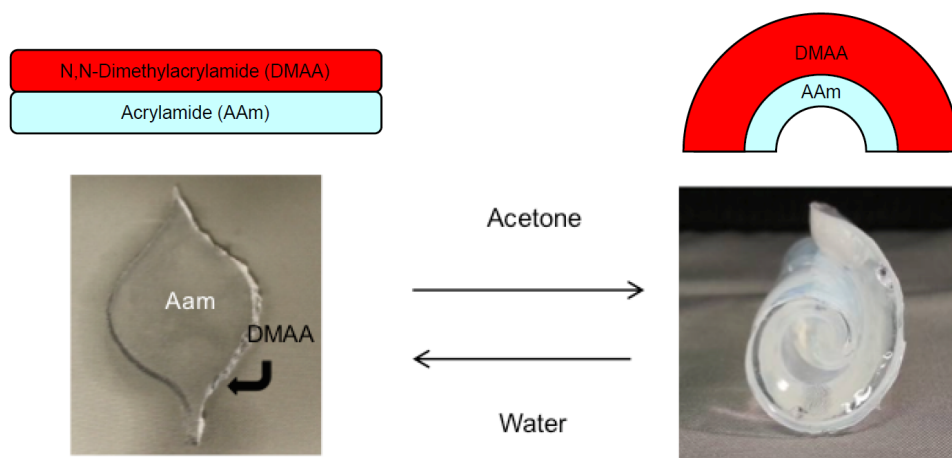


Figure 2.6. Folding of a bilayer hydrogel. The gel is a sandwich of two layers, one made from acrylamide (AAM) and the other from N,N-dimethylacrylamide (DMAA). The AAM layer shrinks in the presence of acetone, and the resulting swelling mismatch between the layers causes the whole gel to curl.⁴²

In 1995, the first example of a self-folding hydrogel was reported by Hu and co-workers.⁴³ Their system was a bilayer gel having two distinct layers, an example of which is shown in Figure 2.6. The bilayer in Figure 2.6 is composed of two gels sandwiched

together: a layer of N,N-dimethylacrylamide (DMAA) adjacent to a layer of AAm. Both swell to similar extents in water. However, when the solvent is replaced with > 50% acetone the AAm layer shrinks, while the DMAA layer remains swollen. The shrinking of the one layer induces an anisotropic strain within the bilayer structure, and to alleviate this strain the structure curls toward the shrinking layer. It should be noted that for this behavior to occur two conditions must be fulfilled: (1) the layers must be attached strongly at the interface, since a weak attachment will cause the layers to delaminate, and (2) the layers must be deformable, i.e., they must not have a very high elastic modulus. This type of folding behavior has been demonstrated in response to other stimuli as well, such as temperature and pH.^{38,39,43}

Chapter 3

Multilayered Spherical Capsules

3.1 Introduction

Nature is increasingly providing the inspiration for the design of new materials.⁴⁴⁻⁵⁰ Significant efforts have been devoted to mimicking the microstructure or nanostructure found in natural materials like opals, nacre, gecko feet, bird beaks, etc.⁴⁷⁻⁵⁰ However, the large-scale (i.e., over mm to cm) structure of natural materials can also be very interesting and provide a source of inspiration. Consider the examples of a plant seed, an egg, a spinal disc, and an onion (see Figure 2.1).^{1,3,4} A common theme to all these materials is that they have many different layers, roughly arranged in a concentric fashion. In the case of an egg (and embryos in general), the yolk and the genetic material form the inner core, and this is surrounded by the albumen, then multiple protein membranes, and finally the inorganic outer shell.¹ Many tissues and body parts are also multilayered.^{1,3} For instance, the spinal discs located between consecutive vertebrae in the spine have two layers: a soft core surrounded by a stiffer shell.³ One final example is that of an onion, which has a developing bud in the center, followed by many water-rich concentric layers, and a drier outer scale.⁴ A key point from these examples is that the concentric layers in a given material often have different composition, which in turn dictates their distinct function in the overall material. Can this design principle be adapted for the design of new materials? That is, can we create materials having multiple layers, each of a different composition and thereby different properties?

In addition to structure, another noteworthy aspect of natural materials deals with the manner of their growth. The growth of a specific structure and shape in nature is termed morphogenesis.^{51,52} To form a multilayered structure, such as an egg, it is evident that the core must form first, followed by the next several layers, and finally the outer shell. Moreover, natural growth invariably occurs from the inside-out.⁵¹ That is, not only does the core form first, but it can dictate the subsequent growth, which occurs in a direction radiating outward from the center. For instance, consider how a seed (or an egg) develops into a full-fledged organism.⁴ The growth begins at the surface of the seed and proceeds radially outward, utilizing nutrients from the external medium. Importantly, the seed (core) controls the growth rate and extent. This strategy is fundamentally different from common processes used in materials synthesis, such as nucleation-and-growth, self-assembly, or additive manufacturing.^{50,53} In nucleation-and-growth, for example, nuclei can grow outward to form macroscopic crystals, but the rate and form of growth is controlled by the availability of external precursor, not by the core nucleus.^{53,54} In additive manufacturing (3-D printing), macroscopic objects can be formed by adding one layer of material at a time, but this is basically a deposition scheme controlled from the outside; thus the core of the object does not dictate the growth.⁵⁵ To our knowledge, true inside-out strategies have rarely been exploited in materials design, especially in the context of soft materials.

Here, we describe the synthesis of multilayered polymer capsules, for which we have developed an inside-out strategy. Polymer capsules are structures in which a polymeric shell surrounds a liquid core.^{56,57} Such capsules are used to store and release solutes, and they find a variety of applications ranging from cosmetics to drug-

delivery.^{30,31,56} Research in this area has focused on stimuli-responsive capsules, where the release of solutes can be modulated by an external trigger, such as temperature, pH, or light.^{30,31} Recently, capsules have also been synthesized with many concentric, but identical, layers.^{17,19,21,23,24,58-61} However, to our knowledge, there have been no reports in which diverse polymeric layers (shells) are integrated together in a capsule. This was our focus, and we demonstrate that a strategy involving successive free-radical polymerizations around an initial gel core can lead to multiple layers with very different composition and properties. The key in our strategy is that the initiator for the polymerization is present only in the core, and therefore layer growth is controlled by the diffusion of initiator from this core (hence the term ‘inside-out’ for this strategy). Significantly, both the thickness and composition of each layer can be independently tuned. We particularly highlight the interesting cases where one (or some) of the polymeric layers are responsive to a stimulus, viz. pH or temperature. Solute release from such responsive capsules is shown to follow step-like (pulsatile) profiles, which suggests their potential utility in delivery applications.⁶²⁻⁶⁴ More generally, our strategy can be used to create new multifunctional materials that mimic the remarkable structures found in nature.

3.2 Experimental

Materials. The monomers N,N-dimethylacrylamide (DMAA) and N-isopropylacrylamide (NIPA), and the accelerant, N,N,N',N'-tetramethylethylenediamine (TEMED) were from TCI America. All other chemicals were from Sigma-Aldrich, including the cross-linker N,N'-methylenebis(acrylamide) (BIS) and the monomer sodium acrylate (SA). Three biopolymers were used: alginate, i.e., medium viscosity alginic acid, sodium salt

from brown algae, chitosan (medium molecular weight), and xanthan gum (from *Xanthomonas campestris*). Other chemicals included calcium chloride dihydrate (CaCl_2) salt, ammonium persulfate (APS) initiator, glutaraldehyde (GA), glacial acetic acid, and Brilliant Yellow (BY) dye. Deionized (DI) water was used in all the experiments.

Synthesis of Gel Cores. To form the alginate gel cores, a 2 wt% alginate solution was first made in DI water. This was then added drop-wise using a transfer pipette or syringe into a solution of 0.5 M CaCl_2 under mild stirring. After incubation for 30 min, Ca^{2+} -cross-linked alginate gels were obtained. To form the chitosan gel cores, a 2 wt% chitosan solution was made in 0.2-M acetic acid. This was then added drop-wise (as above) to a solution of 2 wt% GA. After incubation for 24 h, chitosan gels crosslinked by GA were obtained. To form gel cores with diameters <1 mm, a pulsed-gas micro-capillary device was used.^{65,66} The biopolymer solution of interest was sent through a capillary of 80- μm inner diameter at a flow rate of 3 $\mu\text{L}/\text{min}$. Pulses of nitrogen gas (4 Hz frequency at 9 psi) were applied to the tip of the capillary, leading to the formation of microscale droplets, which were then cross-linked as above.

Synthesis of Multilayer Capsules. Multilayer capsules were synthesized by the procedure described below (see Figure 3.1). First, the gel core prepared in the previous step was placed in an aqueous solution of 15 mg/ml APS initiator for 10 or more minutes. The gel was then removed from the solution and blotted with a Kimwipe to remove excess solution. The APS-soaked gel was then transferred into the desired monomer solution. Typically, the monomer (e.g., DMAA or NIPA) was at a concentration of 1 M. A cross-linker

(typically BIS) was added at a concentration of 2.2 mol% with respect to the monomer. In addition, 15 mg/ml of the accelerant TEMED and 0.5–0.75 wt% of xanthan gum were added to the solution. The function of the TEMED was to accelerate the polymerization, thereby allowing it to be conducted at room temperature. The xanthan gum was used to increase the viscosity of the solution, which was important to keep the capsule suspended during polymerization. Thereafter, free-radical polymerization, initiated by persulfate ions from the APS, was carried out at room temperature. The time for polymerization was dictated by the time needed for the layer thickness to saturate, which was typically around 10–20 min (see Figure 3.4). In many cases, polymerization was continued for a period of 24 h to allow ample time to reach a steady state. Once the first layer was formed, the polymer capsule was washed with water and stored in DI water. To form the next layer, the above procedure was repeated. In the case of the pH-responsive multilayer capsules shown in Figure 3.7, a mixture of DMAA (nonionic) and SA (anionic) in a molar ratio of 9:1 DMAA:SA was used for the pH-responsive layer, with the total monomer concentration being 1 M as above.

Optical Microscopy. Bright field images of capsules were captured with a Zeiss Axiovert 135 TV microscope. Images were taken using either a $\times 2.5$ or a $\times 10$ objective. In some cases, the microscopy was performed with slight under-focus, which helped to clearly define the outlines of the layers and/or the overall capsule.

Scanning Electron Microscopy (SEM). A two-layer capsule with an inner layer of NIPA and an outer layer of DMAA was frozen rapidly in a -80 °C freezer, and subsequently

lyophilized. Next, the capsule was fractured with a razor and affixed to a viewing platform. The capsule was then sputter coated with gold. A Hitachi SU-70 Schottky field emission SEM was used to obtain images of the sample.

Compression Tests. An AR 2000 stress-controlled rheometer (TA Instruments) was used to conduct the compression tests at 25 °C. From the rheometer software, the squeeze-test mode was chosen, and the tests were done using steel parallel plates (40 or 20 mm diameter). The spherical sample of interest (gel or capsule) was placed at the center of the plates. Compression was done at a rate of 10% strain per minute, which was determined based on initial sample diameter. The plates were coated with a thin layer of mineral oil to avoid excessive adhesion to the samples during compression. The normal-stress transducer was used to collect the normal force during compression, and this was converted to stress based on the initial surface area of the capsule.

Controlled Release Experiments. For the dye release studies (Figures 3.8 and 3.9), capsules were loaded with BY dye by soaking in a 500 μM dye solution for 24 h. Capsules were then added to 100-ml Erlenmeyer flasks filled with DI water, and the flasks were placed in a temperature-controlled water bath (Julabo). To monitor the dye concentration, a 1.5-ml sample was taken every 10 min from the supernatant surrounding the capsule, and this was analyzed using a Cary 50 UV-Vis spectrophotometer. After analysis, the sample was returned to the flask containing the capsule.

3.3 Results and Discussion

3.3.1 Synthesis of Multilayer Capsules

We present a step-wise technique for generating polymeric multilayer capsules, as shown schematically in Figure 3.1. First, a gelled core is created by the physical cross-linking of a biopolymer. We have used many biopolymer gels for this purpose, including those based on chitosan, gelatin, and agarose.⁶⁷ But for most of the studies described in this paper, the cores are made from the biopolymer, alginate.^{68,69} To create the gelled cores, a solution of 2 wt% sodium alginate is added drop-wise to a solution of 0.5 M calcium chloride (CaCl_2) using a syringe (Figure 3.1a). The alginate droplets become cross-linked by the Ca^{2+} ions into gelled beads, with the bead diameter typically being 0.5–5 mm. The inset in Figure 3.1a shows the structure of this alginate gel; note that the Ca^{2+} ions form junctions between alginate chains.⁶⁹ The alginate bead is then loaded with ammonium persulfate (APS), which is a water-soluble initiator for free-radical polymerization. For this, the bead is incubated in a solution of 15 mg/ml initiator for at least 10 min (Figure 3.1b). The incubation time was set at 10 min based on a calculation from Fick's 2nd law for diffusion, which revealed that this time was ample for the center of a 4-mm bead to equilibrate to roughly the bulk concentration.³⁶

Next, the initiator-loaded gel is transferred to a solution containing a monomer (labeled monomer 1 in Figure 3.1c) such as N-isopropyl acrylamide (NIPA) at a 1 M concentration, a crosslinker like N,N'-methylenebis(acrylamide) (BIS) at 2.2 mol% with respect to the monomer, and accelerant. Free-radical polymerization is then conducted at room temperature (Figure 3.1d). Polymerization begins as the persulfate ions diffuse from

the core into the surrounding solution and react with the monomers. A layer (shell) of cross-linked polymer thus forms around the core. As shown in the inset to Figure 3.1c, the polymer layer grows in a radial direction outward from the core because of the diffusion of initiator from the core. That is, the initiator concentration is highest at the surface of the core and decreases in a radial direction towards the bulk solution.³⁶ We term this growth an inside-out process. Once a layer of sufficient thickness has formed (typically this takes ~10 min), we can remove the structure, wash it with water and store it in water or buffer. At this point, we have a gelled core surrounded by a layer of polymer 1 (NIPA), which can be clearly seen in the inset image.

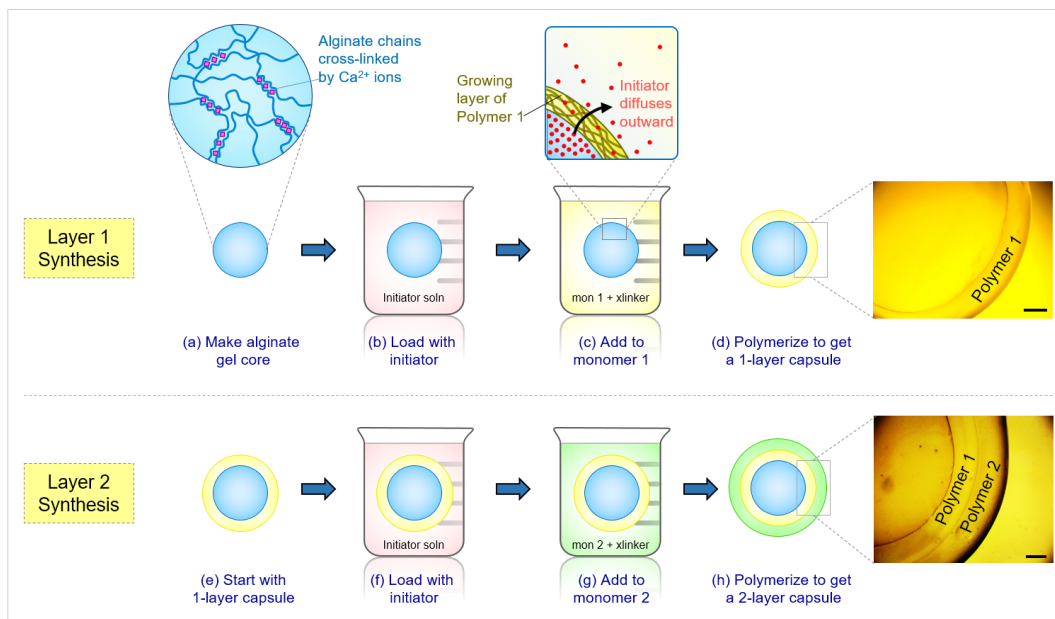


Figure 3.1. Synthesis of multilayer capsules. An alginate gel core is first made (a) and this is loaded with free-radical initiator (b). The gel is then introduced into a solution of monomer 1 (along with cross-linker and accelerant) (c). Upon polymerization, a layer of polymer 1 is formed around the gel core (d). The inset in c shows that this layer is formed by diffusion of initiator outward from the core into the monomer solution. This process is then repeated with the onelayer capsule (e), which is loaded with initiator (f) and then contacted with monomer 2 (g). Upon polymerization, a second layer of polymer 2 is formed (h). The process can be further repeated to introduce additional layers. Scale bars are 500 μm .

The above process is repeated to form a layer of a second polymer, as shown in Figure 3.1. For this, we reload the above structure with APS initiator and place it in a solution of monomer 2, i.e., N,N'-dimethylacrylamide (DMAA), along with the same BIS crosslinker and accelerant. A second polymerization step then yields a second concentric layer of polymer 2 (Figure 3.1h). The second layer grows from the surface of the first layer, again consistent with inside-out growth. We now have a spherical capsule with an alginate core (Alg), then a surrounding layer of polymer 1 (NIPA), and finally an outer layer of polymer 2 (DMAA), as shown in the image in Figure 3.1h. This capsule is designated as Alg–NIPA–DMAA, which signifies the order of layers outward from the core. The same process can be further repeated to give additional concentric layers of different polymers. Also, the alginate core in the capsule can be ungelled to form a liquid core. This can be done by immersing the capsule in a solution of a calcium chelator like sodium citrate or ethylene diamine tetracetic acid (EDTA).⁶⁸ For most of the experiments described below, however, we have left the core intact. For other gelled-cores made from gelatin or agarose, the biopolymer gels are thermoresponsive and hence the core gels can be liquefied by moderate heat.⁶⁷

Figure 3.2a shows the alginate core next to a single-layer capsule and a two-layer capsule generated by sequential polymerization. The alginate core has a diameter of 4 mm. The first surrounding layer is a network of NIPA (~550 μm thick) and the second layer is a network of DMAA (~750 μm thick). The optical microscope image (Figure 3.2b) clearly shows the presence of two distinct layers that are not interpenetrated. Scanning electron microscopy (SEM) images of such Alg–NIPA–DMAA capsules after freeze-drying

(Figure 3.2c) further confirm the discrete nature of the two layers. Each layer appears porous in these images, which is consistent with their being polymer networks. The pores appear to be oriented along slightly different directions, allowing the layers to be distinguished. Note that the SEM images are of two capsules with identical layer composition but synthesized separately. The similar microstructure in both cases shows that these multilayer capsules can be reproducibly synthesized. Overall, the presence of multiple concentric layers in our capsules is reminiscent of natural multilayered materials like the onion.

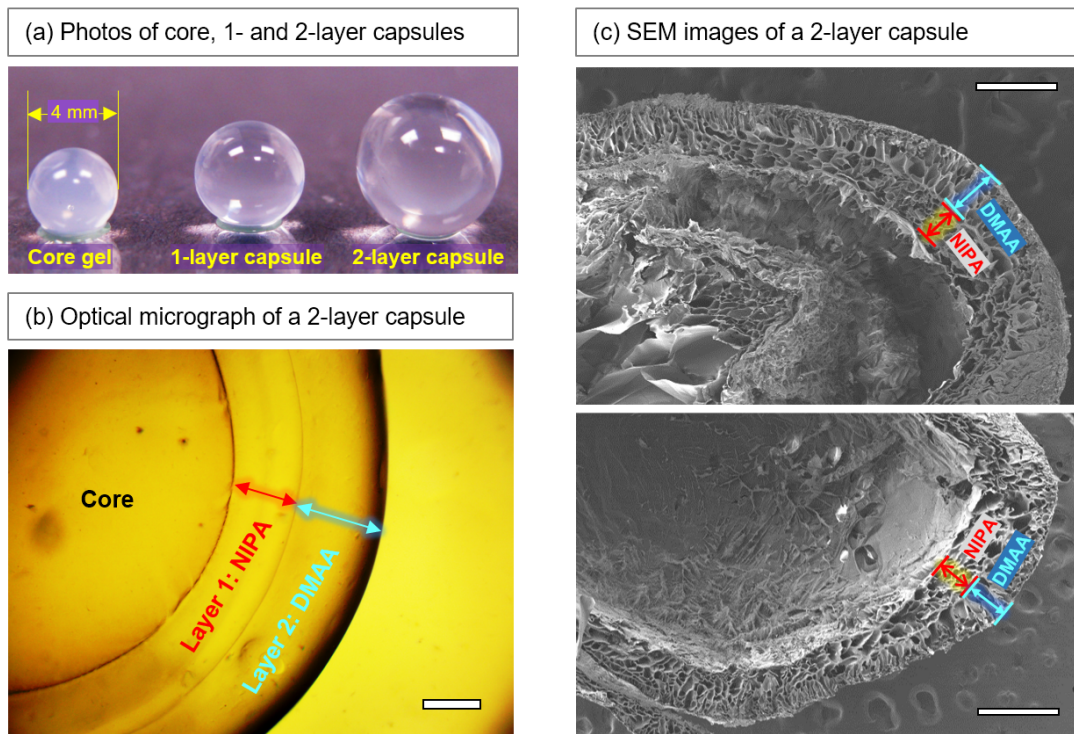


Figure 3.2. Images of multilayer capsules at different length scales. (a) Photos of the alginate gel core and the corresponding one-layer and two-layer capsules. (b) Optical micrograph of a capsule with an alginate (Alg) core, an inner layer of N-isopropylacrylamide (NIPA) and an outer layer of N,N'-dimethylacrylamide (DMAA). The overall structure is denoted as Alg–NIPA–DMAA. The scale bar is 500 μm. (c) Scanning electron micrographs of two Alg–NIPA–DMAA capsules (after freeze-drying). The boundaries between the layers can be distinctly seen in both cases. Scale bars in the images are 500 μm.

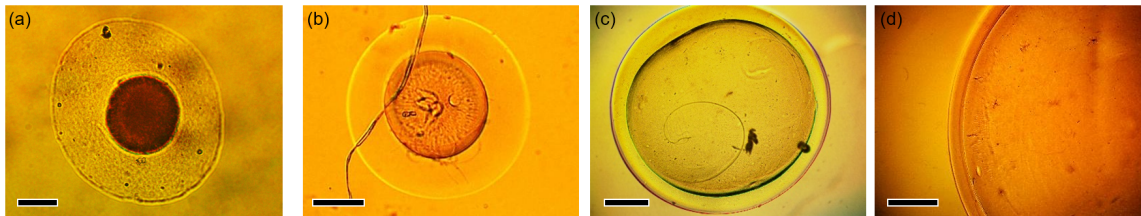


Figure 3.3. Single-layer capsules over a range of length scales. Optical micrographs are shown of capsules with a crosslinked polymeric shell surrounding a biopolymer gel core. In (a), the core (chitosan/GA) has a diameter of 185 μm , and the shell (SA) has a similar thickness (scale bar is 100 μm). In (b), the core (chitosan/GA) has a diameter of 400 μm and the shell (DMAA) has a thickness of ~ 150 μm (scale bar is 200 μm). In (c), the core (alginate) has a diameter of 2.8 mm and the shell (DMAA) is 250 μm thick (scale bar is 700 μm). In (d), the core (alginate) has a diameter of 6.0 mm and the shell (DMAA) is 230 μm thick (scale bar is 800 μm).

The above procedure can be used to synthesize multilayer capsules over a range of sizes. We have varied the diameter of biopolymer cores over approximately two orders of magnitude: from ~ 10 mm to about 200 μm . Optical images of single-layer capsules over this size range are shown in Figure 3.3. Note that, to create biopolymer gel cores with diameters < 1 mm, we resorted to a microfluidic technique developed in our laboratory in which pulses of compressed gas are used to shear off biopolymer-bearing aqueous droplets from the tip of a capillary.^{65,66} Once cores of a given size are created, the rest of the procedure is the same as shown in Figure 3.1, i.e., the cores are loaded with APS initiator, then placed in a solution of monomer, cross-linker and accelerant. The images in Figure 3.3 show that a polymer shell is formed around the core in all cases.

3.3.2 Kinetics of Layer Growth

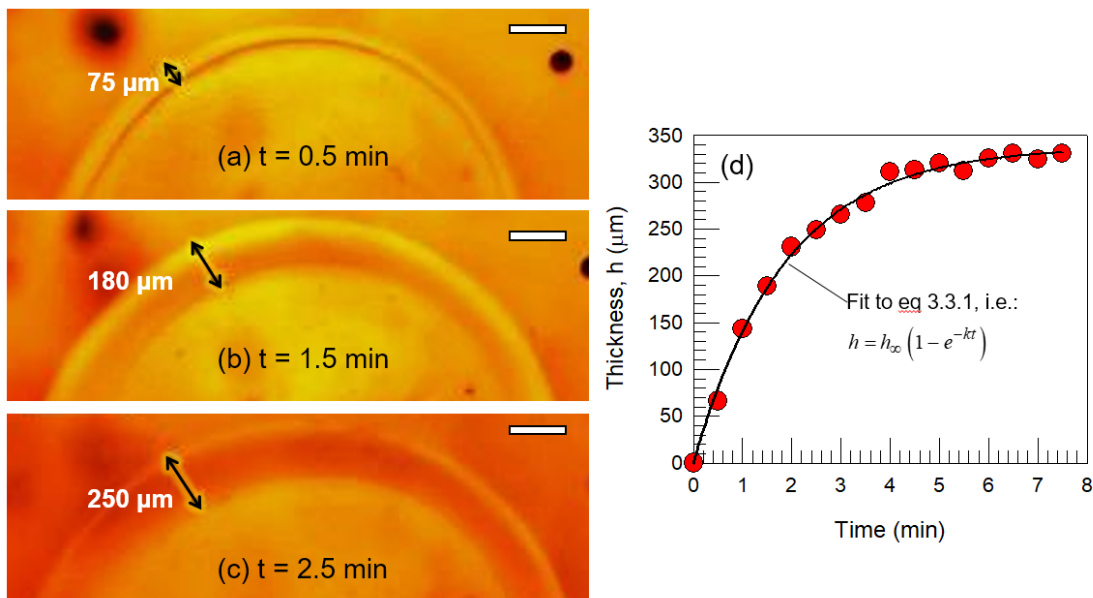


Figure 3.4. Kinetics of layer growth, visualized directly by optical microscopy. At time $t = 0$, an alginate gel core of 2 mm diameter, loaded with 15 mg/ml ammonium persulfate (APS) initiator, is placed in a solution of 1 M DMAA monomer (together with cross-linker and accelerant). Still images at various time points are shown in a, b, and c, and these reveal the growth of the polymer layer around the core. Scale bars in the images are $200 \mu\text{m}$. In d, a plot of the layer thickness h vs. t is shown, and the solid curve through the data is a fit to eq 3.1.

As mentioned, each polymer layer in the capsule grows from the inside out, and we now show that this growth can be visualized in real time. For this, we prepared an alginate core of 2-mm diameter and loaded it with 15 mg/ml of APS initiator. At time $t = 0$, we placed this sphere in a solution of 1 M DMAA with cross-linker and accelerant. The sphere was then observed by optical microscopy (Figure 3.4). Based on the images, a layer of polymer can be discerned around the core within 30 s (Figure 3.4a), and as time progresses, this layer grows outward. The layer thickness h at each time point can be extracted from the images, and this quantity is plotted vs. time t in Figure 3.4d. Note that within about 8 min, the growth of the layer is complete and it saturates at a value around $338 \mu\text{m}$. Even

after a period of 24 h, the layer thickness remains at this steady-state value h_{∞} . We can then fit the $h(t)$ data to the following functional form³⁶:

$$h = h_{\infty} \left(1 - e^{-kt}\right) \quad (3.1)$$

The only adjustable parameter in the above equation is the effective rate constant k . Eq 3.1 gives a very good fit to the data in Figure 3.4d with $k = 0.54$. Note that k accounts for the combination of two steps occurring in series: mass transfer (i.e., diffusion) of initiator from the core into the external solution, followed by the kinetics of the polymerization reaction.³⁶

Based on the above results, the layer thickness h around a given core can be fixed by arresting the polymerization at a particular time, i.e., by replacing the monomer-laden solution with water at this time. Alternately, the layer thickness at steady-state h_{∞} can be varied systematically by modulating the reaction kinetics. The parameters that affect the kinetics include: the concentration of initiator in the core; the concentrations of monomer and crosslinker in the external solution; the reaction temperature; and the viscosity of the external solution.⁷⁰ A detailed study on these parameters is beyond the scope of this initial study. But as an example, we have varied the concentration of APS initiator. Using an identical setup to the one above, we reduced the APS in the core from 15 mg/ml to 7.5 and 3.75 mg/ml. All other conditions were kept the same and the polymerization was conducted for 24 h in each case to allow the layer-thickness to reach steady-state. We found that reducing the initiator decreases the layer thickness: while h_{∞} was 338 μm for 15 mg/ml of APS in Figure 3.4d, reducing the APS by a factor of 4 to 3.75 mg/ml resulted in a drop in h_{∞} to $\sim 90 \mu\text{m}$.

3.3.3 Mechanical Properties

Our multilayered capsules tend to have very different mechanical properties compared to their gel cores. The properties depend on the composition of each layer and on the number of layers. While a detailed study on these aspects is beyond the scope of this paper, we highlight a couple of aspects here. Most importantly, the addition of even a thin shell to a core can radically alter its mechanical response. This is best demonstrated in tests under compression, as shown in Figure 3.5. Here, we contrast an Alg core and an Alg–DMAA capsule with compositions identical to those described above. The Alg core is a gel of diameter 4.6 mm. The Alg–DMAA capsule is created with an identical Alg core and adding a DMAA shell of thickness 200 μm (i.e., 0.2 mm) to it; the shell is thus 1/20th the diameter of the core, i.e., it is very thin in comparison.

First, consider the Alg gel core (Photos a1 to a3 in Figure 3.5). When this is compressed, the initial sphere is squished into an ellipsoidal (disc or pancake) shape. If the compressive strain is 50% or more, then the sphere remains squished as a disc (Photo a3). In other words, the gel suffers a plastic (irreversible) deformation when compressed. Indeed, such a response is familiar to researchers who work with gels of biopolymers like alginate, and it is known that these gels have limited mechanical resilience.^{69,71} Next, consider the response of the Alg–DMAA capsule (Photos b1 to b3 in Figure 3.5). In this case, even when the initial sphere is compressed by 60%, it still recovers to its initial size after the compression. That is, the deformation is reversible, and the response is elastic. The above behavior can be easily confirmed by taking these objects and squeezing them between one's fingers. We consistently find that the Alg cores are squishy and plastic while

Alg–DMAA capsules respond as elastic objects. In short, adding a thin shell to the gel core makes it much more resilient and elastic.

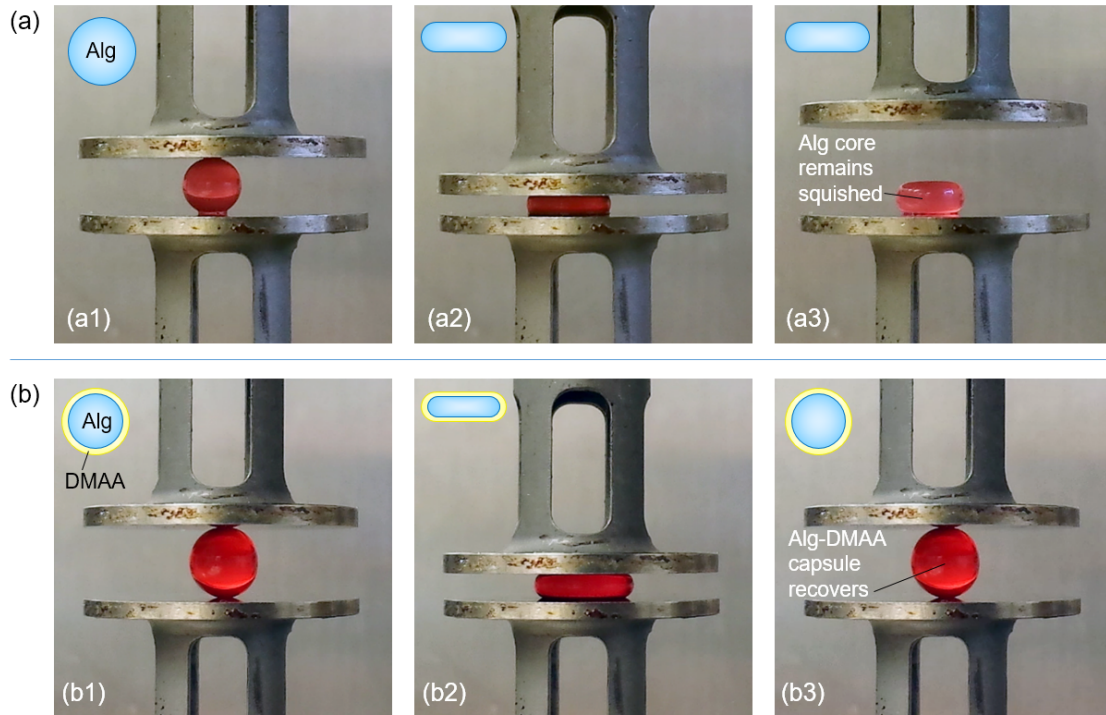


Figure 3.5. Contrasting mechanical properties of a core gel particle versus a single-layer capsule. Photos are shown of an Alg gel particle (a) and an Alg–DMAA capsule (b) being compressed between parallel plates. Both have the same core diameter of 4.6 mm, with the DMAA shell being 200 μm thick. Photos a1 to a3: when the Alg gel is compressed by 50%, it remains squished and does not recover when the compression is removed (plastic response). Photos b1 to b3: when the Alg–DMAA capsule is compressed by 60%, it recovers as soon as the compression is removed (elastic response). Thus, the addition of the thin DMAA shell ($1/20^{\text{th}}$ the thickness of the core) dramatically alters the mechanical properties.

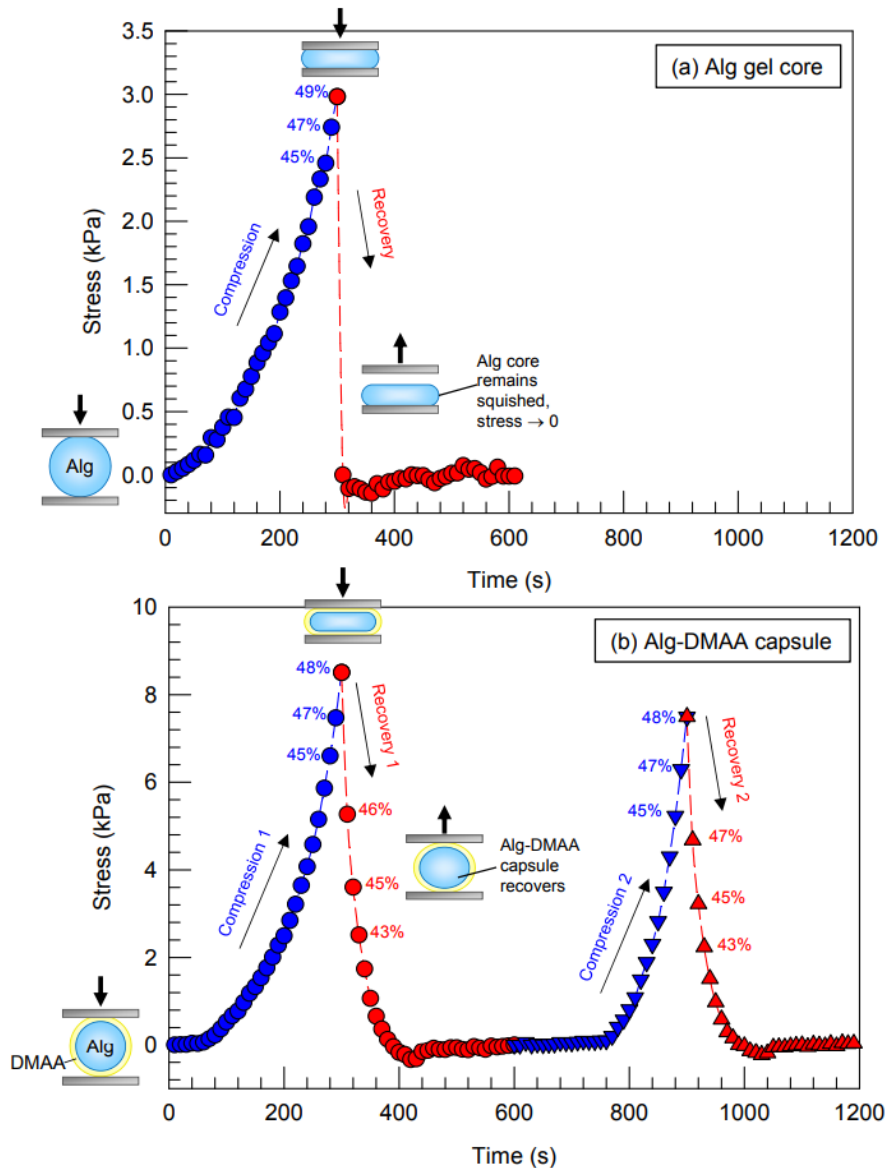


Figure 3.6. Compression tests on an Alg gel core and an Alg-DMAA capsule. The sample is placed between parallel plates at time zero. During the compression cycle the top plate is brought down, while during the recovery cycle the top plate is lifted up (both at 10% strain per minute). The measured compressive stress is plotted against time in the two plots, with the compressive strain indicated for selected points. (a) When the Alg gel core is compressed up to ~ 50% strain, it is irreversibly squished into a disc shape (plastic behavior). Thus, the sample does not recover when the plate is lifted up. (b) When the Alg-DMAA capsule is compressed up to ~ 50% strain, it responds elastically, and recovers to its initial size when the plate is lifted up during the recovery cycle. A second compression-recovery cycle is then applied on the capsule, and the data for this cycle closely track those from the first cycle.

We have attempted to quantify the differences seen in Figure 3.5. For this, we placed the above structures between the plates of a rheometer and compressed them at 10% strain/min.^{72,73} The compressive stress was measured and is plotted in Figure 3.6a for the Alg core and in Figure 3.6b for the Alg–DMAA capsule. These data confirm the visual observations. That is, during the first loading cycle, the Alg core gets irreversibly compressed. When the stress is released, the top plate detaches from the sample, and the stress therefore plummets to zero. The Alg–DMAA capsule, on the other hand, can be subjected to multiple compression-recovery cycles, which reflects its elastic response (akin to a cross-linked rubber). Note that the non-linearity of the response makes it difficult to extract an elastic modulus from the initial portion of the data. We briefly mention two other points of interest here. First, the failure mode of the capsule is also distinct from that of the core. That is, when compressed beyond a critical strain, the Alg core ruptures into many pieces⁷⁴, whereas the Alg–DMAA capsule suffers a break in its shell, with the core then ejecting out as a distinct entity. Secondly, the elastic nature of the capsule is also reflected in its ability to bounce off a hard surface. That is, the Alg–DMAA capsule bounces to a greater height compared to the Alg core, i.e., its coefficient of restitution is much higher.

3.3.4 Stimuli-Responsive Layers

A key feature of our synthesis scheme is that it allows integration of different polymeric layers into the same capsule. The interesting combinations are when one (or more) of the layers are responsive to external stimuli while others are not. We present two examples to illustrate these capabilities. First, we consider pH as a stimulus. It is well-known that ionic polymer gels exhibit a different response to pH compared to nonionic

polymer gels^{29,33,34}. For example, an anionic gel based on a monomer such as sodium acrylate (SA) will be swollen at high pH when all its carboxylate groups are ionized and shrunken at low pH when the same groups lose their charge.^{32,75,76} Nonionic gels, on the other hand, will exhibit the same volume at low and high pH. These differences are highlighted by a two-layer capsule in Figure 3.7a where the inner layer is nonionic while the outer layer is anionic. To make this capsule, we first created a pH-insensitive core of chitosan (an amine-rich polysaccharide) cross-linked with glutaraldehyde (GA).^{65,77} The core was made as before by adding the chitosan solution drop-wise into a solution of the GA; note that GA forms covalent bonds between the amines on chitosan.⁶⁷ We then polymerized a layer of nonionic DMAA around this core by the procedure described earlier (Figure 3.1). Next, we polymerized an anionic layer around the first layer. For this, the capsule from the previous step was loaded with initiator and placed in a solution containing DMAA and SA (at a molar ratio 9:1) as well as crosslinker (BIS) and accelerant. Figure 3.7a shows an image of the the two-layer capsule in a pH 3 solution. In this case, the two layers have about the same thickness, i.e., ~900 μm . This is because the carboxylate groups of SA are not ionized under acidic conditions. Next, Figure 3.7a shows the same capsule in a pH 7 solution. While the inner DMAA layer remains at the same thickness as at pH 3, the outer DMAA–SA layer is now swollen to about 2000 μm , which is an increase by more than 100%. This illustrates the pH-responsive properties of our multilayer capsule.

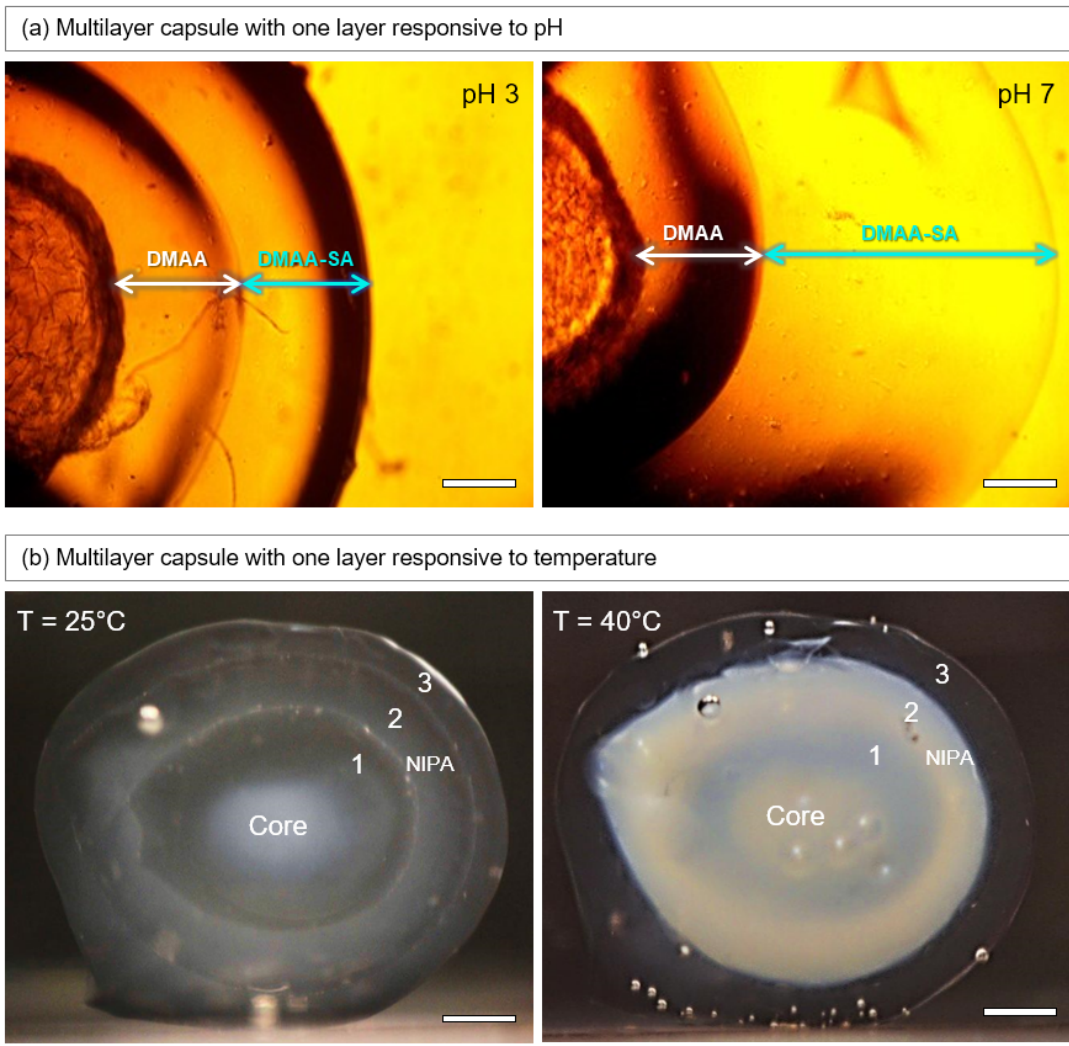


Figure 3.7. Multilayer capsules with specific layers responsive to external stimuli. In (a), a two-layer capsule is shown with an inner layer of nonionic polymer (DMAA) and an outer layer of anionic polymer, obtained by copolymerization of DMAA with sodium acrylate (SA) (designated as DMAA–SA). At pH 3, the two layers have the same thickness. At pH 7, the carboxylate groups in the DMAA–SA layer become deprotonated, causing the anionic gel to swell, and thus the thickness of the DMAA–SA layer increases substantially. In (b), a three-layer capsule is shown, where layers 1 and 3 are DMAA (non-responsive), while layer 2 is NIPA (thermo-responsive). At ambient temperature (25°C), all layers are transparent gels. Upon heating to 40°C, which is above the lower critical solution temperature (LCST) of NIPA, the NIPA layer becomes turbid. Scale bars are 500 μm in (a) and 1 mm in (b).

Next, we consider temperature as a stimulus. NIPA is well-known to be a thermo-responsive polymer, i.e., NIPA gels shrink when heated above the polymer’s lower

critical solution temperature (LCST) of 32°C.^{34,35} DMAA, on the other hand, is not affected by temperature.⁷⁶ Figure 3.7b shows a three-layer capsule where layer 1 and 3 are DMAA and layer 2 is NIPA (the core is alginate/Ca²⁺, as before). The photo taken at 25°C clearly shows all three layers, with each layer being about 1 mm thick. Next, a photo is shown of the same capsule after heating to 40°C, which is above the LCST of NIPA. In this case, the NIPA layer (2) has become opaque, and this is because the NIPA chains turn hydrophobic above the LCST and the gel begins to expel water.^{36,72} In contrast, the DMAA layers (1 and 3) are unaffected by temperature and are actually both clear (the inner layer 1 of DMAA may seem somewhat turbid, but that is only because it is obscured by the surrounding NIPA layer 2). Overall, the above capsule shows a visible macroscopic change in response to temperature.

3.3.5 Solute Release from Temperature-Responsive Capsules

We now study the release of small-molecule solutes from the above kind of temperature-responsive capsules. As mentioned earlier, capsules are frequently used for the delivery of drugs and other solutes.^{30,31} In this context, the proximity of NIPA's LCST to human body temperature (37°C) has made this polymer of particular interest in drug delivery.³⁴ For example, a number of groups have demonstrated pulsatile release of drugs from thermosensitive NIPA gels through temperature control.⁶²⁻⁶⁴ Inspired by these past studies, we investigated whether the multilayer structure of our capsules could make them interesting candidates for drug delivery. For these experiments, we worked with two-layer capsules having concentric layers of DMAA and NIPA, but in different order. First, we consider an Alg–DMAA–NIPA capsule, i.e., with DMAA as the inner layer and NIPA as

the outer layer. This capsule was loaded with brilliant yellow (BY) dye by soaking in a 500- μ M dye solution for 24 h at room temperature. The capsule was then heated in the dye solution up to 40°C, a temperature that exceeds the LCST of NIPA. This causes the outer NIPA layer to shrink, thereby preventing release of dye from the inner portions of the capsule (see more details below).

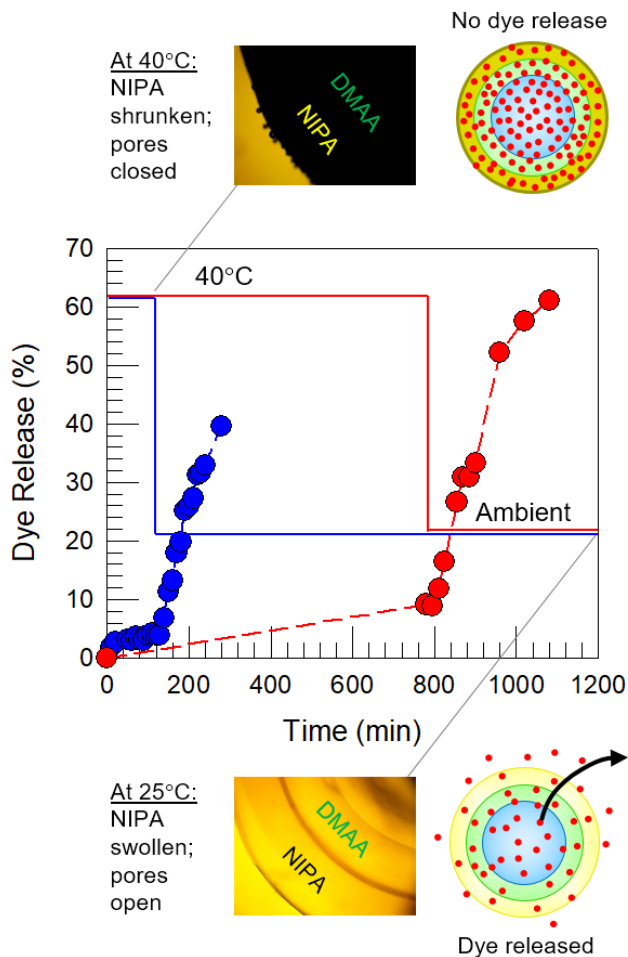


Figure 3.8. Temperature-responsive release of dye from a two-layer DMAA–NIPA capsule. Here, DMAA is the inner layer and NIPA is the outer layer. At 40 °C (above the LCST of NIPA), the pores in the outer NIPA layer are closed; thus, the dye remains in the capsule. This is indicated by the schematic, and the corresponding micrograph shows a dark capsule due to the turbidity of the outer layer. After a certain time (110 min for the blue curve; 780 min for the red curve), the temperature is lowered to ambient (25 °C). The pores in the NIPA layer open up, causing the dye to release. This is shown by the schematic, and in this case the micrograph shows a transparent capsule. The y-axis is normalized to the dye released into solution after a long time (2 days).

Next, the capsule was rinsed briefly with deionized (DI) water at 40°C, and then transferred to a flask maintained at 40°C and containing 100 ml of DI water. The dye concentration in the external solution was then monitored as a function of time, and this is plotted in Figure 3.8. As long as the temperature is at 40°C, we find negligible dye to be released from the capsule, with the % release (blue curve) saturating at ~5%. Next, at the 110 min mark, we stopped heating the flask and allowed it to cool to ambient temperature. As the temperature drops below the LCST of NIPA, we observe a sharp increase in dye release. Within the next 180 min (3 h), more than 40% of the dye gets released. Note that the y-axis in Figure 3.8 is normalized to the dye in the solution 2 days later at ambient temperature, i.e., at a state when all the dye has been released from the capsule.

A similar experiment was repeated, where an identical capsule to the above was held at 40°C in the flask for 13 h (780 min). Even over this longer period (red curve in Figure 3.8), only about 10% of the dye gets released. When heating is stopped and the system is cooled, the dye release is again triggered and over the next 300 min, more than 60% of the dye is released. A key result from these experiments is that small-molecule solutes can be kept encapsulated for extended periods of time by exploiting the thermoresponsive properties of NIPA. When a NIPA gel is heated above its LCST, its chains become hydrophobic and the gel becomes turbid.^{36,70} Similarly, when the Alg–DMAA–NIPA capsule is observed under a microscope at 40°C, the capsule appears dark (see image in Figure 3.8) because the NIPA layer is turbid and it is the outer layer. We believe the hydrophobic NIPA chains close the pores in the NIPA layer, akin to forming a precipitate around the pores. This allows the dye to be retained in the core. When

temperature is decreased to 25°C, the capsule becomes clear again (see image in Figure 3.8). In this state, the pores in the outer NIPA layer are reopened, allowing the dye to diffuse out. Overall, Figure 3.8 shows that we can engineer a one-step release profile, i.e., with no release under one value of the stimulus, followed by rapid release under a different value of the same stimulus.

Next, we consider an Alg–NIPA–DMAA capsule, i.e., with NIPA as the inner layer and DMAA as the outer layer. We again loaded the capsule with BY dye; note that some of the dye will be in the alginate core and inner NIPA layer, while some of it will be in the outer DMAA layer. The capsule was then transferred to a flask at 40°C containing 100 ml of DI water. The release profile (Figure 3.9) shows an initial rapid release of dye, followed by a saturation around the 45 min mark. This released dye corresponds to that in the outer DMAA layer. The dye in the core is prevented from diffusing out because the pores in the NIPA layer are closed at 40°C. In the corresponding microscope image in Figure 3.9, the core and NIPA layer appear black, but the DMAA layer is clear. When the heat is removed at the 45 min mark, the system cools to ambient temperature, and at this point the entire capsule appears clear. In turn, the pores in the NIPA layer are opened, allowing dye trapped within the core to be released. Thus, the release profile shows a second bump followed by a saturation at about the 180 min mark. The y-axis in Figure 3.9 is normalized by the final dye concentration in the solution; thus, ~60% of the dye in the capsule is released at 40°C, while the remaining 40% of the dye is released upon cooling. Overall, by changing the capsule architecture, i.e., order of layers, we have now been able to engineer a two-step

release profile, with some of the solute being released at one value of the stimulus, and the rest of the solute being released at a different value of the stimulus.

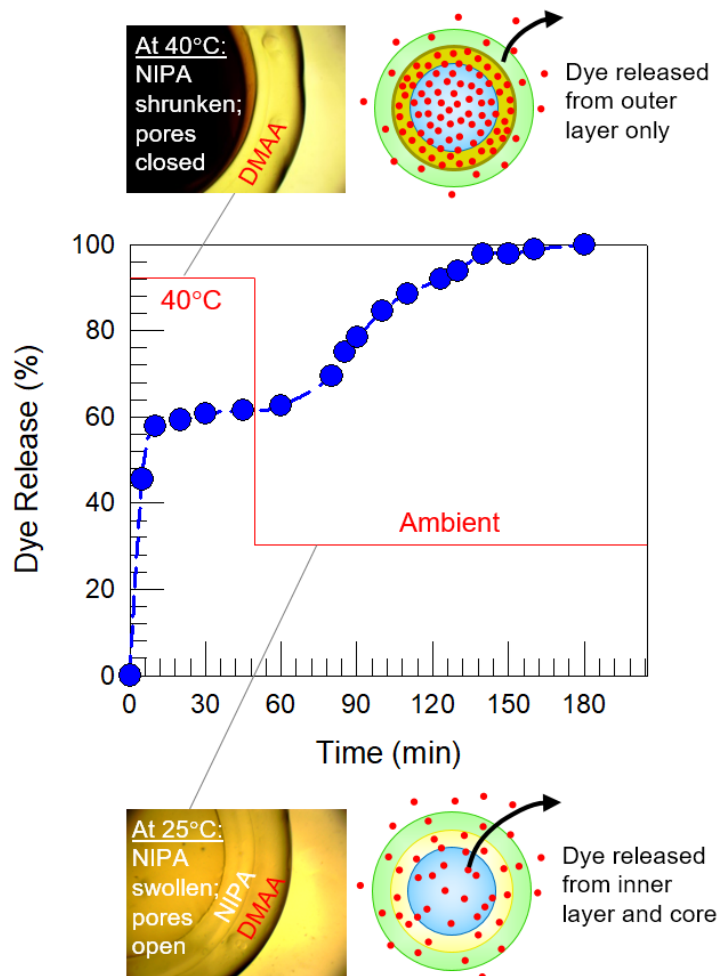


Figure 3.9. Temperature-responsive release of dye from a two-layer NIPA–DMAA capsule. Here, NIPA is the inner layer and DMAA is the outer layer. At 40°C (above the LCST of NIPA), the pores in the inner NIPA layer are closed. In this case, the dye in the outer DMAA layer alone is released, as shown by the schematic. The corresponding micrograph shows a dark inner portion due to the turbidity of the NIPA layer, while the outer layer is transparent. At the 45 min mark, the temperature is lowered to ambient (25°C). The pores in the NIPA layer open up, causing the inner dye to also release. This is shown by the schematic and in this case the entire capsule is transparent.

3.4 Conclusions

We have demonstrated an inside-out technique for creating multilayered polymer capsules, with each layer being a crosslinked polymer gel. The technique is very simple to implement, and does not require complex multiphase precursors such as double emulsions, nor does it require strong interactions (electrostatic or hydrophobic) between adjacent layers. As a result, a wide variety of polymers can be used to form the layers. The technique uses a gelled core that is loaded with water-soluble initiator and then placed in a solution containing monomer, crosslinker and accelerant. The initiator diffuses out of the core into the surrounding solution, whereupon polymerization begins at the surface of the core. A polymer layer is formed by freeradical polymerization, and as time progresses, this layer grows outward. The process can be sequentially repeated with different monomers to generate additional layers. Layer thickness can be controlled based on the polymerization time or by varying the amount of initiator in the core.

The utility of this technique is shown by juxtaposing layers of a non-responsive polymer next to either a temperature or pH-responsive polymer. In these cases, the thickness of the stimuli-responsive layer can be altered substantially by varying the external stimulus while the non-responsive layer remains at the same thickness. In addition, the permeability of small molecules through the stimuli-responsive layers is also altered. For example, when NIPA is one of the layers, the release of a small-molecule dye from the capsule is very slow above the LCST of NIPA but much faster below the LCST. As a result, a two-layer capsule with an inner DMAA and outer NIPA layer shows a one-step release profile with varying temperature. Conversely, when NIPA is the inner and DMAA the outer

layer, the capsule shows a two-step release when subjected to the same temperature profile. Thus, new modes of pulsatile release are made possible by these multilayer capsules.

The multilayer capsules described here can be extended in numerous ways. Unusual combinations of polymeric layers can be incorporated into a given capsule. Also, nanoparticles of different kinds can be incorporated into specific layers during synthesis. We have also briefly shown that these multilayer capsules can have remarkable mechanical properties; these also depend on the composition of each layer and on the number of layers. In addition, the optical properties of these capsules can also be tuned based on the content of each layer. We hope that the versatility of this technique will prove attractive to researchers. Many new kinds of multilayer capsules with expanded functionalities are envisioned in the future, with potential applications in fields, such as catalysis, biomimetics, and the delivery of drugs and therapeutics.

Chapter 4

Multilayer Tubes

4.1 Introduction

In nature the structural motif of multilayered materials is pervasive.¹⁻⁵ These include roughly spherical structures such as seeds, eggs, onions, etc., as discussed in Section 2.1. In addition, cylindrical tubes used in the body to transport fluids and nutrients, including veins and arteries, as well as the intestines, all have multilayered walls.^{1,2,5,6,26,27} The number of layers in the tube wall as well as the thickness and composition of each layer vary depending on the type of tube.^{26,27} Veins and arteries are typically three-layered, as discussed in Section 2.1 (interestingly, capillaries, which have the shortest inner diameter have only a single layer).^{1,2,78} As noted earlier, each layer of such tubes is essential to their function. In particular, all these tubes have to be flexible, yet robust. Moreover, since each layer is formed from cells, they all contain water.¹ Thus, we infer that tubes with multiple layers of soft, gel-like materials are ubiquitous in biology.

A large body of research has been dedicated to synthesizing hollow tubes out of polymers. Techniques used for this purpose include molding, electrospinning, and additive manufacturing (3D printing).⁷⁹⁻⁸⁶ In many of these cases, the walls of the tubes are solid materials rather than water-swollen gels.^{79,82,86} Gelled walls are possible in the case of tubes made by molding.^{80,87} The simplest approach here is to pour a monomer solution into a mold formed by the annulus between two solid cylinders, followed by free-radical polymerization. This approach, however, is difficult to extend to form multilayered tubes.

If a second layer is polymerized around a first one, the two layers will be weakly bonded and will tend to delaminate. Thus, there exists the need for a new technique for the creation of multilayered tubes in a fast, simple, and precise manner utilizing biocompatible constituent materials.

Towards this end, we describe a new route for creating multilayer tubes through a biomimetic “inside-out” polymerization technique (see Chapter 3). Briefly, the technique employs a template (in this case a cylindrical gel made from agar) loaded with a free-radical initiator. This initiator-laden template is then placed into a solution with a monomer and a crosslinker. In this solution, the initiator diffuses outward and initiates the polymerization of the monomer and crosslinker to form a layer around the template. Thus, the polymeric layer is formed in an “inside-out” manner. We can then repeat the procedure with different monomers to add more concentric layers outside the first. After the synthesis, the template can be removed by heat to yield a hollow tube. The resulting tubes are mechanically robust and flexible. We can control the lumen diameter, and the thickness and composition of individual layers in the tube wall. We can also construct different kinds of patterned tubes, including a longitudinally-patterned “Janus tube” with different top and bottom halves that curls spontaneously into a circle in response to stimuli. Also, we have made a patterned tube in which there is a local change in lumen diameter in response to a temperature change. This is reminiscent of blood vessels, which can undergo vasoconstriction or vasodilation over a particular segment.

4.2 Experimental

Materials. The following were purchased from Sigma-Aldrich: the initiator ammonium persulfate (APS); the accelerant N,N,N',N'-tetramethylethylenediamine (TEMED); the monomers sodium acrylate (SA), N,N'-dimethylacrylamide (DMAA), and N-isopropylacrylamide (NIPA); the crosslinker N,N'-Methylenebis(acrylamide) (BIS); the cationic dye methylene blue (MB); xanthan gum (XG); fluoresceinamine (F-NH₂); and N-hydroxysuccinimide (NHS). The coupling agent 1-ethyl-3-(3-dimethylaminopropyl) carbodiimide (EDC) was purchased from Carbosynth. Agar was purchased from Living Jin. The nanoclay laponite XLG (LAP) was obtained as a gift from Southern Clay Products. Deionized (DI) water from a Millipore system was used for all experiments.

Synthesis of Agar Template Cylinders. Agar powder was dissolved in ~ 95°C DI water at a concentration of 5 wt%. This hot solution was then inserted into a length of Tygon® tubing (available from ~0.700 mm to 25.4mm inner diameter) of the desired inner diameter. After ~ 30 min at room temperature, the agar solidifies. Water was then injected into the tube end to force the agar cylinder out of the tubing. The cylinder was then cut to the desired length using a razor blade. Tubes were stored in DI water at 4°C until use

Synthesis of Multilayer Polymer Tubes. First, the agar template cylinder was incubated in a 15 mg/mL solution of APS. After 15 min, the cylinder was removed, blotted with a Kimwipe®, and placed in a monomer solution contained in a rectangular trough. A typical monomer solution had 10 wt% monomer, 0.34 wt% BIS (crosslinker), 0.5 wt% XG, and 15 mg/mL TEMED. The XG was added to increase the viscosity of the solution; note that

the template stayed suspended in the middle of the viscous solution in the dish, allowing polymerization to occur on all sides of the template. Instead of BIS, LAP particles could be used as cross-linkers, and in that case, the composition was: 10 wt% monomer, 0.005 wt% BIS, 3 wt% LAP and 15 mg/mL TEMED. The XG was not used with the LAP because the LAP particles themselves aggregate and make the solution viscous. To synthesize multilayer tubes, the above process was repeated with a different monomer. Once the template with a desired number of polymerized layers was synthesized, it was washed with water and taken out of the solution. A razor blade was used to cut the caps off the structure, thus exposing the agar template. Thereafter, the whole structure was placed in water at ~90°C to melt the agar and thereby remove the core template. In some cases, to ensure full removal of the agar, hot water was forced through the lumen of the tube using a syringe.

Fluorescent Modification of Polymer Tubes. A two-layer tube was employed with an inner layer being a copolymer of SA and DMAA (10:90 ratio by weight of the total monomer) while the outer layer was solely DMAA. The tube was placed in water at pH 4.5 and to this EDC and NHS were added at concentrations that were 1.5× the molar equivalent of the SA in the tube (each SA monomer has a carboxylate group, which is the one that reacts with the EDC). After 30 min of incubation, a solution of 0.01 g/mL of F-NH₂ in methanol was added dropwise to the above tube while stirring. The amount of F-NH₂ added was half the molar equivalent of the SA. The sample was then covered with aluminum foil to prevent photobleaching and maintained at 65°C under moderate magnetic stirring for 24 h to allow the reaction to proceed. The tube was then washed once with a 50/50 methanol/water solution, and three more times with water adjusted to a pH of 4.5.

Optical Microscopy. All microscope images were taken using a Zeiss Axiovert 135 TV inverted microscope. Images were typically taken using a 2.5× objective. A microruler and the image analysis software ImageJ were used to determine tube dimensions from collected images. To visualize the green fluorescence from F-NH₂, which is green, images were collected using a band pass excitation filter (450-490 nm) and a band pass emission filter (515-565 nm). The images were then subsequently combined using ImageJ.

4.3 Results and Discussion

4.3.1 Synthesis of Single-Layer Tubes

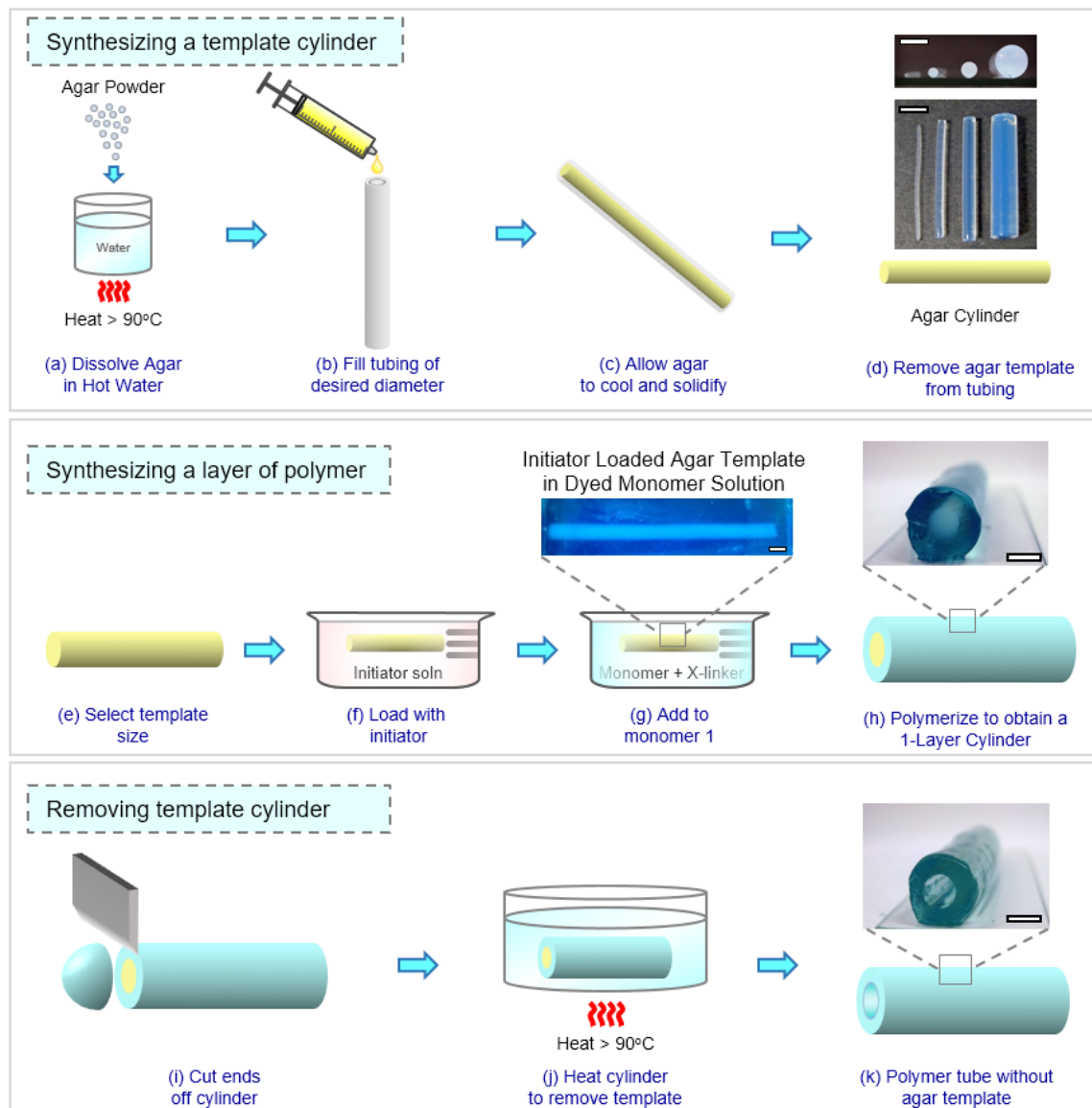


Figure 4.1. Synthesis of a single-layer polymer tube. First, a cylindrical template of agar of desired diameter is created, as shown in (a) to (d). Then, an agar cylinder of specific size (e) is loaded with free-radical initiator (f), and transferred to a solution of monomer (along with crosslinker and accelerant) (g). The initiator diffuses outward, polymerizing a layer of polymer around the template (h). To yield a hollow tube, the ends are cut off (i) and the structure is heated to $\sim 90^{\circ}\text{C}$ (j), whereupon the agar melts away, leaving behind a hollow tube (k). All scalebars in insets are 4.5mm in length.

The technique to generate a single-layer polymer tube is shown schematically in Figure 4.1. First, we synthesize a cylindrical template of the biopolymer agar in a mold (Figure 4.1 a-d). Templates based on other biopolymers like alginate, chitosan, or gelatin can also be used, but agar is particularly convenient for our purpose. Agar gets dissolved in hot water ($\sim 90^{\circ}\text{C}$), and upon cooling to room temperature it sets into a gel. When the gel is reheated to 90°C , it can be melted into a solution. Here, we introduce a hot agar (5 wt%) solution into Tygon® tubing of a pre-determined diameter, and allow the solution to cool into a gel at ambient temperature. The agar cylinder is then removed by injecting DI water into the tubing. The cylinder is then cut into pieces of desired length.

Next, the cylindrical template is incubated in a solution containing a water soluble free-radical initiator (Figure 4.1e, f), typically 15 mg/mL of ammonium persulfate (APS). This is done typically for 15 min, which is sufficient time for the APS to diffuse into the entire tube. This initiator-laden template is then transferred into a solution containing 10 wt% of a monomer (e.g., DMAA), 0.34 wt% BIS as crosslinker, 0.5 wt% XG, and 15 mg/mL of TEMED. The XG makes the solution viscous, while the TEMED allows the free-radical polymerization to occur at room temperature. The initiator diffuses out from the template cylinder into the surrounding solution and induces the growth of a crosslinked polymer layer around the template (Figure 4.1g). Once a layer of desired thickness has formed (Figure 4.1h), the structure is removed and washed. Then the hemispherical caps at the ends of the cylinder are cut off with a razor blade (Figure 4.1i) to reveal the inner agar. The whole structure is then placed in a heated water bath (Figure 4.1j) at 90°C for

~20 min to melt away the agar. This results in a hollow tube with a polymeric wall of desired composition and thickness (Figure 4.1k).



Figure 4.2. Single-layer tubes of different lumen diameter. All tubes have a wall composed of a DMAA-BIS network and their lumen (inner) diameter ranges from ~ 0.6 mm on the far right to ~ 4.5 mm on the far left. The scale bar is 5mm in length.

Tubes synthesized by this technique can be created with a variety of lumen diameters and wall thicknesses. Figure 4.2 displays tubes with lumen diameters ranging from 4.5 mm to 0.6 mm, which are made by varying the diameter of the agar templates. All have a wall that is a network of DMAA, cross-linked with BIS. For comparison, it is worth noting that blood vessels in our body range in diameter from ~ 5 μm for the smallest capillaries to > 30 mm for the largest ones like the aorta.^{78,88,89} The wall thicknesses of our tubes in Figure 4.2 are ~ 1 mm with the smallest tube having a wall thickness of ~0.3mm. This thickness can be easily controlled by varying either the initiator concentration or the polymerization time. The latter is shown below.

4.3.2 Kinetics of Layer Growth

The “inside-out” growth of a polymer layer around the core template can be visualized in real-time by optical microscopy. For this, a cylindrical template (1.2 mm diameter) with 15 mg/mL APS was placed in a monomer solution with the composition as

stated above (10% DMAA, 0.34% BIS). A video of the growing layer was captured at room temperature, and still images from the video are shown in Figure 4.3a to 4.3c. The layer thickness can be extracted from the images using ImageJ. The layer grows rapidly, reaching a thickness of 550 μm after 1 min (Figure 4.3a) and saturates at a thickness of 1600 μm by about 15 min (Figure 4.3c).

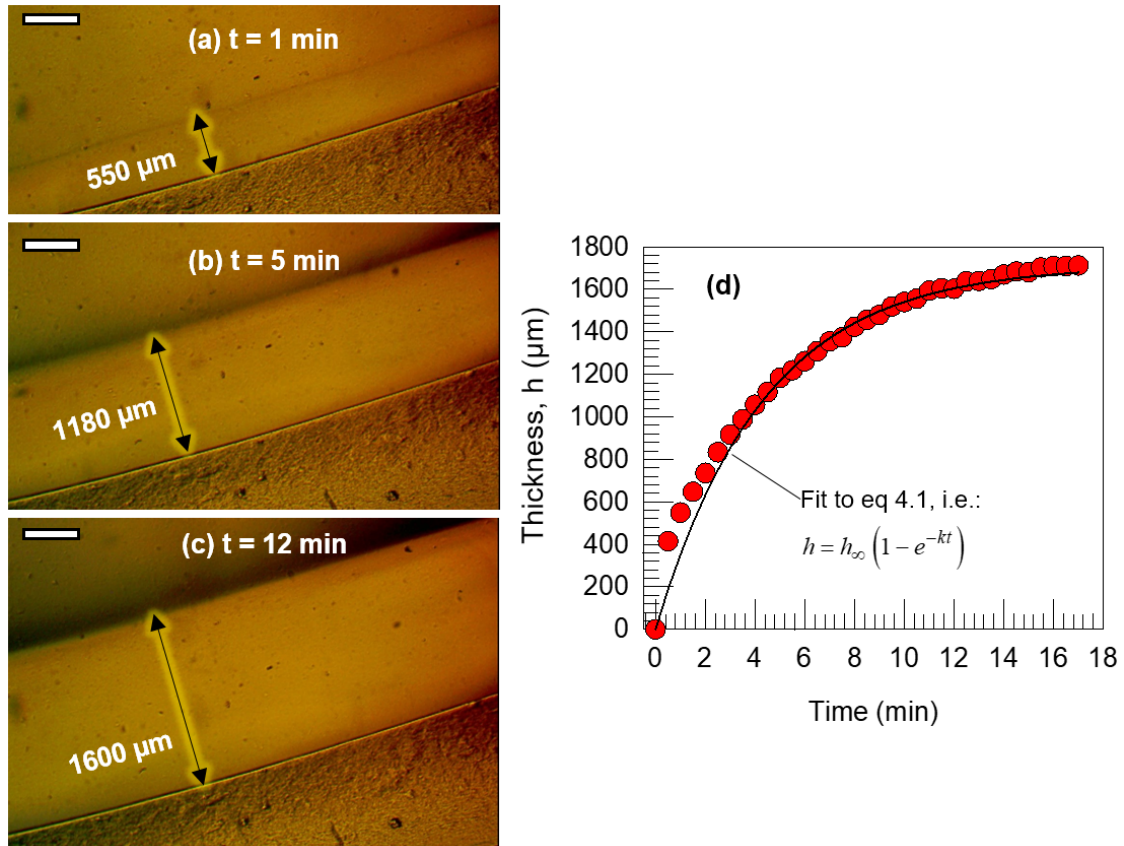


Figure 4.3. Kinetics of polymer layer growth. An agar cylinder loaded with 15 mg/mL APS was placed in a 10 wt% DMAA solution at time $t = 0$. Time-lapse microscope images collected during the polymerization are presented in (a), (b) and (c), showing the growth of the polymer layer over time. Scale bars in the images are 500 μm . In (d), the thickness h of the polymer layer is plotted as a function of time t , and fit to eq 4.1.

Figure 4.3d plots the thickness h of the polymer layer from the above images as a function of time. The data are fit to the following equation:

$$h = h_{\infty} \left(1 - e^{-kt}\right) \quad (4.1)$$

where h_{∞} is the layer thickness at saturation and k is a rate constant. Eq 4.1 fits the data reasonably well, with a value of $k = 0.21 \text{ min}^{-1}$. There is a small deviation from the model in the initial 2 min of layer growth.

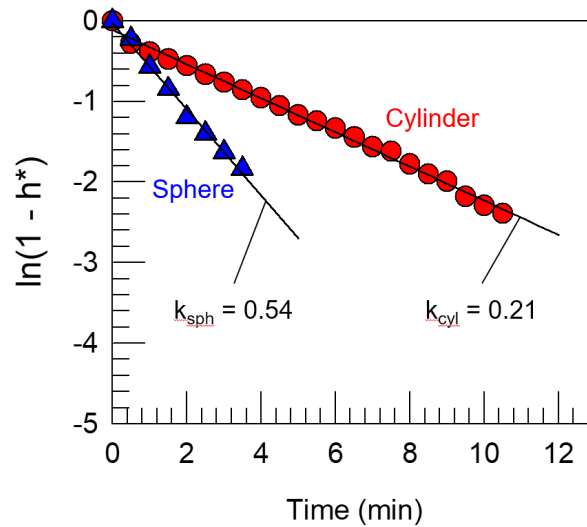


Figure 4.4. Kinetics of layer growth around a spherical vs. cylindrical template. The data from Figures 3.4 and 4.3 are replotted above. Each set of data is normalized by the final layer thickness ($h^* = h/h_{\infty}$). The semilog plots above both follow straight lines, confirming the exponential form for the fit (eq 4.1). From the slope, the rate constants k are calculated, and we find that $k_{\text{sph}} = 0.54$ is much higher than $k_{\text{cyl}} = 0.21$.

We now compare the kinetics of layer growth around a spherical core (data shown in Figure 3.4) vs. that around a cylindrical core (data in Figure 4.3). The monomer solutions used for the two experiments are identical (10 wt% DMAA, 0.34% BIS), and so was the initiator concentration in the core (15 mg/mL APS) as well as the conditions for the polymerization (room temperature). The spherical core was based on alginate and had a diameter of 2 mm, while the cylindrical core above is based on agar and had a diameter of

1.2 mm. The layer of polymer formed around the agar cylinder is noticeably thicker than that around the sphere, i.e., the thickness $h_\infty \sim 1700 \mu\text{m}$ for the former and $h_\infty \sim 340 \mu\text{m}$ for the latter. Also, the layer growth is completed quicker in the case of the sphere ($\sim 7 \text{ min}$) vs. $\sim 15 \text{ min}$ in the case of the cylinder. Figure 4.4 compares the kinetics on a normalized semilog plot of $h^* = h/h_\infty$ vs. t . Consistent with eq 4.1, the two plots follow a straight line. From the slopes, the rate constant $k_{\text{sph}} = 0.54$ is much higher than $k_{\text{cyl}} = 0.21$, indicating that the reaction proceeds more rapidly in the case of the sphere. The exact reasons for these differences are unclear, but may be related to the different materials used for the template (alginate vs. agar). We should also note that the volume of the cylinder is quite a bit larger than that of the sphere, which means there is a larger amount of initiator in the former case.

4.3.3 LAP-Crosslinked Tubes and their Staining

To visualize tubes more clearly, we incorporated the nanoclay laponite (LAP) into our synthesis scheme. LAP is a disk-shaped nanoparticle, 25 nm in diameter and 1 nm in thickness.⁹⁰ It is known to serve as a cross-linker for growing polymer chains^{91,92}, as shown in Figure 4.5a. In addition, the faces of the disks are negatively charged, and these have a high affinity for cationic dyes.^{90,93} We typically use a monomer composition of 10 wt% monomer (e.g., DMAA), 0.005 wt% BIS, 3 wt% LAP and 15 mg/mL TEMED. Thus, LAP particles are the main cross-linkers for the polymer chains, and the advantage is that networks cross-linked by LAP are more flexible and robust than networks cross-linked with BIS. The rest of the procedure is the same as before: the agar template is placed in the monomer solution, and a layer of DMAA-LAP forms around the template in 15 min. A

photo of this tube after removal of the template is shown in Figure 4.5a. The tube wall is nearly transparent and colorless. The tube is then placed in a solution of the cationic dye, methylene blue (MB) at a concentration of $10\ \mu\text{M}$. The MB molecules adsorb on the faces of LAP disks, turning the layer blue. We can impart either a light blue color (Figure 4.5b) or a dark blue color (Figure 4.5c) depending on the time for which the tube is soaked in the MB solution. Note that the dye adsorption is strong and irreversible; thus, the dye does not subsequently diffuse out of the tube if it is placed in water. Also, only tubes with LAP in the walls show this strong, irreversible binding of MB; thus, we can distinguish layers based on this staining technique. Through the course of this work we will employ this technique for visualization purposes.

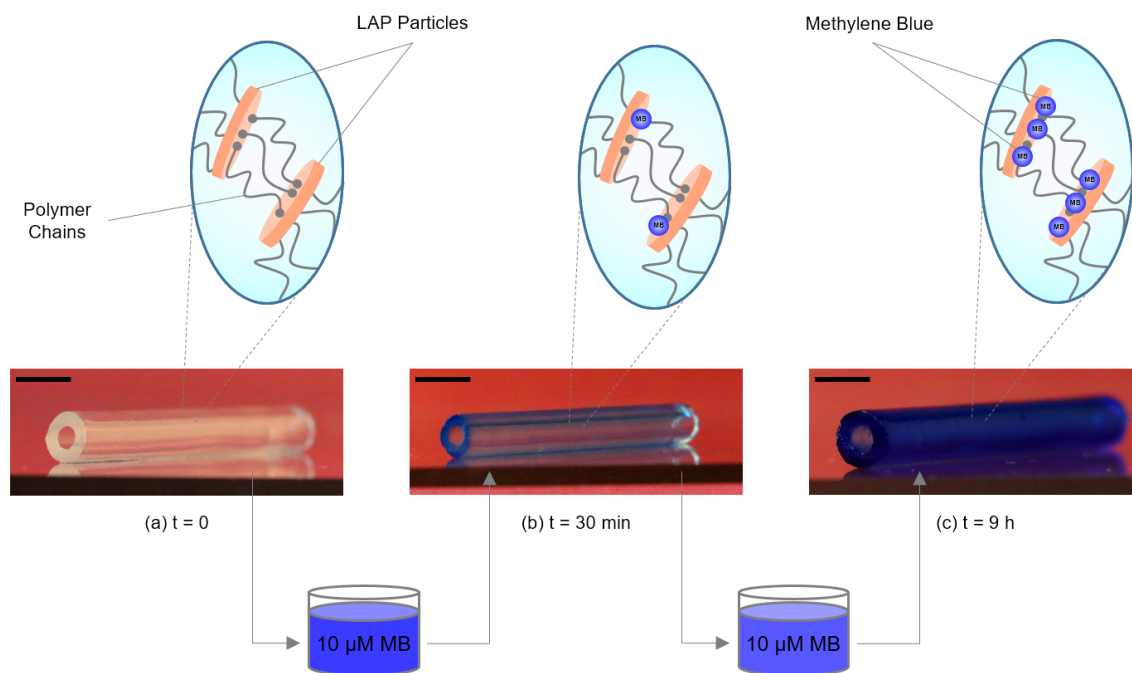


Figure 4.5. Tube with a polymer layer crosslinked by LAP and staining of this layer. LAP particles serve as crosslinkers for growing polymer chains, leading to a network, as shown by the schematics. A tube with a layer of DMAA-LAP is transparent (a). When placed in a $10\ \mu\text{M}$ solution of methylene blue (MB) for 30 min, the tube wall takes on a light-blue color (b), while incubation in the same solution for 9 h gives it a dark blue color (c). The color is due to adsorption of the cationic MB on the anionic faces of the LAP particles, as shown by the schematics. Scale bars are 5 mm.

4.3.4 Mechanical Robustness of the Tubes

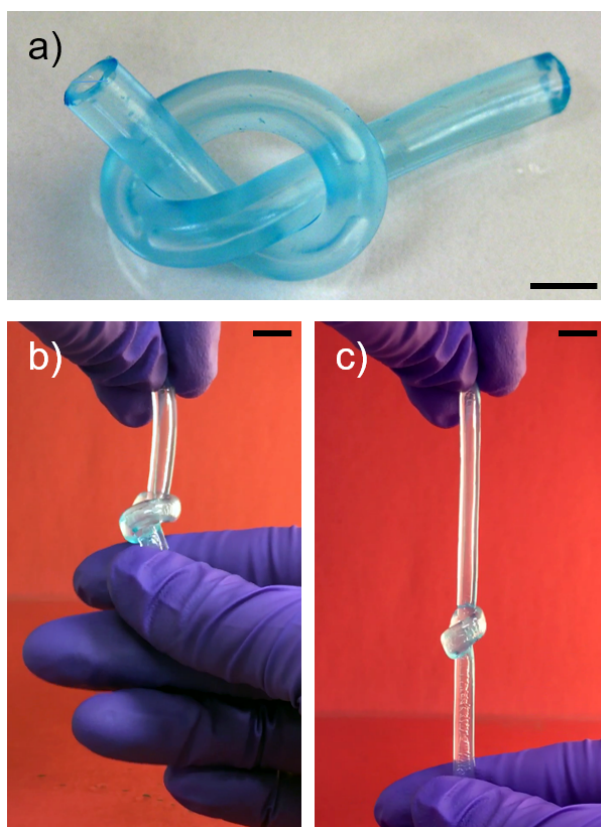


Figure 4.6. Photos showing the mechanical properties of tubes. This 1-layer tube of DMAA-LAP is flexible and robust enough to be bent and tied into a knot (a). The images in (b) and (c) show a knotted tube being further stretched up to ~150% of its initial length without breaking. All scale bars are 5mm.

Our method generates tubes that are mechanically robust. For example, the tubes can support the steady flow of liquids through their lumen. Tubes made with LAP as the cross-linker (Section 4.3.3) are especially robust, and they are also flexible and stretchable (Figure 4.6). The tubes have a light blue color due to exposure to MB for just 1-2 min. The photos in Figure 4.6 show that the tube is stretchable, flexible, and robust. The tube can be tied into a knot, and the knotted tube can be stretched to nearly 150% of the original length

(Figure 4.6b-c) without rupture. The stretchability is a well-known property of LAP-crosslinked gels, and this is most likely due to the increased length of polymer chain segments between crosslinking junctions.

4.3.5 Tubes Patterned with Stimuli-Responsive Polymers

Biological tubes, i.e., veins and arteries, display an ability to spontaneously shrink or enlarge their lumen diameter over certain tube segments (this behavior is termed vasoconstriction and vasodilation). These phenomena occurs in response to changes in body temperature and blood pressure, and is responsible for manipulating a steady flow of blood. To our knowledge, these behaviors have not been shown by synthetic polymer tubes. To mimic these with our tubes, the challenge was to synthesize tubes with patterned regions of different polymers in the same material, of which one (or more) polymers could be a stimuli-responsive one.

First, we show the ability to synthesize tubes with *lateral* patterns (Figure 4.7), where different lateral segments of a tube are made with different polymers. For this, we use the same synthesis scheme as shown in Figure 4.1, but we use more than one monomer solution in our container. Figure 4.7a illustrates lateral patterning into three zones, each with different monomers. To do this, we exploited the fact that highly viscous solutions will not mix. All monomer solutions had 10 wt% of the monomer, and were made viscous either by adding 0.5% XG or by using 3 wt% LAP. In a rectangular trough, we placed two glass slides vertically at discrete points, as shown in Figure 4.7a. This divides the trough into three compartments. The three monomer solutions were then added to the three

compartments. The glass slides were then removed, whereupon due to their high viscosity, the adjacent solutions did not mix. A cylindrical template loaded with initiator was then positioned perpendicularly across the three monomer solutions, as shown in Figure 4.7a, and this was left to polymerize.

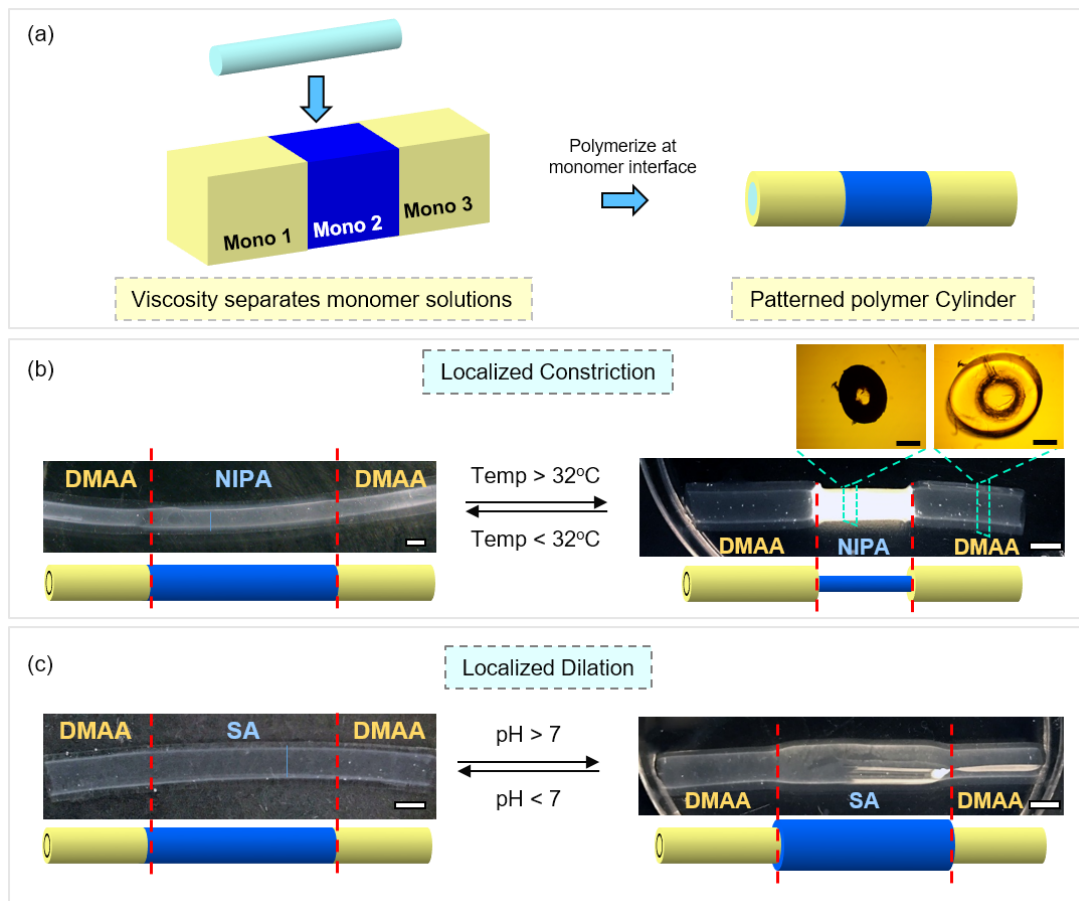


Figure 4.7. Synthesis of laterally patterned tubes, and two examples of the same. (a) The synthesis is achieved by placing an initiator-loaded cylindrical agar template in a rectangular trough containing two or more highly viscous monomer solutions. The solutions do not mix due to their viscosity. (b) A tube with three lateral segments corresponding to DMAA-NIPA-DMAA. When heated above 32°C, the middle NIPA segment shrinks, and the tube narrows. The lumen diameter (inset micrographs of a separate, microscale tube which shows inner diameter change; scale bar 500 μm) decreases by ~50%. (c) A tube with three lateral segments corresponding to DMAA-SA-DMAA. At pH > 7, the SA segment swells and the tube dilates. The lumen diameter increases from 4.5 mm to 5.7 mm. Photograph scale bars are 4.5mm.

Figure 4.7b shows a laterally patterned DMAA-NIPA-DMAA tube, where the middle segment is the thermoresponsive polymer NIPA (all layers crosslinked with BIS). Note that the initial photo reveals a smooth tube with no obvious demarcation of the three zones. The differences emerge upon heating. Above its lower critical solution temperature (LCST) of $\sim 32^{\circ}\text{C}$, a NIPA gel becomes opaque and shrinks. Correspondingly, here, we observe that the NIPA segment of the tube narrows above 32°C . Both the outer (OD) and inner diameter (ID) of the tube are reduced. A microscale tube was synthesized to illustrate the ID change of the tube (inset images in Figure 4.7b). In both cases the ID of the tube decreases by $\sim 50\%$. This change in diameter is reversible, i.e., the original sizes are restored upon cooling.

Next, we show a laterally patterned DMAA-SA-DMAA tube in Figure 4.7c (all layers crosslinked with BIS). The middle segment labeled “SA” is actually a copolymer of SA/DMAA in a 20/80 ratio of the total monomer. Due to the presence of SA, this middle segment is anionic, whereas the segments with DMAA alone are nonionic. When the carboxylate groups are ionized, i.e., at $\text{pH} > 7$, SA gels swell highly whereas the gels are less swollen at lower pH. In our case, the SA segment of the tube gets dilated significantly upon increasing the pH to above 7, with the OD increasing from 6.0 to 7.8 mm. This change is also reversible, i.e., the original sizes are restored when pH is lowered. Overall, the above behavior of the tubes mimics the local vasoconstriction or vasodilation of blood vessels, which is achieved using stimuli-responsive polymers in the tube walls.

Next, we show the ability to create tubes with *longitudinal* patterns, where the top and bottom halves of the tube are made from distinct polymers. Such a tube is akin to a Janus or two-faced material. Here again, we used viscosity to separate our monomer solutions. We simply poured one solution to fill our rectangular trough half-way to the top, then poured our second monomer solution on top of the first. Again, due to their high viscosity, the adjacent solutions did not mix. A cylindrical template loaded with initiator was then positioned such that one half of its height was in contact with the bottom monomer and the other half with the top, as shown in Figure 4.8a.

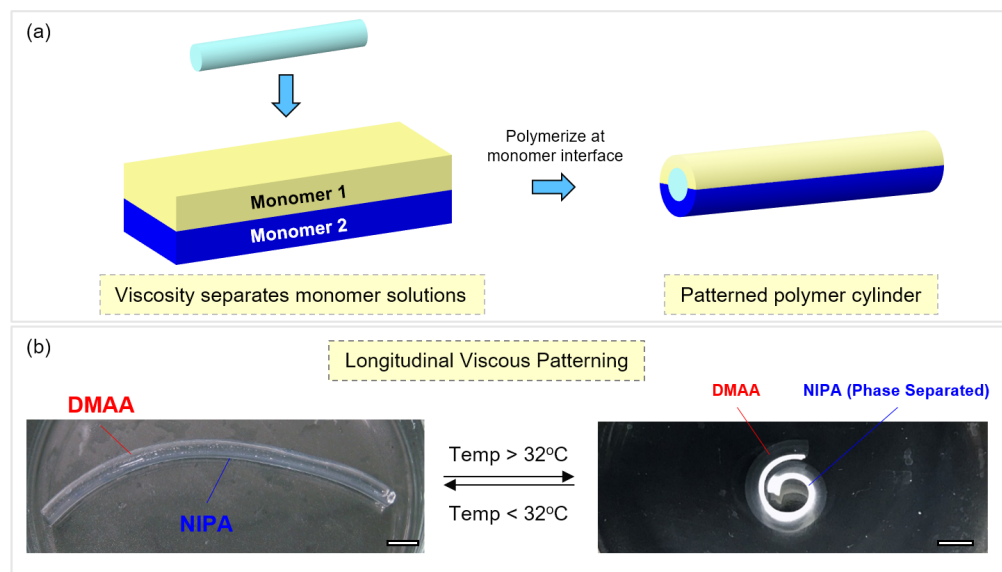


Figure 4.8. Synthesis of longitudinally patterned (“Janus”) tubes, and an example of the same. (a) The synthesis is achieved by placing an initiator-loaded cylindrical agar template in a rectangular trough containing two viscous monomer solutions, poured one after the other. The solutions do not mix due to their viscosity. (b) The Janus tube has a top half of DMAA and a bottom half of NIPA. When heated above 32°C, the NIPA half shrinks. This in turn causes the tube to curl and coil. Scale bars are 5mm.

Figure 4.8b shows a Janus tube with a top half of DMAA and a bottom half of NIPA (both layers crosslinked with BIS). At room temperature, this tube is an extended, straight structure and it is not evident from the photo that the tube is anisotropic. However, when the temperature of the system is increased above the LCST of NIPA (32°C), we observe that the lower half of the tube becomes opaque due to the phase separation of NIPA. Moreover, the tube curls into a coil rather than remaining straight. This curling is because the NIPA half shrinks compared to the DMAA half. This mismatch in swelling degree between the top and bottom halves of the tube creates internal stresses. To relieve this stress, the tube curls with the swollen portion outside and the shrunken portion inside. Similar folding occurs for flat sheets formed by sandwiching DMAA and NIPA.

4.3.6 Multilayered Polymer Tubes

Our technique can be extended to synthesize multilayer tubes, as outlined in Figure 4.9. For this, a cylinder with one polymer layer (with agar intact in the core) is incubated in the APS initiator solution for 15 min (Figure 4.9b), essentially re-activating the structure for another polymerization. The initiator-loaded cylinder is then transferred into a second monomer solution (Figure 4.9c). The initiator diffuses out and induces “inside-out” growth of a second polymer layer distinct from the first layer and on the outside (Figure 4.9d). This process can be further repeated to generate additional layers. Both the composition and thickness of each layer can be controlled. As an example, the multilayer tube (after removal of the agar template) shown in Figure 4.9e,f has 3 layers: (1) DMAA-BIS, (2) DMAA-LAP and (3) DMAA-BIS. That is, the three layers are based on the same monomer, but different crosslinkers. Also, the thicknesses of the three layers are different: (535 μm

for layer 1, 1050 μm for layer 2, 300 μm for layer 3), which is achieved by varying the incubation time of the template in the three successive monomer solutions. To show the differences between the three layers, the entire tube is exposed to MB dye for 24 h and then washed. Only the LAP layer holds onto the MB dye whereas the dye gets washed off from the other layers. Thus, in Figure 4.9f, the inner and outer layers are colorless whereas the middle layer is dark blue.

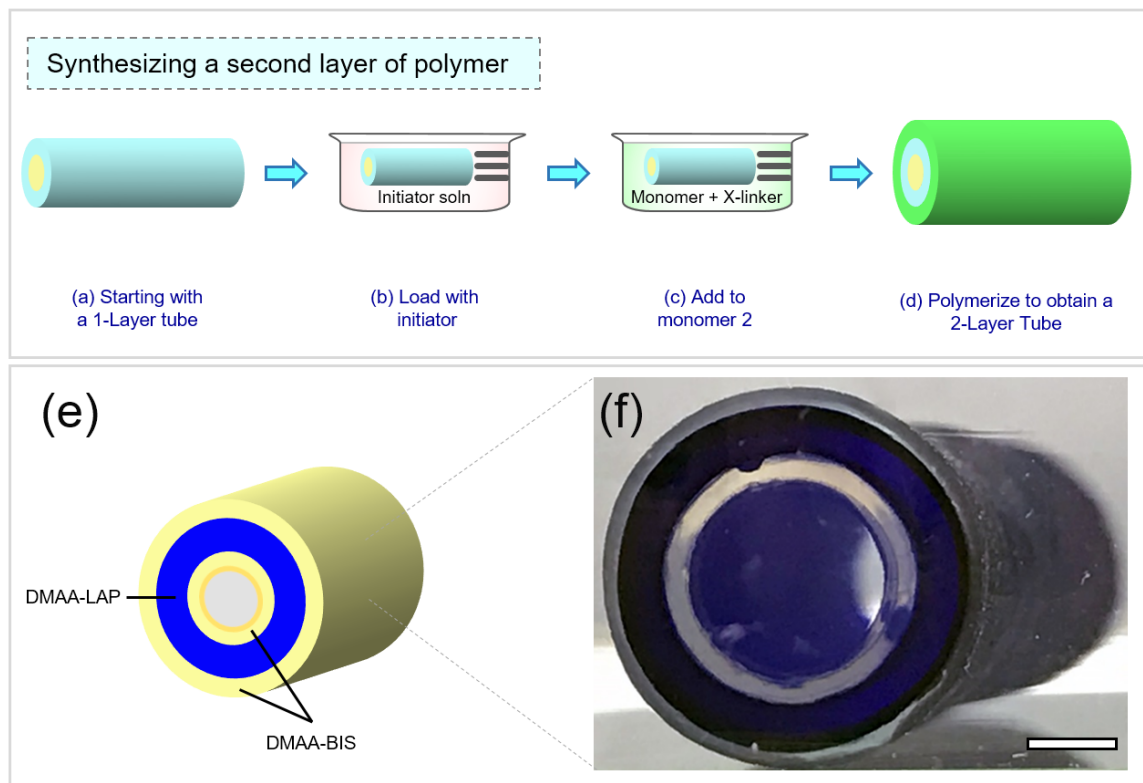


Figure 4.9. Synthesis of multilayer polymer tubes. A one-layer cylinder (with agar intact) is used as a new template for the synthesis of the next outside layer (a). The template is soaked in initiator (b) and then placed in monomer 2 solution (c), yielding a second polymer layer outside the first. This process is repeated to form additional layers. A three-layer tube is shown schematically in (e) and by a photo in (f). The layers differ in the crosslinker used: layers 1 and 3 have BIS as crosslinker while layer 2 has LAP as crosslinker. The differences between the layers are highlighted by the fact that only the LAP layer strongly binds MB dye, giving it a dark blue color. The scale bar is 2 mm.

Next, Figure 4.10 shows the synthesis of a tube that has varying numbers of layers over distinct lateral regions. First, a cylinder with one polymer layer (with agar intact in the core) is reloaded with initiator. This structure is partially submerged vertically in a monomer solution, as shown. The second polymer layer then only grows over the submerged portion. An example of such a tube (after removal of the agar core) is shown in Figure 4.10b. The tube changes from one to two layers at the point indicated by arrows. The inner layer is DMAA-LAP and the outer one is DMAA-BIS. When exposed to MB dye for 24 h, the inner layer alone gets stained dark blue (Figure 4.10c, d).

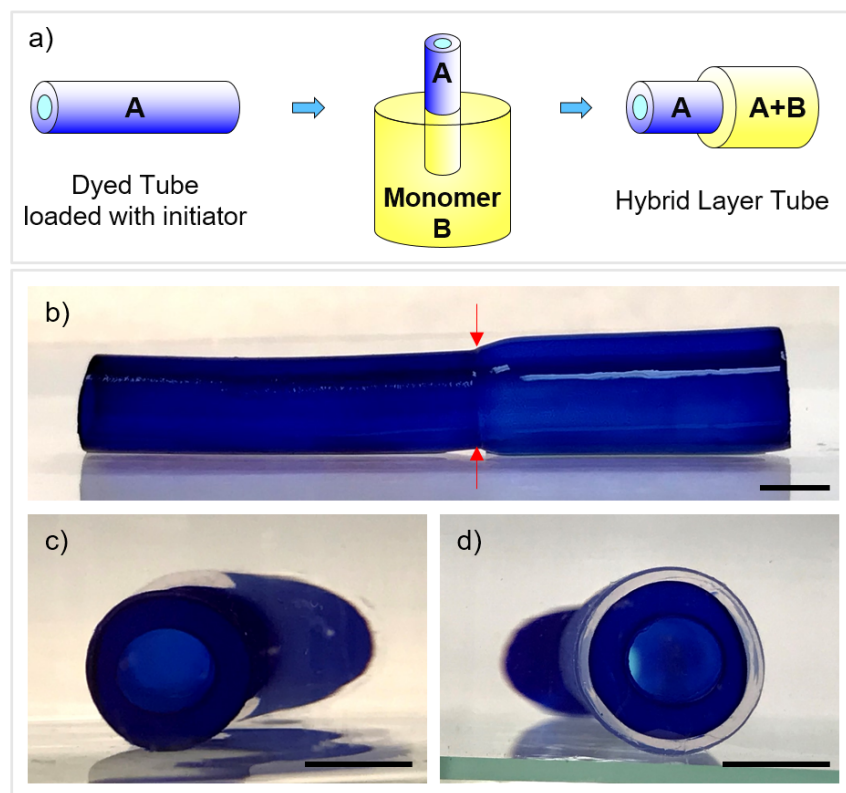


Figure 4.10. Synthesis of tubes with single-layer and multilayer regions. A one-layer cylinder (with agar intact) is loaded with initiator and placed vertically in a second monomer solution such that only a portion of the cylinder is submerged (a). As a result, the second polymer layer only forms over the submerged portion. Photos of such a tube are shown in different views from the top and sides (b-d). The one-layer portion is DMAA-LAP and the second layer is DMAA-BIS. Only the former strongly binds MB dye, giving it a dark blue color. The scale bars are 5 mm.

4.3.7 Chemical Post-Modification of Tube Layers

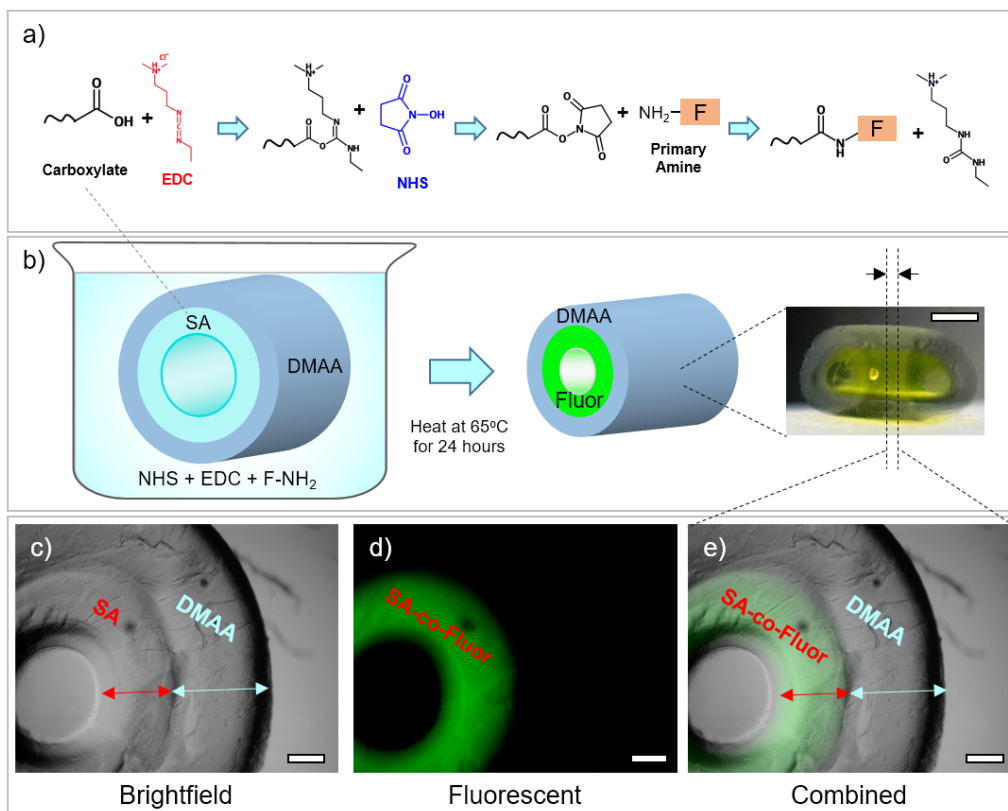


Figure 4.11. Post-modification of a specific layer in a multilayer tube. The tube has an outer layer of DMAA and an inner layer of SA, with the latter having carboxylate groups. The tube is reacted with EDC and NHS, and then with a primary amine via the reaction scheme shown in (a). The result is that the carboxylates become attached to the functional group F on the amine. The amine chosen here is fluoresceinamine (F-NH₂) and it imparts fluorescence to the inner layer. A yellow-green color is selectively seen visually for this layer after modification (b). The scale bar in the photo is 2 mm. The cross-section of the tube is viewed under fluorescence microscopy and the inner layer reveals bright green fluorescence (c-e). Scale bars in the images are 500 μ m.

Multilayer tubes that have different polymers in each layer can also be modified further after synthesis. This allows functionalities to be introduced into precise regions of a tube. For example, a tube could be decorated with molecules that can sense analytes flowing through the lumen, or with biological molecules (e.g. growth factors⁹⁴) to enable their use in tissue engineering. Towards this end, we demonstrate the modification of a

specific layer in a tube with fluorescent markers (Figure 4.11). We start with a two-layer DMAA-SA tube. The outer layer is DMAA while the inner layer is a copolymer of SA/DMAA in a 10/90 ratio of the total monomer (both layers are crosslinked with BIS). This tube is added to a solution containing the coupling agents EDC and NHS, and thereafter reacted with a primary amine, which in this case is fluoresceinamine (F-NH₂). Following reaction and washing, photos of the modified tube are shown in Figure 4.11b and fluorescence micrographs of the cross-section are shown in Figure 4.11c. We find that the F-NH₂ is indeed selectively attached to the inner SA layer while there is no modification to the outer DMAA layer.

4.4 Conclusions

We have presented a technique for the synthesis of polymer tubes with multiple layers, which mimic several features of blood vessels. The technique provides precise control over lumen diameter, wall thickness, numbers of layers and the chemistry of individual layers. Tubes can be patterned with different polymers either in the lateral or longitudinal directions. Patterned tubes based on stimuli-responsive polymers exhibit the ability to spontaneously change their lumen diameter in response to stimuli, or to convert from a straight to a curled shape. Tubes can also be post-modified to attach specific chemicals selectively to a given layer of a multilayer structure.

Chapter 5

Hairy Gel Surfaces

5.1 Introduction

In nature, many structures have hair or finger-like protrusions on them. For example, micro-organisms have hairs called cilia¹, which enable them to move in solution. Similarly, hair-like protrusions are found on the walls of the small intestine, and these are called villi.¹ They are highly flexible, gel-like structures and their primary function is to increase the surface area of the intestinal wall, which improves nutrient diffusion. The villi are actually hierarchical structures, i.e., each hair has smaller hairs called micro-villi that grow on top of it. Scientific interest in villi comes from their role in mediating various intestinal diseases, such as celiac disease and Crohn's disease.^{95,96} Some attempts have been made at synthesizing surfaces covered with hair-like structures.^{97,98} However, there still exists a need for a biocompatible and versatile method based on aqueous polymers for forming such hairy surfaces.

Herein, we report a technique to synthesize complex, hair-covered surfaces through “inside-out” polymerization. Briefly, the technique involves loading a template with a water-soluble free radical initiator and exposing this to a monomer solution. As the initiator diffuses out of the template, a layer of polymer grows outward from the surface of the template. To create hairs, we confine this outward growth to occur within channels carved out of a mold. Our method provides control over the length of the polymer hairs, their surface density, and most importantly, the composition of the hairs. We show that the

presence of hairs increases the surface area for adsorption of a solute from a bulk solution. Moreover, we create patterns of hairs of different kinds co-existing on the surface, including polymeric hairs that respond to stimuli, including temperature and magnetic fields. We also show that a hair-covered sheet can be induced to fold into a tube, thus giving rise to a structure similar to that of the small intestine, i.e. a tube with hairs emanating from the walls.

5.2 Experimental

Materials. The following were purchased from Sigma-Aldrich: the initiator ammonium persulfate (APS); the accelerant N,N,N',N'-tetramethylethylenediamine (TEMED); the monomers sodium acrylate (SA), acrylamide (AAM) and N,N'-dimethylacrylamide (DMAA); the crosslinker N,N'-methylene-bis(acrylamide) (BIS); the cationic dye methylene blue (MB); xanthan gum (XG); Agar was purchased from Living Jin. The nanoclay laponite XLG (LAP) was obtained as a gift from Southern Clay Products. Iron (III) oxide, magnetic Nanoarc® powder (MNPs) was purchased from Alfa Aesar. Carbon black (EC-600JD) (CB) was purchased from Akzo Nobel. Deionized (DI) water from a Millipore system was used for all experiments.

Fabrication of Agar Templates with an Array of Holes/Channels. An agar gel with an array of holes was created as follows (see Figure 5.1). First, agar powder was dissolved in 95°C DI water at a concentration of 5 wt%. Syringe needles were affixed on a glass microscope slide using epoxy adhesive, such that the needles formed an ordered array. This array was then placed in a beaker and the hot agar solution was poured to surround the

needles up to a given height (this height eventually determines the length of the hairs). After ~ 30 min at room temperature, the agar solidifies into a gel around the needles, and the needles were then removed. This leaves behind an agar gel with an array of holes running all the way through it. The dimensions of the holes depends on the diameter of the needles used. Typically, with 22.5-gauge needles, the holes were 0.71 mm in diameter.

Polymer Base Gel Fabrication. Single-layer polymer gels to use as the base for the hairs were fabricated by adding a given monomer solution into a Petri dish, followed by free-radical polymerization. A typical monomer solution had 10 wt% monomer, 0.34 wt% BIS (crosslinker), 15 mg/mL TEMED, and 4 mg/mL APS. Polymerization was conducted for 1 h under a nitrogen atmosphere. Subsequently, the polymer gel was removed and cut to the desired dimensions using a razor blade.

Multilayer polymer bases were fabricated in a similar way, but with controlled thicknesses. First, a solution of monomer 1 (e.g., DMAA, with overall composition as above), was placed between two glass slides separated by a spacer of 1 mm thickness. This was polymerized as above. Next, the spacer thickness was increased to 2 mm and a solution of monomer 2 (e.g., AAm) was introduced into the vacant space and polymerized. The slides were then removed to yield a multilayer gel, with two layers (DMAA and AAm), each of 1 mm thickness. This gel was then cut to the desired dimensions using a razor blade.

Synthesis of Hairy Gels. Hairy gels were fabricated using the holey agar template and the polymer base gel (Figure 5.1). First, the base gel was incubated for 20 min in a 20 mg/mL solution of APS initiator. Simultaneously, the holes (channels) in the agar template were loaded with monomer. A typical monomer solution had 10 wt% monomer, 0.34 wt% BIS (crosslinker), 1 wt% LAP particles, and 10 mg/mL TEMED. Loading of monomer into the channels was done either by capillary rise or by filling each channel directly using a micropipette. The latter was used if the channels were relatively long (> 13 mm) or wide (> 1.25 mm in diameter). The agar template with monomer-filled channels was allowed to rest in a container in ~ 0.5 mm depth of monomer solution to prevent monomer from evacuating the channels. The initiator-loaded base gel was then placed over the top of the agar template. This system was allowed to polymerize at room temperature for 2 h under a nitrogen atmosphere. At this point, polymer hairs are connected to the base gel, but are surrounded by agar. To remove the agar template, the entire structure is placed in 90°C DI water for 1 h, whereupon the agar gel melts to a liquid. This reveals the hairs on the surface of the base gel.

Patterns of Hairs. The process for creating spatial patterns of different hairs on a gel is identical to that for making a gel with one type of hair. In this case, selected channels are filled with different monomer solutions. For magnetic hairs, the monomer solution contained 10 wt% DMAA, 0.1 wt% BIS, 2 wt% LAP, 10 mg/mL TEMED, and 0.2 wt% MNPs. For black hairs, the MNPs in the above solution were replaced with 0.1 wt% CB.

Dye Adsorption Experiments. The comparison of dye adsorption between a base gel and hairy gel was done with the following materials. First, base gels were synthesized from a solution of 10 wt% DMAA, 0.34 wt% BIS, 1 wt% LAP, 4 mg/mL APS and 15 mg/mL TEMED. Two square base gels with a side length of 22.5 mm and a thickness of 1.5 mm were cut from the above base gel. One base gel was stored in DI Water. On the second base gel a 5 × 5 array of hairs of 10 mm length and 0.9 mm diameter were These hairs were composed of 10 wt% DMAA, 0.34 wt% BIS and 1 wt% LAP, which is the same composition as the base gel.

The dye adsorption tests were performed in two separate beakers, each containing 30 mL of 10 μM MB dye. The base and hairy gel were placed into the separate beakers, and the solution was stirred with a magnetic stir bar. At different time points, a 1 mL aliquot of the supernatant was removed from each solution and analyzed on a Cary 50 UV-Vis spectrophotometer at a wavelength of 665 nm (absorbance peak of MB). Photos were also taken of the beakers over time. Following a 2 h period, the beakers were transferred to a shaker table, where they were allowed to mix for a full 24 h, at which point a final sample was analyzed in each case.

Multilayer Hairs. Multilayer hairs were synthesized using a hairy gel as a template. The hairy gel used here had hairs made as noted earlier: the base was DMAA-BIS, and the hairs were DMAA-BIS-LAP. Also, the hairs were colored blue by exposure to MB dye. This hairy gel was incubated in a 20 mg/mL solution of APS for 20 min. The gel was then removed and placed at the bottom of a container having a second monomer solution. The

composition of this solution was 10 wt% AAm, 0.34 wt% BIS and 10 mg/mL TEMED. Additionally, 0.1wt% of xanthan gum (XG) was added to this solution to make it slightly viscous. XG was included to prevent hairs from moving excessively during the polymerization of the second layer. After a layer of sufficient thickness had formed, which took ~ 10 min, the whole gel was removed and washed with DI water.

5.3 Results and Discussion

5.3.1 Synthesis of Hairy Gel Surfaces

Our technique for producing hair-covered gel surfaces relies on the diffusion of initiator from a base gel through liquid columns in a holey agar template that contain monomer (Figure 5.1). For this, we first make a base polymer gel, typically using the monomer DMAA and BIS as the crosslinker. This gel is then cut to desired dimensions (typically a cuboid with 1 mm depth and a square face with sides of 22 mm) (Figure 5.1 a-b). The holey agar template in which the hairs will grow is synthesized next. For this, we place an array of syringe needles of a selected diameter into a container and pour a hot agar solution around them up to a desired height (Figure 5.1c). The system is allowed to cool to room-temperature, at which point the agar solidifies into a gel. The needles are removed to yield an agar gel with an array of holes (channels) running all the way through it (Figure 5.1d). These channels are then filled with a solution containing 10 wt% of a monomer, 0.34 wt% BIS, 1 wt% LAP particles, and 10 mg/mL of TEMED. Filling of monomer into the channels is done either by capillary rise or by manual pipetting (Figure 5.1e). Next, the base gel is incubated for ~15 min in a 20 mg/mL solution of water soluble free-radical initiator, typically APS (Figure 5.1f). The initiator-loaded base gel is then placed over the monomer-filled agar template (Figure 5.1g) such that the two are in intimate contact. Subsequently, the APS will diffuse through the monomer-filled channels in the agar template, and this will initiate the polymerization of the monomers into a gel. Note that diffusion occurs in a direction away from the initiator-laden gel, i.e., the hair grows downward in Figure 5.1h.

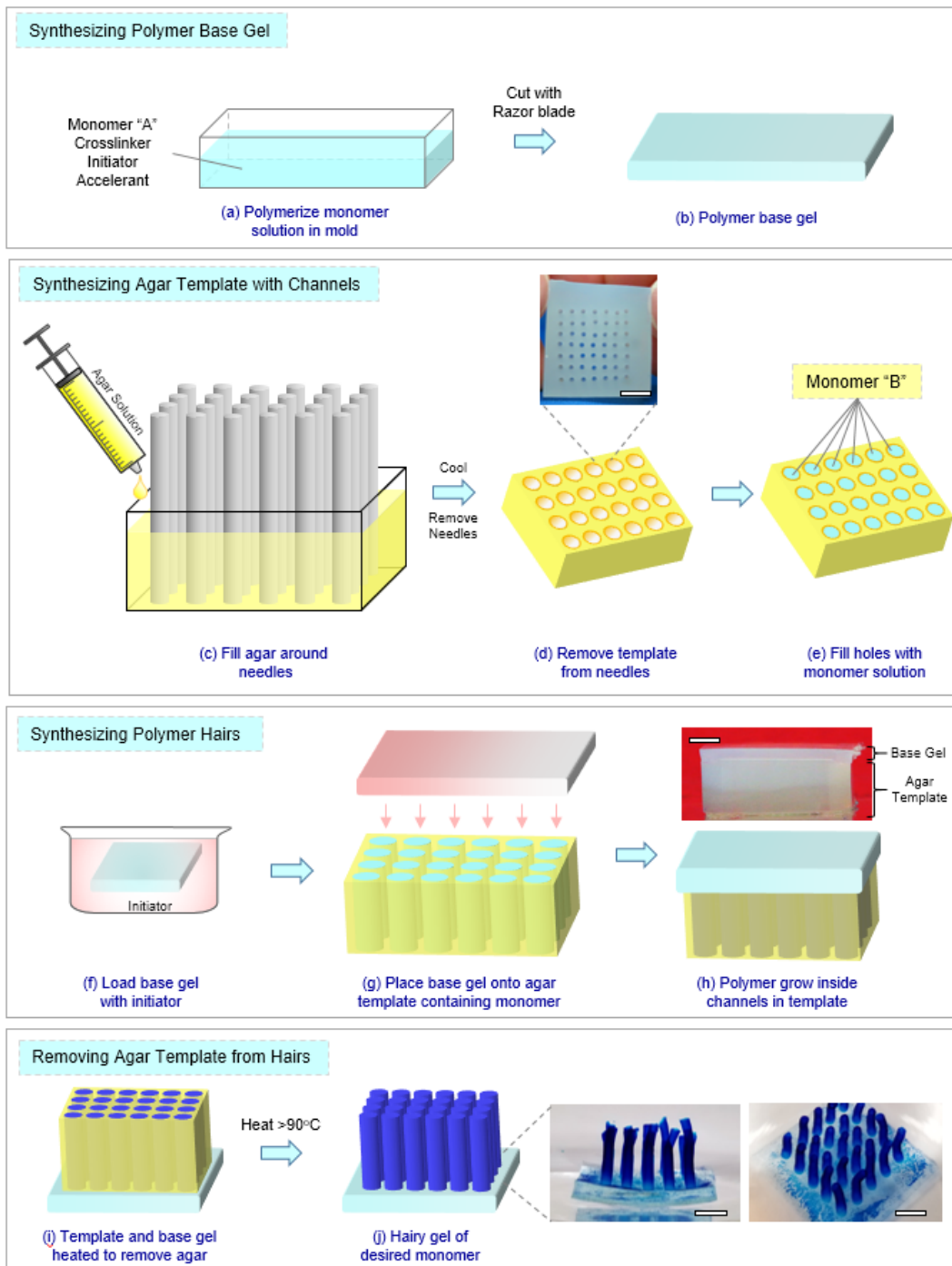


Figure 5.1. Synthesis of Hairy Gels. First a base gel, typically of DMAA, is made and cut to the desired size. Second, agar is poured around a syringe needle array (c) and cooled to produce a gel. When the needles are removed, we have a holey agar template with channels (d), which are filled with a monomer solution (e). The base gel is loaded with initiator (f) and placed atop the monomer-filled agar template (g). The initiator diffuses into the channels and forms polymer (h). Finally, the agar is dissolved by heat (i) to yield a hairy gel (j). Images of hairy gels in (k). All scale bars are 5 mm.

Once the polymerization is complete, the hairs are still embedded in an agar gel. (Figure 5.1i). We then heat the structure to $\sim 90^{\circ}\text{C}$ in DI water to liquefy and get rid of the agar gel, thereby revealing the hairs (Figure 5.1j). The hairs are still attached to the base gel since they grow outward from this gel. (Note that the structure in Figure 5.1j is inverted relative to the same structure during synthesis.) In the scheme above, both the hairs and base are made from the same monomer (DMAA), but with differing crosslinkers. The base is made with BIS as the crosslinker, while for the hairs we use a combination of BIS and LAP particles as the crosslinkers. The reasons for using LAP are described below. The images in Figure 5.1k show dark blue hairs, which show high visual contrast from the base and from the solution they are in. This color is due to adsorption of a blue dye onto the LAP particles in the hairs (see below). The base is colorless since it does not have LAP particles. The hairs in this image are ~ 10 mm long and 1.25 mm in diameter. They are arranged in a 5×5 array with a lateral spacing of 1.5 mm between adjacent hairs. Note also that the hairs are usually studied with the overall structure in solution. If taken out of solution, the hairs tend to collapse sideways, but return to standing when placed in solution.

5.3.2 LAP-Bearing Hairs and their Staining

For most of our hairy gels, the base is synthesized without LAP, and the hairs with LAP. The benefit of LAP is two-fold. First, LAP particles, which are disks of 25 nm diameter and 1 nm thickness, are known to serve as crosslinkers for growing polymer chains (Figure 5.2a). Moreover, the use of LAP leads to gels that are flexible, and this is indeed the case with our hairs, i.e., they are flexible and “wavy” when they contain LAP. Secondly, our hairs (with or without LAP) are optically transparent and hence difficult to

discern. For this reason, it is necessary to provide contrast to the hairs, and one way to do so is by exploiting the anionic nature of LAP disks, which have a high affinity for cationic dyes. This is shown by Figure 5.2. When a colorless hairy gel is placed in a solution of the cationic dye, methylene blue (MB) at a concentration of $10\ \mu\text{M}$, the MB molecules adsorb on the faces of LAP disks, turning the layer blue.^{90,93} We can impart either a light blue (Figure 4.5b) or a dark blue (Figure 4.5c) color, depending on the soaking in the MB solution. Note that dye adsorption to LAP is irreversible; thus, the dye does not subsequently diffuse out of the hairs. Also, the base that does not have LAP does not get stained by the MB, i.e., any absorbed dye in the base gets removed by diffusion.

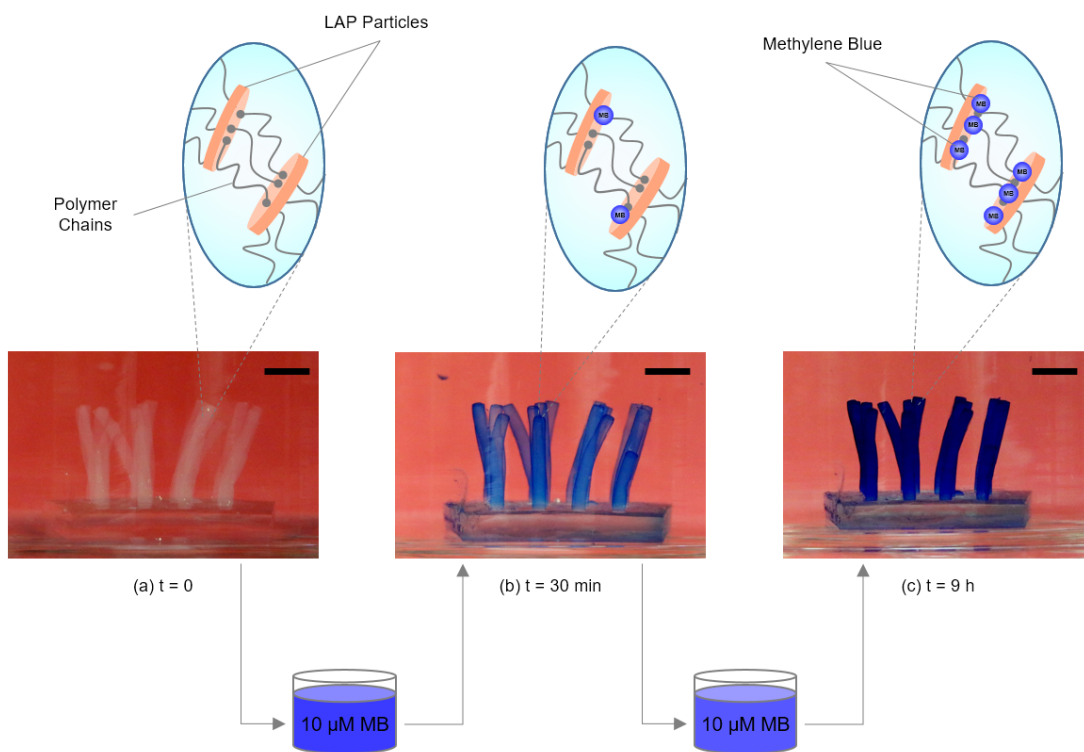


Figure 5.2. Staining of LAP-bearing hairs with a cationic dye. The LAP particles serve as crosslinkers for polymer chains in the hairs, as shown by the schematics. The hairs are initially transparent (a). When placed in a $10\ \mu\text{M}$ solution of methylene blue (MB) for 30 min, the hairs take on a light-blue color (b), while incubation in the same solution for 9 h gives the hairs a dark blue color (c). The color is due to adsorption of the cationic MB on the anionic faces of the LAP particles, as shown by the schematics in (b) and (c). Scale bars in the images are 5 mm.

5.3.3 Hairy Gels with Tailored Dimensions

Biological villi in the small intestine vary between individuals in diameter, height and spacing. Thus, we were interested in modulating the same variables through our synthesis technique. First, we show that we can synthesize hairs in a variety of spacings. Hairs in a 3×3 array, a 5×5 array, and a 8×8 array are shown in Figure 5.3a-c. All were synthesized on a base of the same area, a square of 14.5 mm length. The different arrays correspond to different numbers of needles chosen for the holey agar template. Second, we vary hair thickness. The hairs in Figure 5.3a have a diameter of 2.4 mm (corresponding to 13-gauge needles used in making the template) and those in Figure 5.3b-c have a diameter of 0.71 mm (22.5-gauge needles). Finally, we vary the height of the hairs, which is done by filling the agar solution to different heights in Figure 5.1c. The hairs in Figure 5.3b have a height of ~ 3 mm while those in Figures 5.3a and 5.3c have a height of ~ 10 mm.

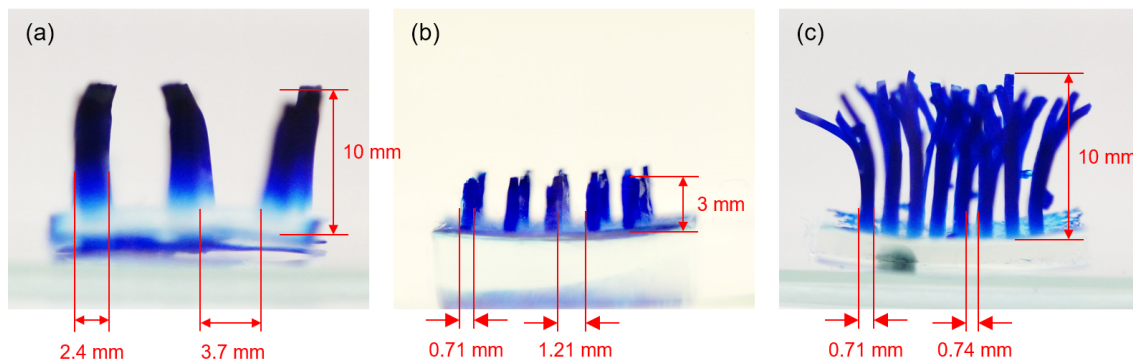


Figure 5.3. Hairs of varying dimensions and spacing. The height, diameter, and spacing between hairs are varied, as shown in the photos. All hairs were fabricated on a base of the same dimensions, i.e. a 14.5×14.5 mm square.

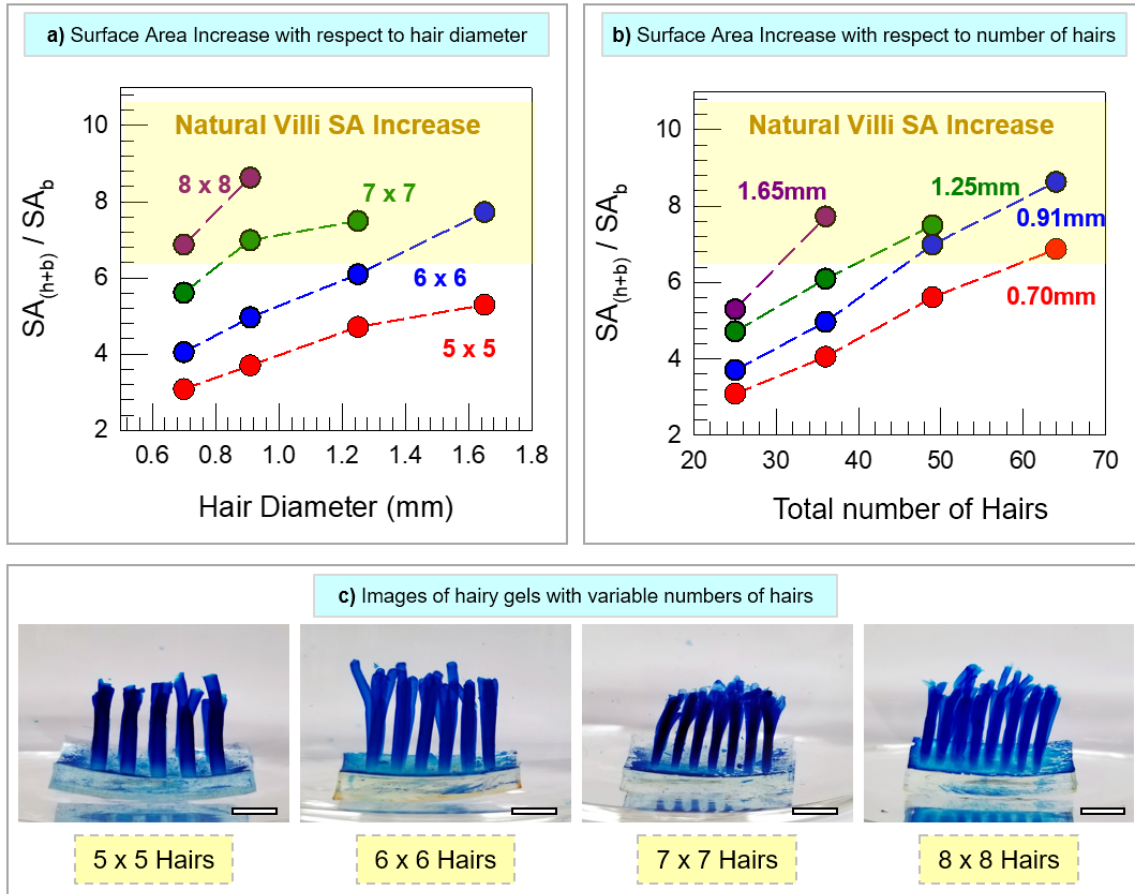


Figure 5.4. Surface area increase for hairy gels vs base gels. The ratio of the surface area of the hairs + base gel, $SA_{(h+b)}$ to the surface area of just a base gel SA_b is plotted in (a) as a function of the hair diameter and in (b) as a function of the total number of hairs. The yellow box demarcates the typical increase in surface area seen for an intestine covered with villi over a flat intestine. Inset (c) shows images of hairy gels with different hair densities, from 5×5 to 8×8 for a constant hair diameter of 0.9 mm. Scale bars are 5mm.

The presence of villi on intestinal walls increases the surface area of the small intestine between 6 and 10 times. In Figure 5.4. we present data for the increase in surface area achieved by various combinations of hair diameters and spacing. The plotted variable on the y-axis is the ratio between the surface area of the hairy gel (i.e. $SA_{(h+b)}$ for Hairs + Base) and the surface area of only the base gel (SA_b). This is plotted as a function of hair diameter in Figure 5.4a and vs. the total number of hairs in Figure 5.4b. Each colored line in Figure 5.4a corresponds to a different array of the hairs (5×5 to 8×8), while each line

in Figure 5.4b corresponds to a different hair diameter. All hairy gels were fabricated on a square base of 14×14 mm, with hairs spaced evenly along the lengths of a side. Hairs were synthesized at a length of 8 mm, and individual hairs were measured using electronic calipers to confirm dimensions post-synthesis. The yellow region across Figures 5.4a and 5.4b indicates the typical surface area increase seen in the case of biological villi.^{25,99} The data show that we approach this biological range with our denser hair arrays.

5.3.4 Dye Adsorption by Hairy vs. Base Gels

As previously stated, villi improve nutrient transport through the small intestine by increasing the surface area for adsorption. To mimic this behavior, we have studied the adsorption of a dye from solution by a flat gel with no hairs (base gel) compared to an identical hairy gel. For this purpose, we synthesized a base gel of the composition 10 wt% DMAA, 0.34 wt% BIS, and 1 wt% LAP. This was sectioned into two 22.5×22.5 mm squares, and one such base gel was used as is. Hairs were grown from the surface of the second base gel, with the hairs having an identical composition to the above. We then compared the two gels for their ability to extract MB from an aqueous solution. Each gel was placed in a separate beaker containing a $10 \mu\text{M}$ solution of MB (Figure 5.5), and monitored for 2 h by UV-Vis spectroscopy. Thereafter, the beakers were transferred to a shaker table, where they were allowed to mix for a full 24 h, at which point a final sample was analyzed in each case. The results are plotted in Figure 5.5c, with the inset showing the data over the first hour. Photos at selected time points of the solution containing the base gel are shown in Figure 5.5a and for the hairy gel in Figure 5.5b.

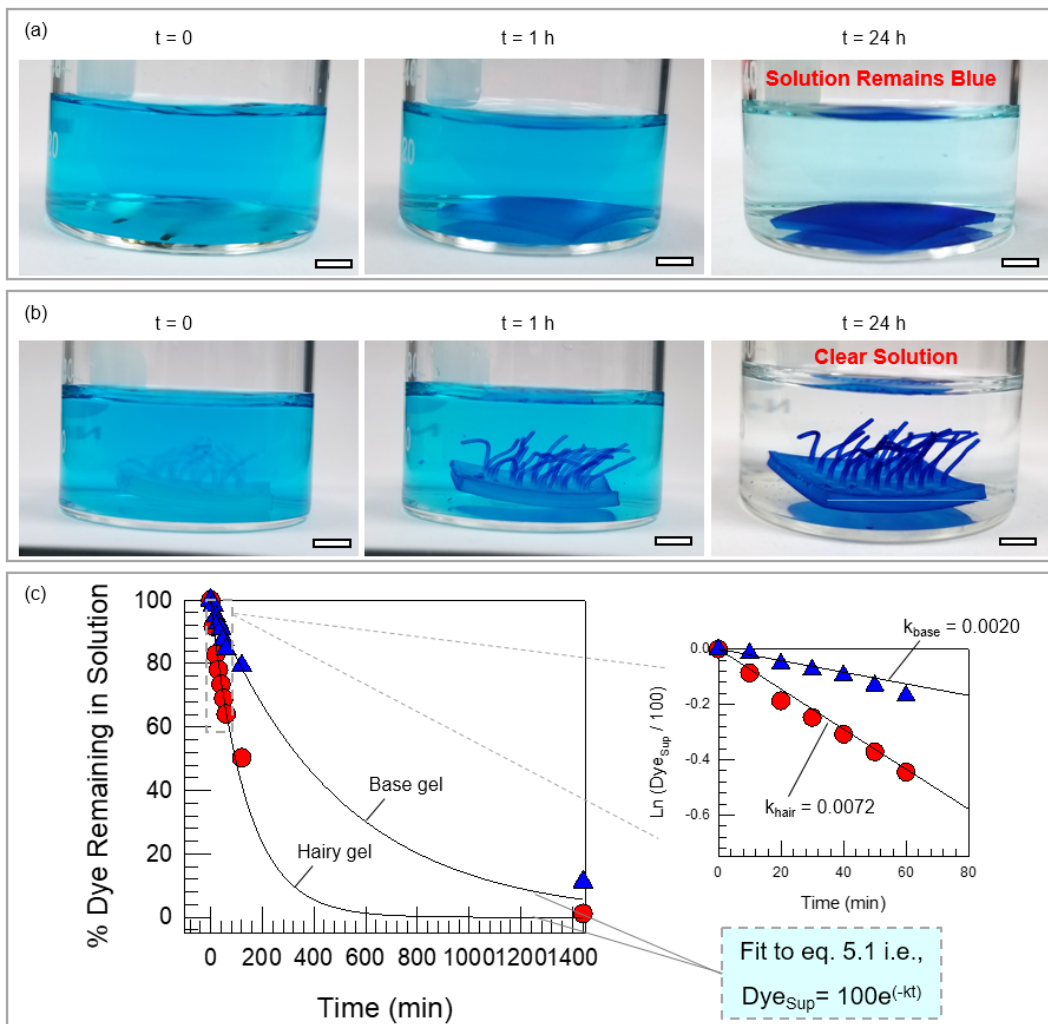


Figure 5.5. Dye adsorption of hairy vs base gels. A base gel and a hairy gel of identical composition (both contain LAP) are compared for their ability to absorb MB dye from water. Photos of the base gel (a) and hairy gel (b) in MB solution at different time points. The hairy gel samples show a lighter color, indicating more dye removal. (c) Dye% in solution as a function of time plotted for the base and hairy gels, confirming more rapid dye removal by the latter. The inset is a semilog plot of the initial ~ 1 h of the data. The slopes of the lines yield the decay constants k for each gel. The value of k_{hair} is about thrice the value of k_{base} . Scale bars are 5 mm.

We note from the photos that after 24 h, the base gel in Figure 5.5a shows a deep blue color while the solution still has a light blue color, indicating residual MB dye in solution. In comparison, the solution containing the hairy gel is practically colorless after 24 h, indicating that most of the MB has been removed. Both the hairs as well as the base

of this gel are deep blue. The UV-Vis data for the dye in the supernatant is normalized and presented in Figure 5.5c. The data indicate faster removal of dye by the hairy gel. Both the hairy gel and base gel data can be fit to an exponential decay:

$$\text{Dye}\% = 100 e^{-kt} \quad (5.1)$$

where Dye% is the percent of dye remaining in the supernatant, and k is a decay constant. The inset shows the data over roughly the first hour of the experiment, and this is plotted in a semilog fashion. From the slopes of the lines on this plot, we can calculate the decay constants. For the hairy gel $k_{\text{hair}} = 7.2 \times 10^{-3} \text{ min}^{-1}$ and for the base gel $k_{\text{base}} = 2.0 \times 10^{-3} \text{ min}^{-1}$. Thus, k_{hair} is more than thrice k_{base} , which confirms the large increase in dye adsorption by the hairy gel.

5.3.5 Gels with Stimuli-Responsive Hairs

In addition to villi in the intestine, other hair-like structures in nature include the cilia on microbes, which exert a characteristic “beating” motion that transports the microbe through fluids. To mimic the “beating” motion, we synthesized hairy gels with magnetic hairs. Alternating rows of magnetic and non-magnetic hairs were polymerized on the surface of a DMAA-BIS base gel. Both hairs contained LAP for flexibility. For the magnetic hairs, we included 0.2 wt% MNPs (Fe_2O_3) in a DMAA-BIS-LAP gel, and these hairs have a brown color. In the non-magnetic hairs, we used the same composition of monomers, but replaced the MNPs with 0.1 wt% CB nanoparticles. These hairs have a black color due to the CB. Figure 5.6 shows the response of the above hairy gel to a magnet placed to the left of the container while the gel is in DI water. Initially, in the absence of a magnetic field, both sets of hairs stand straight up from the surface (Figure 5.6a). In the

presence of a magnetic field, the responsive hairs bend towards the magnet, while the non-magnetic hairs remain vertical (Figure 5.6b). When the magnetic field is removed, the magnetic hairs return to their original position (Figure 5.6c). This behavior demonstrates that the hairs are magnetically responsive, and that a periodic magnetic field can be used to make the hairs “beat” in a manner similar to that of cilia.

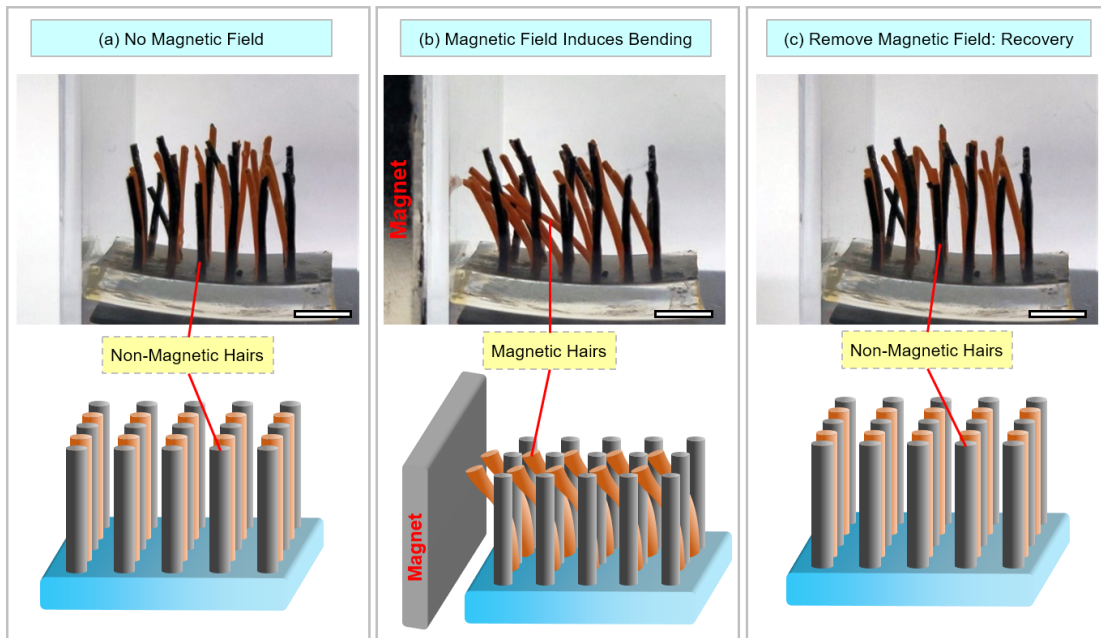


Figure 5.6. Stimuli-responsive rows of hairs. Rows of magnetically responsive hairs (brown color, due to MNPs in the hairs) (brown) alternate with non-responsive hairs (black due to CB in the hairs) on the base gel. Both photos (top) and schematics (bottom) are shown. In (a), with no magnetic field, both hairs stand vertically. In (b), when a magnet is placed on the left, the magnetic hairs bend toward the gel, while the non-responsive hairs remain vertical. In (c), the magnetic field is removed and all hairs return to the vertical position. Scale bars are 5 mm.

5.3.6 Multilayer Hairs

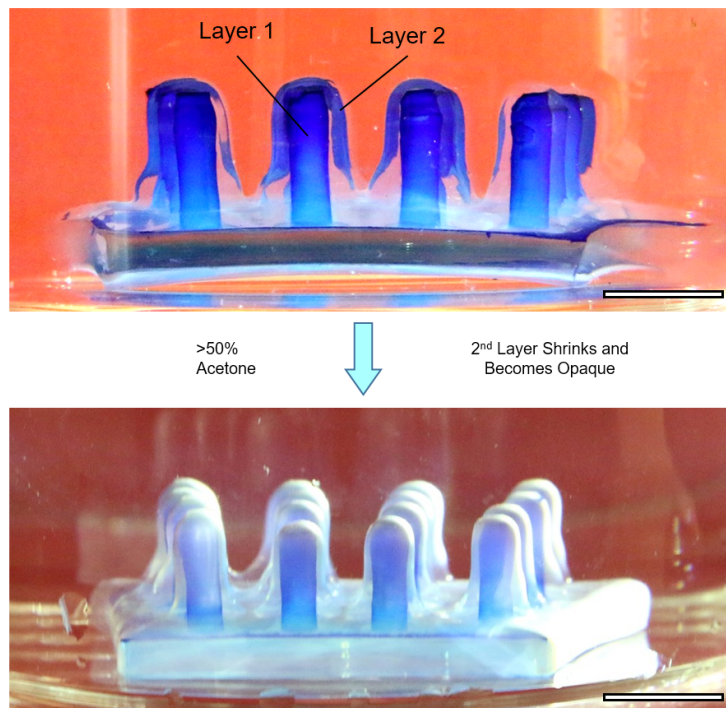


Figure 5.7. Multilayered hairs. Each hair has an inner layer of DMAA-LAP (blue due to adsorbed MB dye) and an outer layer of AAm-BIS. In water (top), both layers are swollen. In 60% acetone the outer AAm layer shrinks and becomes turbid. Scale bars are 5 mm.

To synthesize multilayered hairs, we first start with a previously synthesized hairy gel, specifically one with hairs of DMAA-LAP, with adsorbed MB for visualization. We incubate this gel in a 20 mg/mL APS solution for 20 min, then move it to a container with a second monomer solution, which in this case is acrylamide (AAm) with BIS as the crosslinker. The initiator diffuses outward from the hairs and base to create a second layer of hairs over the first. At this point, we have a hairy gel with an inner blue layer of DMAA-LAP, covered by a transparent layer of AAm-BIS hairs (Figure 5.7a). AAm is known to shrink and become turbid in solutions of $> 50\%$ acetone, whereas DMAA is unaffected by

acetone. Thus, when the whole gel is placed in a 60% acetone solution, we see the inner blue hairs of DMAA-LAP surrounded by the turbid layer of AAm-BIS in Figure 5.7b.

5.3.7 Hairy Gels with Stimuli-Responsive Bases

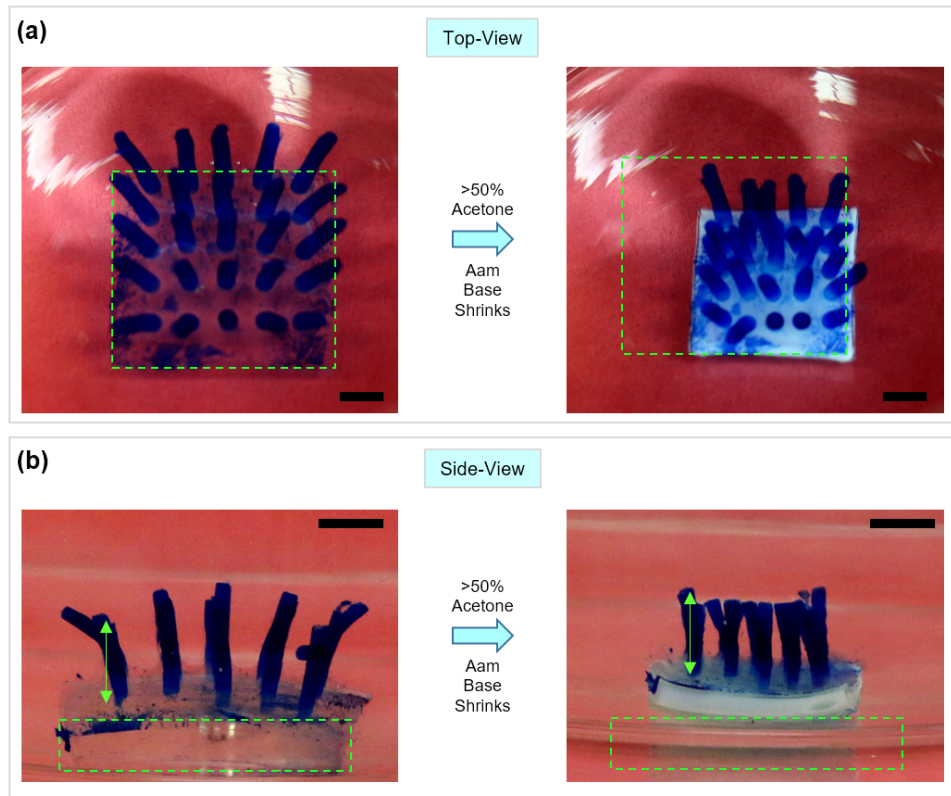


Figure 5.8. Hairy gel with a stimuli-responsive base. The hairs are DMAA-LAP on top of a base of AAm-BIS. The whole gel is placed in a 60% acetone solution. The top-view of the response is shown in (a) and the side view in (b). The base gel shrinks, but the hairs remain the same height. The dashed lines show the initial dimensions of the base gel. Due to the shrinking, the distance between adjacent hairs shrinks from 2.7 to 1.3 mm. Scale bars are 5 mm.

Previously we studied how hairs created from stimuli-responsive materials behave in interesting ways. Next, we study the case where the base alone is stimuli-responsive. Here, the hairs are made of DMAA-LAP and are stained blue by MB. The base is AAm-BIS. Figure 5.8 shows images of this gel immersed in a 60% acetone solution. As was

noted in Figure 5.7, AAm shrinks and becomes turbid while DMAA is unaffected. Thus, in this case, the base shrinks by about 50% of its initial area, and so all the original hairs are packed more densely in a smaller area. The spacing between hairs along the front edge of the gel changes from ~ 2.7 mm initially to ~ 1.3 mm once the base shrinks. The vertical arrows indicate that the hairs remain at roughly the same height.

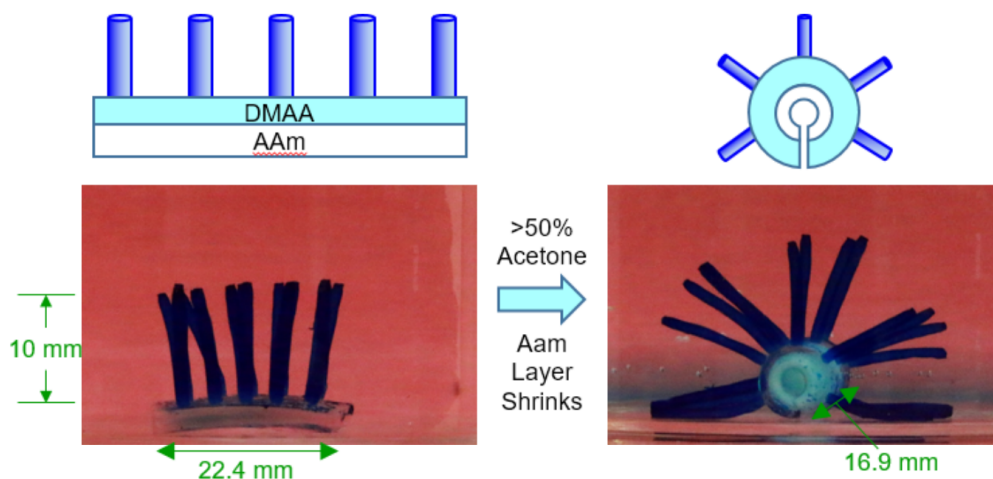


Figure 5.9. Hairy gel with a bilayer base showing a shape change to an insect-like structure in response to solvent composition. The base has two layers, AAm and DMAA, both crosslinked with BIS, and hairs of DMAA-LAP are grown on the DMAA side of the bilayer. In acetone, the AAm layer shrinks, causing the base to curl into a tube. The DMAA layer, and the hairs, are on the outside of this tube, which thereby resembles an insect.

Next, we create hairs on a bilayer base. Bilayer bases are formed by polymerizing a first layer of monomer, followed by adding a second monomer and polymerizing that one as well. The two polymer networks in the bilayer are bonded at the interface because the second monomer will interpenetrate a bit into the first layer before it is polymerized. The first bilayer base studied here has a lower AAm and an upper DMAA layer, both crosslinked with BIS (Figure 5.9). We then form DMAA-LAP hairs on the DMAA layer

of the base, and these are again stained blue by MB. When this hairy gel is placed in 60% acetone, the AAm layer shrinks. This shrinking causes the bilayer base gel to curl toward the AAm layer, away from the hairs. Ultimately, this results in a tubular structure with hairs on the outside, which on the whole resembles an insect.

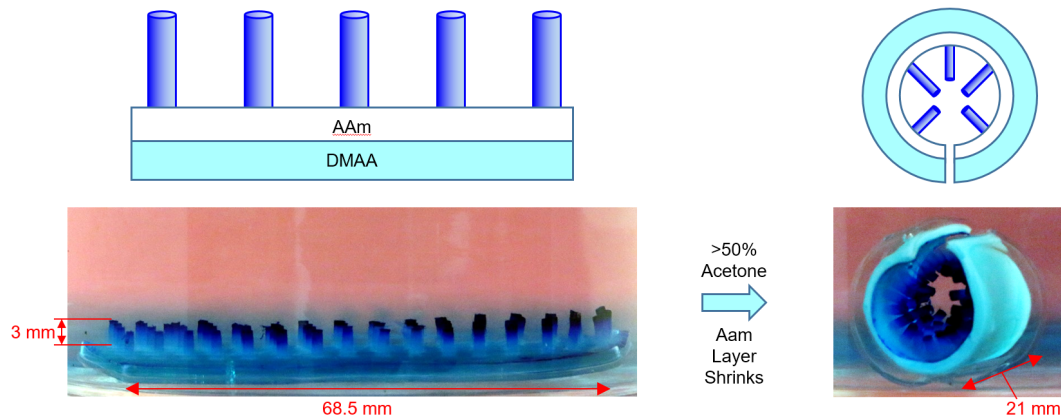


Figure 5.10. Hairy gel with a bilayer base showing a shape change to an intestine-like tube in response to solvent composition. The base has two layers, AAm and DMAA, both crosslinked with BIS, and hairs of DMAA-LAP are grown on the AAm side of the bilayer. In acetone, the AAm layer shrinks, causing the base to curl into a tube. The hairs are attached to the AAm layer, which means the hairs are now positioned on the inside of the tube. This structure is similar to that of the small intestine.

Next, we study the opposite case, in which hairs of DMAA-LAP are formed on the AAm side of the AAm/DMAA bilayer gel, as shown in Figure 5.10. Again, the hairy gel is placed in 60% acetone, and the AAm layer shrinks. The result is that the bilayer base gel curls towards the AAm layer, leading to a curled tubular structure with hairs on the inside of the tube. This structure is similar to that of the small intestine, which has the villi on the inside wall. To our knowledge, this is the first example of such a complex shape in the literature.

5.4 Conclusions

We have presented a technique for the synthesis of biomimetic hair-like structures that grow outward from a base polymer gel. The addition of hairs serves to increase the net surface area of the base gel by nearly 10-fold. This increase is comparable to the surface area increase provided by villi on the inner walls of small intestines. We can impart stimuli-responsive properties to the hairs (e.g., magnetic properties), and we can also induce such hairy gels to fold into tubes with hairs on the outside or inside. We believe the complex and unique structures of these gels are unlike any in the current literature. These types of materials should hold great interest for study as biomimetic models and as possible tissue engineering scaffolds.

Chapter 6

Conclusions and Recommendations

6.1 Project Summary and Principal Contributions

In this dissertation, we have presented a novel “inside-out” synthesis technique to create biomimetic multilayered materials. Specifically, we created multilayered spheres, tubes and surfaces with controlled morphology. The individual layer chemistry, and size, of each material can be tailored precisely over a range of length-scales (i.e. micro to centimeter sizes). Additionally, all the synthesized materials were created with hydrogels, which are similar to biological tissue.

In Chapter 3, we present a bioinspired “inside-out” technique for the synthesis of multilayered capsules. First, we present the synthesis of capsules with concentric layers of responsive and non-responsive polymers. We demonstrate that changes in external stimuli cause the thickness of individual layers to change dramatically. Additionally, we use stimuli-responsive layers to control the permeability of small molecules. Thus, we demonstrate pulsatile and step-wise release of solutes, which could be employed in the release of drugs or other compounds. Finally, we demonstrate that the addition of a thin, elastic layer of polymer to a fragile core particle improves the mechanical properties of the core. This layer provides protection to the encapsulated material.

In Chapter 4, we extend our “inside-out” technique to the synthesis of multilayered polymer tubes. Here, we demonstrate precise control over individual tube inner diameter, polymer layer thickness and chemistry. Additionally, we demonstrate the patterning of stimuli-responsive materials in tubes. The triggering of these stimuli-responsive materials

by external sources causes unique behavior in the polymer tubes. For example, spontaneous changes in lumen diameter, or causing a straight tube to curl. Behavior like the spontaneous change in diameter is similar to blood vessels found in the body. Furthermore, we demonstrate the chemical modification of a specific layer within a multilayered tube architecture with a fluorescent dye, which may be extended to modification with other chemicals (e.g. growth factors, catalysts, etc.).

In Chapter 5, we employ our technique to create hair-like protrusions on the surface of polymer gels. We demonstrate specific control over hair diameter, length and spacing. Hair-like protrusions in nature serve to increase the surface area of materials, and we demonstrate that our hair covered surfaces achieve the same purpose. We demonstrate this surface area increase through a dye adsorption experiment in which a hair covered gel removes solutes from a solution much faster than a gel without hairs. We incorporate stimuli-responsive materials into the hairs, and demonstrate the movement of hairs based on an external stimulus. Finally, we demonstrate that by growing hairs on stimuli-responsive surfaces we can cause these surfaces to fold into unique tubular structures, with hairs on the inner or outer surface depending on orientation. The former is mimetic of the structure of the small intestine, a tube with hairs on the inside surface.

6.2 Recommendations for Future Work

6.2.1 Mechanical Properties of Multilayered Capsules

In Chapter 3 we discuss the synthesis of capsules with thin layers of elastic materials. The elastic nature of the polymer layer helps to protect fragile cargo (e.g. alginate

core particles). Here, we propose to further study the mechanical properties of multilayered capsules. We have observed that, in addition to the protective properties of these elastic polymer layers, the elastic layers cause these capsules to bounce. In this study we will examine the complex interplay between core and polymer layer mechanical properties. For example, in a simple case, an Alginate core does not bounce much, but when surrounded by a small layer of DMAA the whole capsule bounces noticeably more. We will extend this study to a number of other cases to better learn how to tune the mechanical properties of these capsules. For example, what happens when there are multiple elastic layers in structure? What if some of the layers are elastic, and other layers are non-elastic? If shear-thickening materials are incorporated into the core, or specific layers, does this change the overall properties of the capsule? We intend to examine these qualities through Coefficient of Restitution (which is directly related to elasticity of a collision) measurements in conjunction with Rheological studies of the materials present. We believe the ability to predictively tune the mechanical properties of these capsules, and their layers, could be useful in applications from drug delivery to industrial reactions.

6.2.2 Multilayered Hydrogel Materials as Tissue Engineering Scaffolds

The field of tissue engineering has grown immensely in recent years, with the ultimate goal of augmenting or replacing existing tissues within the body. Hydrogels are attractive materials for tissue engineering applications, due to their similarity to tissues.^{100,101} Most of the scaffolds employed in tissue engineering are simple, and lack the level of complexity found in natural tissues.^{79,82,87} We propose to employ the materials synthesized in Chapters 4 and 5 as complex tissue engineering scaffolds. We believe this may be accomplished in two ways. First, through the incorporation of monomers which

are known to promote the growth of cells. For example, materials like methacrylate-modified gelatins^{102,103} have been successfully employed as tissue scaffolds. This type of material can be directly incorporated into our “inside-out” polymerization technique to generate multilayered tubes and hairy surfaces which would act as scaffolds for tissue growth. The second way these materials could be modified to act as tissue scaffolds is through the direct conjugation of growth factors for different types of cells. It has been reported in literature that conjugation or incorporation of growth factors into tissue scaffolds promotes the growth of certain types of cells.^{94,104,105} In Chapter 4 we demonstrated the direct modification of a specific zone of polymer within a multilayered architecture. Multilayered tubes and hairy surfaces could be similarly chemically modified with growth factors to promote the growth of certain cells on these structures.

6.2.3 Organic-Inorganic Hybrid Materials

Throughout this dissertation we have discussed the fascinating structure of the egg as a multilayered material. However, the egg is also interesting in that it combines organic (e.g. yolk, albumin, etc.) and inorganic (e.g. eggshell) components in one structure.^{1,7} We observe a number of other interesting materials in nature which also exhibit this organic-inorganic hybrid structure. For example, the structure of bone in the body, which is also a complex, multilayered structure containing organic components surrounded by inorganic materials.¹⁰⁶ The inorganic components of these hybrid materials vary from calcium carbonate in eggs, to hydroxyapatite in bones.^{1,7,106} We propose to extend our “inside-out” synthesis technique to the fabrication of hybrid organic-inorganic multilayered materials. To accomplish this a variety of inorganic chemistries are available.¹⁰⁷⁻¹⁰⁹ We will focus on two chemistries, silica sol-gel and hydroxyapatite synthesis techniques. In the silica sol-

gel chemistry a silica precursor reacts with water in a hydrolysis which is accelerated by an acid or base. We will employ the diffusion of an acid or base from a template particle, in an “inside-out” manner, to create a shell of silica around a template. There are a variety of techniques to synthesize hydroxyapatite reported in literature. For example, the reaction of orthophosphoric acid (H_3PO_4) with calcium hydroxide ($\text{Ca}(\text{OH})_2$).¹¹⁰ Organic-Inorganic hybrid materials could exhibit interesting permeability for the release of solutes. Additionally, these types of materials might find use as novel tissue engineering platforms for the reconstruction of bone.

References

- [1] OpenStaxCollege *Biology*; Downloadable at <http://cnx.org/content/col11448/latest/>, 2013.
- [2] Patel, A.; Fine, B.; Sandig, M.; Mequanint, K. "Elastin biosynthesis: The missing link in tissue-engineered blood vessels." *Cardiovasc. Res.* **2006**, *71*, 40-49.
- [3] Gray, H. *Anatomy of the Human Body*; Bartleby: New York, 2000.
- [4] Mauseth, J. D. *Botany: An Introduction to Plant Biology*; Jones & Bartlett Learning: New York, 2011.
- [5] Buckley, J. A.; Fishman, E. K. "CT evaluation of small bowel neoplasms: spectrum of disease." *Radiographics* **1998**, *18*, 379-392.
- [6] Lack, L.; Weiner, I. M. "In vitro absorption of bile salts by small intestine of rats and guinea pigs." *Am. J. Physiol.* **1961**, *200*, 313.
- [7] Nys, Y.; Gautron, J.; Garcia-Ruiz, J. M.; Hincke, M. T. "Avian eggshell mineralization: biochemical and functional characterization of matrix proteins." *C. R. Palevol* **2004**, *3*, 549-562.
- [8] Decher, G.; Hong, J.-D. "Buildup of ultrathin multilayer films by a self-assembly process, I consecutive adsorption of anionic and cationic bipolar amphiphiles on charged surfaces." *Macromol. Symp.* **1991**, *46*, 321-327.
- [9] Decher, G.; Hong, J. D. "Buildup of Ultrathin Multilayer Films by a Self-Assembly Process: II. Consecutive Adsorption of Anionic and Cationic Bipolar Amphiphiles and Polyelectrolytes on Charged Surfaces." *Berich. Bunsen. Gesell.* **1991**, *95*, 1430-1434.
- [10] Decher, G.; Hong, J. D.; Schmitt, J. "Buildup of ultrathin multilayer films by a self-assembly process: III. Consecutively alternating adsorption of anionic and cationic polyelectrolytes on charged surfaces." *Thin Solid Films* **1992**, *210*, 831-835.
- [11] Polomska, A.; Leroux, J.-C.; Brambilla, D. "Layer-by-Layer Coating of Solid Drug Cores: A Versatile Method to Improve Stability, Control Release and Tune Surface Properties." *Macromol. Biosci.* **2017**, *17*, 1600228-n/a.
- [12] Quintana, G.; Simões, M. G.; Hugo, A.; Alves, P.; Ferreira, P.; Gerbino, E.; Simões, P. N.; Gómez-Zavaglia, A. "Layer-by-layer encapsulation of *Lactobacillus delbrueckii* subsp. *Bulgaricus* using block-copolymers of poly(acrylic acid) and pluronic for safe release in gastro-intestinal conditions." *J. Funct. Foods* **2017**, *35*, 408-417.

- [13] Chojnacka-Gorka, K.; Rozpedzik, A.; Zapotoczny, S. “Robust polyelectrolyte microcapsules reinforced with carbon nanotubes.” *RSC Adv.* **2016**, *6*, 114639-114643.
- [14] Hu, N.; Frueh, J.; Zheng, C.; Zhang, B.; He, Q. “Photo-crosslinked natural polyelectrolyte multilayer capsules for drug delivery.” **2015**, *482*, 315-323.
- [15] Caruso, F.; Spasova, M.; Susha, A.; Giersig, M.; Caruso, R. A. “Magnetic Nanocomposite Particles and Hollow Spheres Constructed by a Sequential Layering Approach.” *Chem. Mater.* **2001**, *13*, 109-116.
- [16] Caruso, F.; Caruso, R. A.; Hwang, H. “Nanoengineering of Inorganic and Hybrid Hollow Spheres by Colloidal Templating.” *Science* **1998**, *282*, 1111-1114.
- [17] Choi, C.-H.; Weitz, D. A.; Lee, C.-S. “One step formation of controllable complex emulsions: From functional particles to simultaneous encapsulation of hydrophilic and hydrophobic agents into desired position.” *Adv. Mater.* **2013**, *25*, 2536-2541.
- [18] Kang, J.-H.; Lee, S. S.; Guerrero, J.; Fernandez-Nieves, A.; Kim, S.-H.; Reichmanis, E. “Ultrathin Double-Shell Capsules for High Performance Photon Upconversion.” *Adv. Mater.* **2017**, *29*, 1606830-n/a.
- [19] Kim, S.-H.; Weitz, D. A. “One-step emulsification of multiple concentric shells with capillary microfluidic devices.” *Angew. Chem. Int. Edit.* **2011**, *123*, 8890-8893.
- [20] Abate, A. R.; Weitz, D. A. “High-Order Multiple Emulsions Formed in Poly(dimethylsiloxane) Microfluidics.” *Small* **2009**, *5*, 2030-2032.
- [21] Duan, J.; Hou, R.; Xiong, X.; Wang, Y.; Wang, Y.; Fu, J.; Yu, Z. “Versatile fabrication of arbitrarily shaped multi-membrane hydrogels suitable for biomedical applications.” *J. Mater. Chem. B* **2013**, *1*, 485-492.
- [22] Haase, M. F.; Brujic, J. “Tailoring of High-Order Multiple Emulsions by the Liquid-Liquid Phase Separation of Ternary Mixtures.” *Angew. Chem. Int. Edit.* **2014**, *53*, 11793-11797.
- [23] Ladet, S.; David, L.; Domard, A. “Multi-membrane hydrogels.” *Nature* **2008**, *452*, 76-79.
- [24] Dai, H.; Li, X.; Long, Y.; Wu, J.; Liang, S.; Zhang, X.; Zhao, N.; Xu, J. “Multi-membrane hydrogel fabricated by facile dynamic self-assembly.” *Soft Matter* **2009**, *5*, 1987-1989.
- [25] Helander, H. F.; Fändriks, L. “Surface area of the digestive tract—revisited.” *Scand. J. Gastroentero.* **2014**, *49*, 681-689.

- [26] Pignoli, P.; Tremoli, E.; Poli, A.; Oreste, P.; Paoletti, R. "Intimal plus medial thickness of the arterial wall: a direct measurement with ultrasound imaging." *Circulation* **1986**, *74*, 1399.
- [27] Wong, M.; Edelstein, J.; Wollman, J.; Bond, M. G. "Ultrasonic-pathological comparison of the human arterial wall. Verification of intima-media thickness." *Arterioscl. Throm. Vas.* **1993**, *13*, 482.
- [28] Tanaka, T. "Gels." *Sci. Am.* **1981**, *244*, 124-S-17.
- [29] Osada, Y.; Gong, J. P.; Tanaka, Y. "Polymer gels." *J. Macromol. Sci., Polym. Rev.* **2004**, *C44*, 87-112.
- [30] Esser-Kahn, A. P.; Odom, S. A.; Sottos, N. R.; White, S. R.; Moore, J. S. "Triggered release from polymer capsules." *Macromolecules* **2011**, *44*, 5539-5553.
- [31] Wang, H. C.; Zhang, Y. F.; Possanza, C. M.; Zimmerman, S. C.; Cheng, J. J.; Moore, J. S.; Harris, K.; Katz, J. S. "Trigger chemistries for better industrial formulations." *ACS Appl. Mater. Interfaces* **2015**, *7*, 6369-6382.
- [32] Beltran, S.; Baker, J. P.; Hooper, H. H.; Blanch, H. W.; Prausnitz, J. M. "Swelling equilibria for weakly ionizable, temperature-sensitive hydrogels." *Macromolecules* **1991**, *24*, 549-551.
- [33] Qiu, Y.; Park, K. "Environment-sensitive hydrogels for drug delivery." *Adv. Drug Delivery Rev.* **2001**, *53*, 321-339.
- [34] Ahn, S. K.; Kasi, R. M.; Kim, S. C.; Sharma, N.; Zhou, Y. X. "Stimuli-Responsive Polymer Gels." *Soft Matter* **2008**, *4*, 1151-1157.
- [35] Hirokawa, Y.; Tanaka, T. "Volume phase transition in a nonionic gel." *J. Chem. Phys.* **1984**, *81*, 6379.
- [36] Bird, R. B.; Stewart, W. E.; Lightfoot, E. N. *Transport Phenomena*, 2nd ed.; Wiley: New York, 2002.
- [37] Dunlop, J. W. C.; Weinkamer, R.; Fratzl, P. "Artful interfaces within biological materials." *Mater. Today* **2011**, *14*, 70-78.
- [38] Ionov, L. "Biomimetic Hydrogel-Based Actuating Systems." *Adv. Funct. Mater.* **2013**, *23*, 4555-4570.

- [39] Gracias, D. H. "Stimuli responsive self-folding using thin polymer films." *Curr. Opin. Chem. Eng.* **2013**, *2*, 112-119.
- [40] Dawson, C.; Vincent, J. F. V.; Rocca, A.-M. "How pine cones open." *Nature* **1997**, *390*, 668-668.
- [41] Forterre, Y.; Skotheim, J. M.; Dumais, J.; Mahadevan, L. "How the Venus flytrap snaps." *Nature* **2005**, *433*, 421-425.
- [42] Athas, J. C. Designing Hydrogels that Transform their Shape in Response to Molecular Cues. Ph.D., University of Maryland - College Park.
- [43] Hu, Z.; Zhang, X.; Li, Y. "Synthesis and application of modulated polymer gels." *Science* **1995**, *269*, 525.
- [44] *Biofabrication: Micro- and Nano-Fabrication, Printing, Patterning and Assemblies*; Forgacs, G.; Sun, W., Eds.; William Andrew: New York, 2013.
- [45] *Bio-Inspired Materials for Biomedical Engineering*; Brennan, A. B.; Kirschner, C. M., Eds.; Wiley: New York, 2014.
- [46] Fratzl, P. "Biomimetic materials research: What can we really learn from nature's structural materials?" *J. R. Soc. Interface* **2007**, *4*, 637-642.
- [47] Bhushan, B. "Biomimetics: lessons from nature - an overview." *Philos. Trans. R. Soc. A* **2009**, *367*, 1445-1486.
- [48] Chen, P. Y.; McKittrick, J.; Meyers, M. A. "Biological materials: functional adaptations and bioinspired designs." *Prog. Mater. Sci.* **2012**, *57*, 1492-1704.
- [49] Zhao, N.; Wang, Z.; Cai, C.; Shen, H.; Liang, F. Y.; Wang, D.; Wang, C. Y.; Zhu, T.; Guo, J.; Wang, Y. X.; Liu, X. F.; Duan, C. T.; Wang, H.; Mao, Y. Z.; Jia, X.; Dong, H. X.; Zhang, X. L.; Xu, J. "Bioinspired materials: From low to high dimensional structure." *Adv. Mater.* **2014**, *26*, 6994-7017.
- [50] Zhang, C. Q.; McAdams, D. A.; Grunlan, J. C. "Nano/micro-manufacturing of bioinspired materials: A review of methods to mimic natural structures." *Adv. Mater.* **2016**, *28*, 6292-6321.
- [51] Thompson, D. A. W. *On Growth and Form*; Cambridge University Press: Cambridge, 1917.

- [52] Turing, A. M. "The chemical basis of morphogenesis." *Philos. Trans. R. Soc. B* **1952**, 237, 37-72.
- [53] Evans, D. F.; Wennerstrom, H. *The Colloidal Domain: Where Physics, Chemistry, Biology, and Technology Meet*; Wiley-VCH: New York, 2001.
- [54] Granasy, L.; Puszta, T.; Tegze, G.; Warren, J. A.; Douglas, J. F. "Growth and form of spherulites." *Phys. Rev. E* **2005**, 72, 011605.
- [55] Murphy, S. V.; Atala, A. "3D bioprinting of tissues and organs." *Nat. Biotechnol.* **2014**, 32, 773-785.
- [56] Stadler, B.; Price, A. D.; Chandrawati, R.; Hosta-Rigau, L.; Zelikin, A. N.; Caruso, F. "Polymer hydrogel capsules: En route toward synthetic cellular systems." *Nanoscale* **2009**, 1, 68-73.
- [57] Ariga, K.; Ji, Q. M.; Richards, G. J.; Hill, J. P. "Soft capsules, hard capsules, and hybrid capsules." *Soft Mater.* **2012**, 10, 387-412.
- [58] Lima, A. C.; Custódio, C. A.; Alvarez-Lorenzo, C.; Mano, J. F. "Biomimetic methodology to produce polymeric multilayered particles for biotechnological and biomedical applications." *Small* **2013**, 9, 2487-2492.
- [59] Nita, L. E.; Chiriac, A. P.; Nistor, M. T.; Tartau, L. "Upon some multi-membrane hydrogels based on poly(N,N-dimethyl-acrylamide-co-3,9-divinyl-2,4,8,10-tetraoxaspiro (5.5) undecane): Preparation, characterization and *in vivo* tests." *J. Mater. Sci. Mater. Med.* **2014**, 25, 1757-1768.
- [60] Xiong, Y.; Yan, K.; Bentley, W. E.; Deng, H. B.; Du, Y. M.; Payne, G. F.; Shi, X. W. "Compartmentalized multilayer hydrogel formation using a stimulus-responsive self-assembling polysaccharide." *ACS Appl. Mater. Interfaces* **2014**, 6, 2948-2957.
- [61] Yan, K.; Xiong, Y.; Wu, S.; Bentley, W. E.; Deng, H. B.; Du, Y. M.; Payne, G. F.; Shi, X. W. "Electro-molecular assembly: Electrical writing of information into an erasable polysaccharide medium." *ACS Appl. Mater. Interfaces* **2016**, 8, 19780-19786.
- [62] Yoshida, R.; Kaneko, Y.; Sakai, K.; Okano, T.; Sakurai, Y.; Bae, Y. H.; Kim, S. W. "Positive thermosensitive pulsatile drug-release using negative thermosensitive hydrogels." *J. Control Rel.* **1994**, 32, 97-102.
- [63] Dinarvand, R.; D'Emanuele, A. "The use of thermoresponsive hydrogels for on-off release of molecules." *J. Control Rel.* **1995**, 36, 221-227.

- [64] Bhalla, A. S.; Siegel, R. A. "Mechanistic studies of an autonomously pulsing hydrogel/enzyme system for rhythmic hormone delivery." *J. Control Rel.* **2014**, *196*, 261-271.
- [65] Arya, C.; Oh, H.; Raghavan, S. R. "'Killer' microcapsules that can selectively destroy target microparticles in their vicinity." *ACS Appl. Mater. Interfaces* **2016**, *8*, 29688-29695.
- [66] Ghaffarian, R.; Perez-Herrero, E.; Oh, H.; Raghavan, S. R.; Muro, S. "Chitosan-alginate microcapsules provide gastric protection and intestinal release of ICAM-1-targeting nanocarriers, enabling GI targeting in vivo." *Adv. Funct. Mater.* **2016**, *26*, 3382-3393.
- [67] Payne, G. F.; Kim, E.; Cheng, Y.; Wu, H. C.; Ghodssi, R.; Rubloff, G. W.; Raghavan, S. R.; Culver, J. N.; Bentley, W. E. "Accessing biology's toolbox for the mesoscale biofabrication of soft matter." *Soft Matter* **2013**, *9*, 6019-6032.
- [68] Lee, K. Y.; Mooney, D. J. "Alginate: Properties and biomedical applications." *Prog. Polym. Sci.* **2012**, *37*, 106-126.
- [69] Fundueanu, G.; Nastruzzi, C.; Carpov, A.; Desbrieres, J.; Rinaudo, M. "Physico-chemical characterization of Ca-alginate microparticles produced with different methods." *Biomaterials* **1999**, *20*, 1427-1435.
- [70] Odian, G. *Principles of Polymerization*, 4th ed.; Wiley: New York, 2004.
- [71] Chan, E.-S.; Lim, T.-K.; Voo, W.-P.; Pogaku, R.; Tey, B. T.; Zhang, Z. "Effect of formulation of alginate beads on their mechanical behavior and stiffness." *Particuology* **2011**, *9*, 228-234.
- [72] White, J. C.; Saffer, E. M.; Bhatia, S. R. "Alginate/PEO-PPO-PEO composite hydrogels with thermally-active plasticity." *Biomacromolecules* **2013**, *14*, 4456-4464.
- [73] White, J. C.; Stoppel, W. L.; Roberts, S. C.; Bhatia, S. R. "Addition of perfluorocarbons to alginate hydrogels significantly impacts molecular transport and fracture stress." *J. Biomed. Mater. Res. A* **2013**, *101*, 438-446.
- [74] Gong, J. P.; Katsuyama, Y.; Kurokawa, T.; Osada, Y. "Double-network hydrogels with extremely high mechanical strength." *Adv. Mater.* **2003**, *15*, 1155-1158.
- [75] Cipriano, B. H.; Banik, S. J.; Sharma, R.; Rumore, D.; Hwang, W.; Briber, R. M.; Raghavan, S. R. "Superabsorbent hydrogels that are robust and highly stretchable." *Macromolecules* **2014**, *47*, 4445-4452.

- [76] Gargava, A.; Arya, C.; Raghavan, S. R. "Smart hydrogel-based valves inspired by the stomata in plants." *ACS Appl. Mater. Interfaces* **2016**, *8*, 18430-18438.
- [77] Arya, C.; Kralj, J. G.; Jiang, K. Q.; Munson, M. S.; Forbes, T. P.; DeVoe, D. L.; Raghavan, S. R.; Forry, S. P. "Capturing rare cells from blood using a packed bed of custom-synthesized chitosan microparticles." *J. Mater. Chem. B* **2013**, *1*, 4313-4319.
- [78] Hunziker, O.; Abdel'al, S.; Schulz, U. "The Aging Human Cerebral Cortex: A Stereological Characterization of Changes in the Capillary Net." *J. Gerontol.* **1979**, *34*, 345-350.
- [79] Ju, Y. M.; Ahn, H.; Arenas-Herrera, J.; Kim, C.; Abolbashari, M.; Atala, A.; Yoo, J. J.; Lee, S. J. "Electrospun vascular scaffold for cellularized small diameter blood vessels: A preclinical large animal study." *Acta Biomater.* **2017**, *59*, 58-67.
- [80] Alexandre, N.; Amorim, I.; Caseiro, A. R.; Pereira, T.; Alvites, R.; Rêma, A.; Gonçalves, A.; Valadares, G.; Costa, E.; Santos-Silva, A.; Rodrigues, M.; Lopes, M. A.; Almeida, A.; Santos, J. D.; Maurício, A. C.; Luís, A. L. "Long term performance evaluation of small-diameter vascular grafts based on polyvinyl alcohol hydrogel and dextran and MSCs-based therapies using the ovine pre-clinical animal model." *Int. J. Pharm.* **2017**, *523*, 515-530.
- [81] Li, Q.; Mu, L.; Zhang, F.; Mo, Z.; Jin, C.; Qi, W. "Manufacture and property research of heparin grafted electrospinning PCU artificial vascular scaffolds." *Mat. Sci. Eng. C* **2017**, *78*, 854-861.
- [82] Tan, Z.; Gao, X.; Liu, T.; Yang, Y.; Zhong, J.; Tong, C.; Tan, Y. "Electrospun vein grafts with high cell infiltration for vascular tissue engineering." *Mat. Sci. Eng. C* **2017**, *81*, 407-415.
- [83] Melchiorri, A. J.; Hibino, N.; Best, C. A.; Yi, T.; Lee, Y. U.; Kraynak, C. A.; Kimerer, L. K.; Krieger, A.; Kim, P.; Breuer, C. K.; Fisher, J. P. "3D-Printed Biodegradable Polymeric Vascular Grafts." *Adv. Healthc. Mater.* **2016**, *5*, 319-325.
- [84] Hasan, A.; Paul, A.; Memic, A.; Khademhosseini, A. "A multilayered microfluidic blood vessel-like structure." *Biomed. Microdevices* **2015**, *17*, 88.
- [85] Hoch, E.; Tovar, G. E.; Borchers, K. "Bioprinting of artificial blood vessels: current approaches towards a demanding goal." *Eur. J. Cardio-Thorac* **2014**, *46*, 767-778.
- [86] Ju, Y. M.; San Choi, J.; Atala, A.; Yoo, J. J.; Lee, S. J. "Bilayered scaffold for engineering cellularized blood vessels." *Biomaterials* **2010**, *31*, 4313-4321.
- [87] Wang, X.; Mäkitie, A. A.; Paloheimo, K.-s.; Tuomi, J.; Paloheimo, M.; Sui, S. "A tubular PLGA-sandwiched cell/hydrogel fabrication technique based on a step-by-step mold/extraction process." *Adv. Polym. Tech.* **2011**, *30*, 163-173.

- [88] Sandgren, T.; Sonesson, B.; Ahlgren, Å. R.; Länne, T. “The diameter of the common femoral artery in healthy human: Influence of sex, age, and body size.” *J. Vasc. Surg.* **1999**, *29*, 503-510.
- [89] Mao, S. S.; Ahmadi, N.; Shah, B.; Beckmann, D.; Chen, A.; Ngo, L.; Flores, F. R.; Gao, Y. I.; Budoff, M. J. “Normal Thoracic Aorta Diameter on Cardiac Computed Tomography in Healthy Asymptomatic Adult; Impact of Age and Gender.” *Academic Radiology* **2008**, *15*, 827-834.
- [90] Cummins, H. Z. “Liquid, glass, gel: The phases of colloidal Laponite.” *J. Non-Cryst. Solids* **2007**, *353*, 3891-3905.
- [91] Haraguchi, K.; Li, H.-J.; Matsuda, K.; Takehisa, T.; Elliott, E. “Mechanism of Forming Organic/Inorganic Network Structures during In-situ Free-Radical Polymerization in PNIPAA–Clay Nanocomposite Hydrogels.” *Macromolecules* **2005**, *38*, 3482-3490.
- [92] Haraguchi, K. “Stimuli-responsive nanocomposite gels.” *Colloid Polym. Sci.* **2011**, *289*, 455-473.
- [93] Thomas, P. C.; Cipriano, B. H.; Raghavan, S. R. “Nanoparticle-crosslinked hydrogels as a class of efficient materials for separation and ion exchange.” *Soft Matter* **2011**, *7*, 8192-8197.
- [94] Lee, K.; Silva, E. A.; Mooney, D. J. “Growth factor delivery-based tissue engineering: general approaches and a review of recent developments.” *J. R. Soc. Interface* **2011**, *8*, 153-170.
- [95] Tobin, J. M.; Sinha, B.; Ramani, P.; Saleh, A. R. H.; Murphy, M. S. “Upper Gastrointestinal Mucosal Disease in Pediatric Crohn Disease and Ulcerative Colitis: A Blinded, Controlled Study.” *J. Pediatr. Gastr. Nutr.* **2001**, *32*.
- [96] Hüe, S.; Mention, J.-J.; Monteiro, R. C.; Zhang, S.; Cellier, C.; Schmitz, J.; Verkarre, V.; Fodil, N.; Bahram, S.; Cerf-Bensussan, N.; Caillat-Zucman, S. “A Direct Role for NKG2D/MICA Interaction in Villous Atrophy during Celiac Disease.” *Immunity* **2004**, *21*, 367-377.
- [97] Koppes, A. N.; Kamath, M.; Pfluger, C. A.; Burkey, D. D.; Dokmeci, M.; Wang, L.; Carrier, R. L. “Complex, multi-scale small intestinal topography replicated in cellular growth substrates fabricated via chemical vapor deposition of Parylene C.” *Biofabrication* **2016**, *8*, 035011.
- [98] Sung, J. H.; Yu, J.; Luo, D.; Shuler, M. L.; March, J. C. “Microscale 3-D hydrogel scaffold for biomimetic gastrointestinal (GI) tract model.” *Lab Chip* **2011**, *11*, 389-392.

- [99] Daugherty, A. L.; Mersny, R. J. "Transcellular uptake mechanisms of the intestinal epithelial barrier: Part one." *Pharm. Sci. Technol. To.* **1999**, *2*, 144-151.
- [100] Nguyen, K. T.; West, J. L. "Photopolymerizable hydrogels for tissue engineering applications." *Biomaterials* **2002**, *23*, 4307-4314.
- [101] Slaughter, B. V.; Khurshid, S. S.; Fisher, O. Z.; Khademhosseini, A.; Peppas, N. A. "Hydrogels in Regenerative Medicine." *Adv. Mater.* **2009**, *21*, 3307-3329.
- [102] Nichol, J. W.; Koshy, S. T.; Bae, H.; Hwang, C. M.; Yamanlar, S.; Khademhosseini, A. "Cell-laden microengineered gelatin methacrylate hydrogels." *Biomaterials* **2010**, *31*, 5536-5544.
- [103] Naahidi, S.; Jafari, M.; Logan, M.; Wang, Y.; Yuan, Y.; Bae, H.; Dixon, B.; Chen, P. "Biocompatibility of hydrogel-based scaffolds for tissue engineering applications." *Biotechnol. Adv.* **2017**, *35*, 530-544.
- [104] Wang, H.; Feng, Y.; Behl, M.; Lendlein, A.; Zhao, H.; Xiao, R.; Lu, J.; Zhang, L.; Guo, J. "Hemocompatible polyurethane/gelatin-heparin nanofibrous scaffolds formed by a bi-layer electrospinning technique as potential artificial blood vessels." *Front. Chem. Sci. Eng.* **2011**, *5*, 392-400.
- [105] Pauly, H. M.; Sathy, B. N.; Olvera, D.; McCarthy, H. O.; Kelly, D. J.; Popat, K. C.; Dunne, N. J.; Haut Donahue, T. L. "Hierarchically Structured Electrospun Scaffolds with Chemically Conjugated Growth Factor for Ligament Tissue Engineering." *Tissue Eng. Pt. A* **2017**, *23*, 823-836.
- [106] Suchanek, W.; Yoshimura, M. "Processing and properties of hydroxyapatite-based biomaterials for use as hard tissue replacement implants." *J. Mater. Res.* **2011**, *13*, 94-117.
- [107] Hench, L. L.; West, J. K. "The sol-gel process." *Chem. Rev.* **1990**, *90*, 33-72.
- [108] Hench, L. L. "Bioceramics: From Concept to Clinic." *J. Am. Ceram. Soc.* **1991**, *74*, 1487-1510.
- [109] Ribeiro, C. A.; Martins, M. V. S.; Bressiani, A. H.; Bressiani, J. C.; Leyva, M. E.; de Queiroz, A. A. A. "Electrochemical preparation and characterization of PNIPAM-HAP scaffolds for bone tissue engineering." *Mat. Sci. Eng. C* **2017**, *81*, 156-166.
- [110] Ramesha, S.; Adzila, S.; Jeffrey, C.; Tana, C.; Purbolaksonoa, J.; Noora, A.; Hassana, M.; Sopyanc, I.; Tengd, W. "Properties of hydroxyapatite synthesized by wet chemical method." *J. Ceram. Process. Res.* **2013**, *14*, 448-452.

List of Publications

Submitted:

1. Lacey, S.D.; Kirsch, D. J.; Li Y.; Morgenstern, J.T.; **Zarket, B.C.**; Yao Y.; Dai, J.; Garcia, L.Q.; Liu B.; Gao, T.; Xu S.; Raghavan, S.R.; Connel J. W., Hu L.*, “Extrusion-based 3D Printing of Hierarchically Porous Advanced Battery Electrodes.” *Submitted for Publication (2017)*

Accepted:

1. **Zarket, B.C.**; Raghavan, S.R.*, “Onion-like multilayered polymer capsules synthesized by a bioinspired inside-out technique.” *Nat. Commun.* **2017**, *8*, 193.
2. Athas, J.C.; Nguyen, C.P.; **Zarket, B.C.**; Gargava, A.; Nie, Z.H.; Raghavan, S.R.*, “Enzyme-triggered folding of hydrogels: Towards a mimic of the Venus flytrap.” *ACS Applied Materials and Interfaces*, **8**, 19066 (2016)

Manuscripts in Preparation:

1. *Zarket, B.C.*; Wang, H.C., Raghavan, S.R.*, “Multilayered Hydrogel Tubes: Novel Vein and Artery Mimics which Spontaneously Constrict and Dilate Based on External Stimuli”, *Manuscript in Preparation (2017)*
2. *Zarket, B.C.*; Wang, H.C.; Raghavan, S.R.*, “Hydrogels with Hairy Surfaces: Towards Biomimetic Villi”, *Manuscript in Preparation (2017)*
3. *Zarket B.C.*, Raghavan S.R.*, “Multilayered Thin Polymer Coatings Lend Protection and Elasticity to Fragile Cargo Materials”, *Manuscript in Preparation (2017)*

List of Presentations

1. Zarket B.C., Wang H.C., Raghavan S.R., “Multilayer Tubes Displaying Dramatic Shape Change in Response to External Stimuli.” ACS National Meeting, Washington, D.C. 2017.
2. Zarket B.C., Raghavan S.R., “Onion-Like Multilayered Capsules Based on Stimuli-Responsive Polymers - Synthesis by a Bioinspired ‘Inside-Out’ Technique.” Materials Research Society, Phoenix, AZ. 2017.
3. Zarket B.C., Raghavan S.R., “Multilayer hybrid capsules: Towards a biomimetic egg.” ACS Colloids and Surface Science Symposium, Cambridge, MA. 2016.
4. Zarket B.C., Antoszewski S., Coyne T., Yuwono F., Raghavan S.R., “Onion-like polymer capsules with multiple concentric shells.” Pacifichem, Honolulu, HI. 2015.
5. Zarket B.C., Antoszewski S., Coyne T., Yuwono F., Raghavan S.R., “Onion-like polymer capsules with multiple concentric shells.” ResearchFest, College Park, MD. 2015.
6. Zarket B.C., Antoszewski S., Coyne T., Raghavan S.R., “Onion-like polymer capsules with multiple concentric shells.” ACS Colloids and Surface Science Symposium, Philadelphia, PA. 2014

